Repair of Brachial Plexus Avulsion: clinical outcome, strategies for cellular repair and MR imaging protocols

Carolina Kachramanoglou

A thesis submitted to University College, London for the Degree of Doctor of Medicine Research MD(Res)

2013

Department of Brain Repair and Rehabilitation,

UCL Institute of Neurology, Queen Square,

London, WC1N 3BG,

United Kingdom

Declaration

I confirm that the work presented in this thesis is my own. Where information has been derived from other sources, I confirm that this has been indicated below.

The olfactory mucosa biopsies were obtained by Mr. Peter Andrews (Consultant ENT surgeon). The olfactory ensheathing cultures were performed by Stuart Law and Daqing Li. The electrophysiological studies were performed by the Prof. Martin Koltzenburg at the National Hospital for Neurology and Neurosurgery, who was not aware of the patients' clinical status.

The MRI imaging protocol was designed by Dr. Claudia Wheeler-Kingshott and her team in the MNR Research unit. Patients were scanned in my presence by the radiographers at the Functional Imaging Laboratory, part of The Wellcome Trust Centre for Neuroimaging at UCL.

For the statistical analysis, I obtained advise from Dr. Constantinos Kallis and members of the UCL Biostatistics Group at the Joint Research Office.

Dr Carolina Kachramanoglou

Abstract

This thesis comprises of three studies investigating the repair of brachial plexus avulsion injury from three different perspectives. The first aim of this thesis was to investigate the long-term effects of reimplantation surgery in patients with complete brachial plexus avulsion injury using standardized assessments. Patients are assessed with clinical examination, neurophysiological studies and patient-reported outcome questionnaires. It is shown that patients who have undergone brachial plexus re-implantation surgery demonstrate small, yet significant, improved function in motor and sensory recovery compared with patients who have not had this surgical intervention. These results are encouraging, but functional improvements are limited. One strategy aimed at further improving the effects of re-implantationis the transplantation of OECs during the surgical repair. The second study presented in this thesis comprises of a prospective observational study of human biopsies of nasal mucosa by endonasal dissection of the mucosa of the nasal septum during the approach for routine sinus surgery. Samples are cultured in the laboratory, and the yield of olfactory ensheathing cells is compared as to the location, size, and weight of the biopsies and patient characteristics including age, smoking, nasal disease severity. OEC yield is associated with mucosal disease and patients age. The third aim of this thesis is to develop novel MRI techniques that can be used in human trials of cell mediated repair of the brachial plexus to assess patients' spinal cord regeneration after OEC transplantation and provide a more robust outcome measure for comparing different strategies of brachial plexus repair. We focus on magnetic resonance spectroscopy and demonstrate that this technique is sensitive to pathological changes that occur in the spinal cord above the injury. Myo-Inositol to

creatine ratio is correlated with disability and is negatively correlated to time from injury. The implications of the above findings are discussed.

Acknowledgements

First and foremost I would like to thank my principal supervisor Mr. David Choi for offering the opportunity to work at Queen Square and Institute of Neurology. I thank him for providing me with a measured balance among guidance, supervision and freedom to express my thoughts and transfer of his wisdom regarding professional conduct in the research world, interprofessional relationships and efficient working methods.

I would like to warmly thank Dr. Olga Ciccarelli, for her time, patience, support and tireless assistance with the MRI experiment, for listening to me in periods of crisis and for reminding me that things were not as bad as I usually thought.

A huge thanks to members of the Spinal Repair Unit, especially Stuart Law for teaching me the principles of laboratory work and assisting in any type of troubleshooting. I would also like to thank everyone involved in the production of this work. Special thanks to Prof. Carlstedt for introducing me to brachial plexus avulsion injury and repair and trusting me, Mr. P. Andrews for bearing with me in almost every list of his for more than two years and Prof. Martin Koltzenburg performing the electrophysiology tests. Special thanks also goes to all the physicists including Dr. Claudia Wheeler-Kingshott, David Thomas, Enrico DeVita, Torben Schneider, Rebecca Samson and Evelyn Balteau, for designing the MR protocol and reviewing the MR paper. Thank you to Prof Alan Thomson who despite his busy schedule spent time to review my work.

I am grateful to all patients with brachial plexus injury that took part in this study for travelling long distances and giving up their time to be assessed and patients who offered specimens of their olfactory mucosa for the sake of research. This study relied entirely on their generosity. I would also like to express my gratitude to the healthy subjects that took part in this project.

Finally, I would like to thank my long-suffering husband who (semi)patiently supported me throughout the process and my parents for helping me take this path in life.

Thank you.

Publications arising from the work presented in this thesis

Metabolic changes in the spinal cord after brachial plexus root re-implantation, C. Kachramanoglou, E. De Vita, D. L. Thomas, C. A. M. Wheeler-Kingshott, E. Balteau, T. Carlstedt, D. Choi, A. J. Thompson, and O. Ciccarelli, Neurorehabil Neural Repair. 2013 Feb; 27(2):118-24.

Culture of Olfactory Ensheathing Cells for Central Nerve Repair: The Limitations and Potential of Endoscopic Olfactory Mucosal Biopsy, Carolina Kachramanoglou, Stuart Law, Peter Andrews, Daqing Li, David Choi, Neurosurgery. 2013 Feb; 72(2):170-8.

Novel strategies in brachial plexus repair after traumatic avulsion, Kachramanoglou C, Li D, Andrews P, East C, Carlstedt T, Raisman G, Choi D. Br J Neurosurg. 2011; 25(1): 16-27.

Self-mutilation in patients after nerve injury may not be due to deafferentation pain: a case report, Kachramanoglou C, Carlstedt T, Koltzenburg M, Choi D. Pain Med. (2011); 12(11): 1644-8.

Fuzzy partial volume correction of spinal cord DTI parameters (Abstract), Schneider T, Thomas DL, Kachramanoglou C, Ciccarelli O, Alexander DC, Wheeler-Kingshott C. Fuzzy partial volume correction of spinal cord DTI parameters, *Proc. Intl. Soc. Mag. Reson. Med*, (2011); 19: 4556

Reliability of tract-specific q-space imaging metrics in healthy spinal cord (Abstract), Schneider T, Ciccarelli O, Kachramanoglou C, Thomas DL, Wheeler-Kingshott CAM, Proc. Intl. Soc. Mag. Reson. Med, (2011); 19: 680

Spinal cord ^{1}H-MR spectroscopy in patients after brachial plexus root re-implantation (Abstract), De Vita E, Kachramanoglou C, Wheeler-Kingshott CAM, Thomas DL, Choi D, Thompson A, Ciccarelli O. Proc. Intl. Soc. Mag. Reson. Med, (2011); 19: 4290

Multi-parameter mapping of the human cervical cord at 3.0T in less than 20 minutes (Abstract), Samson RS, Ciccarelli O, Kachramanoglou C,Lutti A, Thomas DJ, Weiskopf N, Wheeler-Kingshott CAM. Proc. Intl. Soc. Mag. Reson. Med, (2011); 19: 2754

Table of Contents

List of Figures

Page

Chapter 4

Chapter 5

Chapter 6

List of Tables

Page

Chapter 5

Chapter 6

List of abbreviations

^{1}H-MRS: proton magnetic resonance spectroscopy

ADLs: activities of daily living

ADM: digiti minimi muscle

APB: abductor pollicis brevis muscle

ATP: adenosine triphosphate

BP: brachial plexus

BDNF: brain-derived neurotrophic factor

DASH: Disabilities of the Arm, Shoulder and Hand

DML: distal motor latency

CHESS: chemical-shift-selective water suppression

Cho: Choline

CNS: central nervous system

CMAP: compound muscle action potential

Cr: Creatine

CRLB: Cramer-Rao lower bounds

CSF: cerebrospinal fluid

CSPG: Chondroitin sulfate proteoglycans

CST: corticospinal tract

CT: Computed tomography

CTNF: ciliary neurotrophic factor

DREZ: dorsal root entry zone

DRG: dorsal root ganglion

DML: distal motor latency

EDC: Extenor Digitorum Communis

EMG: Electromyography

FDIO: first dorsal interosseous

FDM: flexor digiti minimi

FDS: flexor digitorum superficialis

FESS: functional endoscopic sinus surgery

FFT: fast Fourier transformation

FoV: field of view

FID: free induction decay

FVC: forced vital capacity

FWHM: fullwidth at half maximum

GDNF: glial cell line-derived neurotrophic factor

GFAP: glial fibrillary acidic protein

GGF2: glial growth factor 2

GPC: glycerophosphocholine

HASTE: Half Fourier Acquisition Single shot Turbo spin Echo

Lac: lactate

LCModel: Linear combination model

MHQ: Michigan Hand Outcomes Questionnaire

m-Ins : myo-Inositol

MRC: Medical Research Council

MRI: Magnetic resonance imaging

MS: multiple sclerosis

MUAP: motor unit action potential

NAA: N-acetyl-aspartate

NSPCs: Neural stem/progenitor

OB: olfactory bulb

OBI: olfactory biopsy instrument

OECs: Olfactory ensheathing cells

p75: low affinity neurotrophin receptor

PC: phosphocholine

PNS: peripheral nervous system

PRESS: point-resolved spectroscopy

PROMs: patient-reported outcome measures

PSWs: positive sharp waves

RF: radiofrequency

ROI: region of interest

SC: Schwann cells

SCV: Sensory conduction velocity

SNAPs: Sensory nerve action potentials

SNR: signal-to-noise ratio

SSR: sympathetic skin response

STEAM: stimulated echo acquisition mode

TR: transitional zone

VAS: visual analogue scale

VIM: vimentin

VOI: volume of interest

Chapter 1

An introduction to the brachial plexus avulsion injury and brachial plexus re-implantation

1.1 The brachial plexus

The brachial plexus (BP) is a network of nerves responsible for cutaneous and motor innervation of the entire upper limb. It is formed by the union of ventral rami of C5 through T1. As all spinal nerves, the brachial plexus also arises from the spinal cord by *rootlets*, which converge to form *rootlet bundles*, which in turn, combine to give ventral and dorsal *roots* (Figure 1.1). The dorsal and ventral roots of each cord segment pass through the corresponding intervertebral foramen, in or near which they unite to form a mixed *spinal nerve* containing both afferent and efferent neurons. The dorsal and ventral roots are functionally distinct. The dorsal roots contain primary afferent neurons running from peripheral sensory receptors to the spinal cord and brainstem. The nerve cell bodies of primary sensory neurons are located in the dorsal root ganglia (DRG). The ventral roots of the spinal nerves carry efferent neurons dendrites, cell body and proximal part of axons motor neuron are located within the ventral horn in the spinal grey mater of the spinal cord. The distal axon emerges from the ventral root and extends to the target muscles.

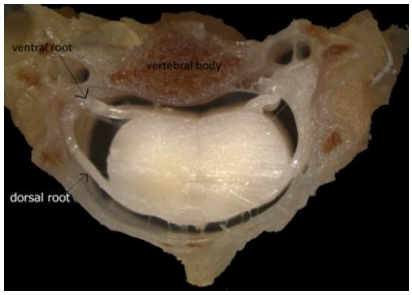

Figure 1.1: *Transverse section through the rodent cervical spinal cord showing the relationship between the spinal cord, dorsal and ventral roots, spinal nerves, and vertebral column.*

1.2 The transitional zone

Each rootlet has an *intramedullary* segment within the central nervous system (CNS), an *emergent* segment, were it passes through the CNS surface, and a *free* segment peripheral to this (Fraher et al. 1985). The *intramedullary* segments contain CNS tissue and the free segment contains peripheral nervous system (PNS) tissue. Where the two meet, they interdigitate to form the PNS-CNS *transitional zone (TR)*. Hence, the TR is characterized by the presence of a projection of CNS tissue from the spinal cord together with PNS tissue in the most proximal part of the root. Nerve fibres in the PNS extend into the CNS or vice versa and traverse the TR. Peripheral to the TR, myelin sheaths are produced by Schwann cells, whereas, central to it myelin sheaths are produced by oligodendrocytes.

The transitional zone may lie in a variety of locations in the rootlet. Central nervous system tissue may project distally beyond the CNS surface. In other cases such as in the cervical spinal cord, this protrusion of CNS tissue in the free part of the rootlet is absent and the transitional zone may rest at the level of the CNS surface or lie slightly deep to the surface of the spinal cord (Fraher et al. 1985). The central nervous system component is covered by a specialized thickening (*glia limitans*) composed of astrocytic foot processes. Astrocytic processes also extend distally into the rootlet among Schwann cells, forming the *glial fringe* that projects about 100 μm distally (Figure 1.2). Closer to the CNS part, the astrocytic fringe is thicker and encloses individual nerve fibres in a cul-de-sac fashion (Carlstedt 1977). Around the perimeter of the fibre bundle at and deep to the plane of the CNS surface, the transitional zone is also surrounded by a thick collar of astrocytic tissue, which is not traversed by any nerve fibres. Where the transitional zone extends well into the

rootlet for long segments, the central tissue component is similar to that of CNS tract with its surface bounded by astrocytic processes continuous to the glia limitans (Fraher 1992).

The basement membrane coating the glial fringe is reflected over to the nerve fibres and is continuous with the Schwann cell basement membrane. Here, there is a unique apposition between astrocytes and Schwann cells. The capillaries in the endoneurial space of the PNS compartment do not cross the PNS-CNS borderline with the nerve fibres but deviate out to join vessels in the pia mater, indicating that the different permeability properties of vessels in the nerve and spinal cord maintain different types of barriers. Therefore, the TR holds a position of conceptual importance with regard to neuronal organization, as well as, a model system for the experimental investigations.

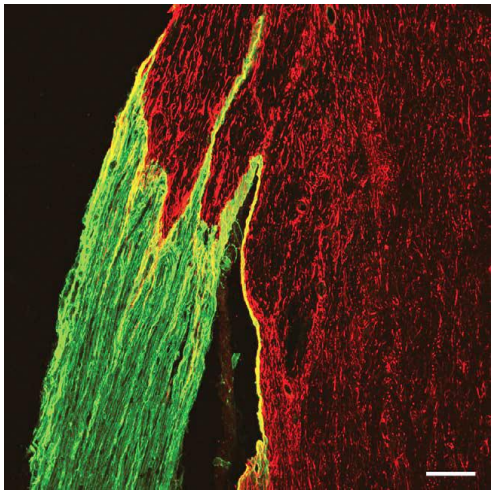

Figure 1.2: *Coronal section through the transitional zone of a normal rodent L4 rootlet. Double immunostaining with laminin (green) and* glial fibrillary acidic *protein (GFAP) (red) to demonstrate peripheral nerve tissue and CNS/spinal cord tissue respectively. Scale bar 100 μm. (Image from Li et al., (2004) Exp Neurol 188(2): 300-8 (Li et al. 2004). Permission to reproduce this image has been granted by Elsevier Limited)*

1.3 Root avulsion injury

In traumatic lesions of the BP, the nerves can be crushed, stretched, ruptured, or avulsed from the spinal cord (Figure 1.3). Ruptures may occur at any site from the spinal nerve distal to the dorsal root ganglion to the terminal branches resulting in postganglionic injuries i.e. a peripheral nervous system injury. Avulsive injury may be of two types: a *peripheral* intradural avulsion occurs if the nerve root is torn proximal to the dorsal root ganglion but remnants of the root remain attached to the spinal cord; a *central* avulsion injury occurs when there is an interruption of root or rootlet continuity at the surface of the spinal cord proximal to or at the transitional zone of the spinal cord; which is effectively a CNS injury (Spinner et al. 2008) and may be considered a "longitudinal spinal cord injury" (Carlstedt 2008).

Combination of complete and partial ruptures and avulsions can also occur. The most frequent pattern is complete avulsion of dorsal and ventral roots. The combination of intact dorsal and avulsed ventral roots is more common than spared ventral and avulsed dorsal roots (Carlstedt 2008).

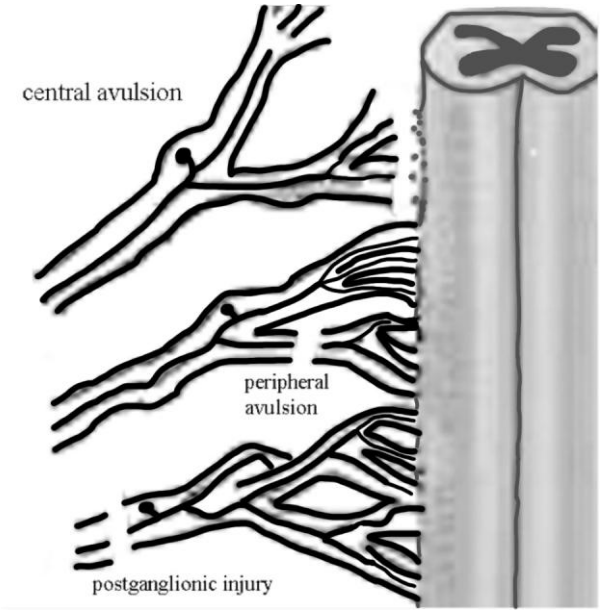

Figure 1.3: *Types of root injury: In central intradural avulsion injury a root is torn off the spinal cord at its surface at the transitional zone of the spinal cord; In peripheral intradural avulsion the nerve root is torn proximal to the dorsal root ganglion but remnants of the root remain attached to the spinal cord; Postganglionic injuries involve ruptures of the nerve distal to the DRG.*

1.4 Clinical features of brachial plexus avulsion

Avulsion of one or more roots is clinically diagnosed in about 70% of severe BP traction injuries (Narakas 1993) and is most often caused by high kinetic motor vehicle accidents (Terzis et al. 2000). The roots supplying the BP are particularly at risk of avulsion due to the loose suspension of the shoulder girdle compared to the lumbosacral plexus, which is better protected within the bony pelvis. In addition, the lower roots of the BP (C8 and T1) are more easily avulsed than the upper roots BP (C5 and C7), because the latter are supported by ligaments at the neural foramina

and former have a more straight course as they are exiting the spinal cord and course towards the exiting foramina (Carlstedt 2008).

A c*omplete brachial plexus* avulsion involves all five sets of dorsal and ventral roots (C5 to T1) supplying the BP. Motorcycle accidents account for most cases due to the increased traction forces applied to the BP when the rider falls on the shoulder, forcing the head and shoulder apart. Other causes of BP injuries in adults include falls from a roof or tree, skiing accidents, penetrating injuries and iatrogenic insults (Terzis et al. 2000; Kandenwein et al. 2005).

Complete brachial plexus avulsion is characterized by a completely paralyzed and anaesthetic arm. Neuropathic pain, which is severe and resistant to pharmacological treatments commonly follows avulsion injuries (Berman et al. 1998; Htut et al. 2006). Interestingly, a significant correlation between pain intensity and number of affected roots has been demonstrated and allodynia was shown to be more frequent in the border zone of affected and unaffected dermatomes (Htut et al. 2006).

1.5 Diagnosis of brachial plexus avulsion

A careful clinical history together with a meticulous clinical examination can often give a good indication of complete BP avulsion injury at presentation. On inspection, a positive Horner's sign, which involves drooping of the upper eyelid from loss of sympathetic innervation to the superior tarsal muscle, anhidrosis and miosis suggests avulsion of the lower roots. This sign, however, is not always present immediately

after injury but develops soon after. Abrasions and ecchymosis in the supraclavicular area suggests tearing of deep structures and give an indication about the force of injury. Fluid collections at the posterolateral aspect of the neck due to rupture of the dural sac and formation of pseudomeningocoeles also indicate violent injury to the forequarter. Paralysis of the ipsilateral hemidiaphragm may also be present if higher roots are also involved (C3, 4, 5).

The BP can be palpated just lateral to the sternocleidomastoid muscle. Often in BP avulsion injury, the plexus is pulled underneath the clavicle and cannot be felt in the neck. Tapping in the supraclavicular area can elicit a sharp electric sensation shooting down the arm in the corresponding dermatomal distribution (positive Tinel's sign), indicating that there is at least one spinal nerve ruptured outside the spinal canal as opposed to intradural avulsion. Spared function in any muscle of the upper limb indicates one or more spinal root rupture or sparing.

On examination, in complete BP injury there is complete loss of motor and sensory function in the whole arm. Specific muscles can be examined to rule out remnant roots. Activity in the serratus anterior muscle, innervated by the long thoracic nerve, indicates the presence of one or more proximal stumps of ventral roots C5-C7. Activity in the clavicular part of pectoralis major indicates sparing or rupture of the upper part of the BP (C5-C7 via the lateral pectoral nerve). Activity in the supraspinatus muscle innervated by the suprascapular nerve indicates sparing of C5 +/- C6 ventral root. All sensory modalities should also be meticulously examined in all dermatomes involving the arm.

Clinical examination, however, cannot regularly distinguish between pre- and post-ganglionic injury. Electrophysiological assessment in the immediate posttraumatic period is of little value as typical denervation signs are evident 2 to 3 weeks following injury. Neurophysiological examination may demonstrate persisting conduction of afferent fibres after pre-ganglionic injury. Furthermore, these investigations are limited by the variation in the distribution of spinal nerves and the presence of more than one lesion, with both pre- and post- ganglionic involvement (Tavakkolizadeh et al. 2001).

The imaging of traction injuries to the adult BP also poses great challenges to the interested radiologist. The aim of imaging is to differentiate between central and peripheral intradural rupture. Myelography may demonstrate individual nerve roots or residual tufts of avulsed roots, a diverticulum at the level of the avulsed spinal, partial elongation of the root pouch with bleb formation or extradural collections. However, it is also associated with high rates of erroneous results. MRI is not an optimal method for visualizing the intraspinal BP, as it is limited by slice thickness, but is best used for visualization of extraspinal parts of the BP and to exclude spinal cord lesions.

The ‘gold standard’ diagnostic tool for root avulsion still remains direct intradural inspection of injured roots via a hemilaminectomy. Complete avulsions, partial avulsions and proximal intradural tears can be visualized. Concomitantly, the components of the BP can be ‘marked’ for subsequent BP repair.

1.6 Pathological processes following root avulsion

Injury at the CNS-PNS junction or proximal to this leads to profound pathological processes regarded as unfavourable to axonal regeneration.

1.6.1 Effects of root avulsion on non-neuronal tissue

Mechanical stress on the TR provokes a vigorous outgrowth of interweaving astrocytic processes and invasion of leptomeningeal cells surrounded by an expanded extracellular space containing numerous collagen fibres, phagocytic inflammatory cells and various extracellular molecules inhibitory to nerve regeneration forming a glial scar (Risling et al. 1993; Nomura et al. 2002). Various kinds of inhibiting factors that are upregulated around the lesion site have been postulated to prevent the regrowth of severed axons beyond the lesion site. Chondroitin sulfate proteoglycans (CSPG), a complex family of macromolecules secreted by almost all cell types at the injury site and especially astrocytes, are well known for their growth-inhibitory effects. They have been shown to induce neurite retraction and growth cone collapse. Other growth-repelling molecules include tenascin (McKeon et al. 1991), semaphorin 3A (Pasterkamp et al. 2001), myelin-associated molecules (Chen et al. 2000) and subtypes of the Eph receptors and their ligands ephrins (Bundesen et al. 2003). Failure of regeneration in the CNS has long been thought to be, in part, due to the development of this growth-inhibitory environment following injury and attempts to eliminate the molecules or neutralize

the inhibitory effect have been reported to enhance axonal regeneration in the damaged brain and spinal cord (Fawcett 1997).

1.6.2 Effects of root avulsion on nerve cells

Avulsion injury leads to rapid death of both primary sensory and motoneurons. Avulsion of ventral roots in experimental animals has demonstrated apoptosis in up to 50% of injured motoneurons within two weeks after the lesion, and further decrease with time to up to 90%. Apoptosis of motoneurones is thought to be due to disconnection from the periphery interrupting the supply of neurotrophic factor support together with vascular trauma (Wu 1993; Koliatsos et al. 1994; Novikov et al. 1995; Kishino et al. 1997; Piehl et al. 1998; Bergerot et al. 2004). Other mechanisms leading to motoneuron death such as inflammatory response to avulsion by means of microglial activation by cytokines have also been described (Olsson et al. 2000). The surviving motoneurons appear to enter a metabolic state with the primary goal being survival and production of new axons. This is reflected by an increase in mRNA expression of proteins linked with cell survival such as growth factors (e.g. brain-derived neurotrophic factor (BDNF)), growth factor receptors and proteins for axonal growth such as GAP-43 (Olsson et al. 2000).

Transection of the spinal nerve close to the DRG provokes apoptotic cell death of primary sensory neurons in the DRG (Hu et al. 2003). After avulsion, a significant increase in apoptotic cell death has been observed in the dorsal columns and dorsal horn of affected animals, which was significantly more than in rhizotomised animals

(Chew et al. 2008), suggesting that avulsion has more severe effects on cell survival than rhizotomy, probably due to the more central location of the lesion. The disappearance of sensory neurons triggers changes in connectivity leading to abnormal signaling (Mannion et al. 2000). This is believed to partly explain the pathophysiological mechanism of the classical neuropathic pain, which affects patients with BP avulsion injury. However, it has also been suggested that a primary sensory afferent injury is not necessary for the development of neuropathic pain, as allodynia and hyperalgesia has been observed after ventral root transection injury in the rat (Li et al. 2002; Sheth et al. 2002). The allodynia induced by ventral root avulsion has also been associated with a glial and inflammatory response in the dorsal gray matter and dorsal funiculus ipsilateral to the lesion (Bigbee et al. 2007). Although pain induced by ventral root avulsion alone is not yet well understood, it has been suggested that Wallerian degeneration of the lesioned efferent axons in mixed nerves causes release of degenerative by-products and subsequent changes in adjacent uninjured primary afferent fibres (Wu et al. 2002).

Furthermore, an increased and prolonged expression of c-fos, a proto-oncogene related to the family of transcription factors, after experimental root transection has been demonstrated in both motor and sensory neurons. Examination of human DRGs following root avulsion injury also showed significantly higher levels of GDNF, a growth factor to both sensory and motoneurones, in avulsed DRG neurons compared to control postmortem human DRGs and increased levels of Interleukin 6, a member of the neuropoietic cytokine family required for nerve regeneration (Bar et al. 1998). These substances may aid survival or have a role in nerve fibre sprouting and regrowth (Carlstedt 2008).

1.7 Regeneration across the ventral root following CNS injury

Observations of Ramon y Cajal in 1928, that severed motor axons after spinal cord injury have the capacity to regrow into neighbouring ventral roots, was reinvestigated by Aguayo and colleagues (Richardson et al. 1980; Aguayo et al. 1987) and confirmed with electron microscopy and intracellular labeling with horseradish peroxidase (Risling et al. 1983). In this experiment, the intramedullary portions of motor axons forming the L7 ventral root of the cat were divided through small longitudinal incisions in the ventral funiculus. During the first postoperative month increasing numbers of unmyelinated and thinly myelinated large-diameter axons coursed through the lesion and entered the denervated ventral root. It was also shown that at least some of the regenerating axons came from large neurons, presumably α-motoneurons in the ventral horn nuclei (Risling et al. 1983). This finding led to a series of experiments in search for factors influencing regeneration.

It was, subsequently, shown that after proximal lesions at the CNS-PNS interface followed by a major loss of motoneurons, a number of reactions occur in the severed cells, which are similar to those that take place after peripheral nerve lesions. Such processes include increased immunoreactivity for the low affinity neurotrophin receptor (p75) (Risling et al. 1992), mRNA for growth-associated protein GAF-43 (Linda et al. 1992), as well as increased immunoreactivity and mRNA for calcitonin gene related peptide (CGRP) (Piehl et al. 1998) and downregulation immunoreactivity and mRNA for the N-methyl-D-aspartate (NMDA) type of glutamate receptor (Piehl et al. 1995). Furthermore, a number of neurotrophic factors have been reported to have a beneficial effect on motoneuron survival and axon

outgrowth, the most important of which include BDNF (Koliatsos et al. 1993), NT-3 and NT-4 (Vejsada et al. 1995). Several other molecules with putative relevance to motoneuron survival and regeneration have been identified but will not be discussed here, as the list is exhaustive and beyond the scope of this background chapter.

With the background that spinal motoneurons are able to survive and generate new axons even after central lesions, it was suggested that motoneurons could be rescued by providing them a peripheral nerve conduit after ventral root avulsion. This could be achieved by re-implanting the avulsed ventral roots back into the spinal cord. Attempts of re-implantation of lumbar ventral roots supplying the hindleg muscles of the rat and cat demonstrated that motoneurons can project myelinated axons and reinnervate the re-implanted ventral root by intracellular recordings and staining with horseradish peroxidase (Carlstedt et al. 1986; Cullheim et al. 1989; Cullheim et al. 1999). These were also shown to possess apposing synaptic boutons, be activated by electrical stimulation of the re-implanted ventral root, fire action potentials secondary to the generation of an excitatory postsynaptic potential (EPSP) following nerve stimulation and cause isometric muscle twitches in the soleus and gastrognemius muscle. It was also demonstrated that the regenerating axon could travel via new roots through CNS tissue and away from the motor nucleus to the re-implanted ventral root for several hundred microns before reaching the PNS.

Re-implantation of the avulsed ventral root has been demonstrated to have both neurotrophic and neurotropic effects on lesioned motoneurons including, an increase in protection and survival of lesioned motoneurons and a stimulation of axonal regeneration into the implanted root (Hallin et al. 1999; Gu et al. 2004; Eggers et al.

2010). Eggers et al., (Eggers et al. 2010) performed unilateral avulsion and re-implantation of lumbar ventral roots L3, L4, and L5 and showed that re-implantation can prolong the survival of motoneurons up to one month post-lesion. The first regenerating motor axons enter the re-implanted ventral roots during the first week and large numbers of fibres gradually enter the lumbar plexus between 2 and 4 weeks, indicating that they enter the re-implanted roots and plexus over an extended period of time.

Furthermore, a single ventral root re-implantation has been shown to exert neurotropic effects in more than one spinal level in multilevel root avulsion (Hoang et al. 2006). A rostro-caudal gradient of this neurotropic effect has also been shown, with the greatest advantage for root reinnervation by axotomized neurons located at the closest proximity to the implantation site (Hoang et al. 2006).

The neurotropic cues, which may be provided by an implanted ventral root and may be responsible for the root reinnervation by both autonomic and motor neurons, are not fully understood. However, a variety of neurotrophic factors provided by the implant may potentially be able to promote the observed axonal regeneration. In Eggers et al., experiments (Eggers et al. 2010) motor axon counts showed that relatively few axons reach the distal sciatic nerve in the 16-week post-lesion period. The observed apparent spatio-temporal decline in the regenerative capacity of motor axons correlated with an observed initial increase and subsequent decline in expression of glial cell line-derived neurotrophic factor (GDNF) and BDNF.

Despite the beneficial effects of re-implantation, in the rat and cat, the ability of the motoneurons to find their original pathways to the muscles is poor, with a substantial degree of cross-innervation and probable functional consequences. Studies in primates provided evidence for a larger potential for plasticity. In the initial reinnervation phase, there was synkinesis of antagonistic muscles succeeded by adequate voluntary movement. Adequate movements were primarily observed in proximal muscle groups in the arm 2-3 months after corrective surgery but reinnervation of distal targets remained poor (Carlstedt et al. 1993; Hallin et al. 1999). It has been suggested that the distal nerve is losing its capacity to support regenerating motor axons following prolonged denervation.

Work has, therefore, concentrated in finding adjuvant strategies aiming at further improving and supporting the effects of re-implantation. A growing list of pharmacological agents and neurotrophic factors has been tested in rodent models of BP and cauda equina injuries. Proof for the neuroprotective effects of BDNF and GDNF has been demonstrated using a variety of delivery methods including intrathecal administration, application of gelfoam soaked with GDNF-containing solution and gene therapy approaches (Li et al. 1995; Novikov et al. 1997; Blits et al. 2004). In a more recent study, Riluzole, a drug used for the treatment of amyotrophic lateral sclerosis, has demonstrated a significant neuroprotective effect of motoneurons after a lumbar ventral root avulsion injury. The combination of GDNF and riluzole caused an augmented production of new processes in an already reduced population of motoneurons and drastically improved function in experimental animals (Bergerot et al. 2004). Other putative pharmacological candidates that have received extensive attention with promising effects on regeneration include

nimodipine, N-acetyl cysteine and minocycline hydrochloride (Havton et al. 2009).

Varieties of cell types and grafting platforms are also being studied because of their considerable potential for promoting axonal regeneration. Particular emphasis has been given to glial cells of the peripheral system such as Schwann cells (SCs) and olfactory ensheathing cells (OECs) due to their dual capacity for stimulating fibre growth, as well as, remyelination. Chapter 3 focuses on the properties of OEC to introduce the second experiment of this thesis. SCs are by far the most extensively studied cell type. SCs have neurotrophic, extracellular matrix and cell adhesion properties favourable to axonal regeneration in the peripheral nervous system. Numerous studies have demonstrated that peripheral nerve grafts can induce and support axonal regeneration over long distances from CNS neuronal populations (Bray et al. 1987; Li et al. 1994). Behavioural efficacy in chronic rodent spinal cord contusion models has also been reported (Takami et al. 2002; Barakat et al. 2005). In addition, a number of preclinical studies have demonstrated the ability of SCs to enhance the regeneration of sensory axons from the dorsal root ganglia as well as propriospinal axons adjacent to the injury site. These studies, however, also pointed out the limitations of SCs in that they do not permit axons that enter SCs grafts to exit and re-enter the host spinal cord. In addition, they provoke a more robust astrocytic reaction resulting in less effective integration into the host spinal cord. Lastly, although harvesting of SCs is relatively easy, it takes several weeks before enough cells can be generated for transplantation.

Neural stem/progenitor (NSPCs) cells are said to be precursors of neurons, astroglia and oligodendrocytes. They can be harvested from the subventricular zones of rodent

brain and spinal cord. Expressions of astrocytes, oligodendrocytes and neuronal markers have been observed to variable degrees, although they differentiate primarily into astroglial cells with some oligodendrocytes. Neuronal differentiation is rare (Karimi-Abdolrezaee et al. 2006; Parr et al. 2007). Behavioural improvements have been shown in contusion, compression and sharp lesion models of SCI, including acute primate cervical contusion model (Iwanami et al. 2005). Given the controversy over the use of human abortion material in most countries, the optimal source for NSPC for transplantation purposes is yet to be determined (Kachramanoglou et al. 2011).

Other potential candidates include neural and glial restricted precursors. Convincing behavioural improvements with glial precursors have only been demonstrated when used in conjunction with overexpression of a neurotrophin (Cao et al. 2005). Studies on these cells are limited, and the extent to which the observed benefits are related to myelination, neuroprotection or plasticity are still speculative. Harvesting from abortion materials meets the same ethical and practical issues to NSPCs (Kachramanoglou et al. 2011).

Furthermore, during the last one-half century, devices and systems have been developed that can apply electrical currents to neural tissues in a synchronized fashion for the purpose of restoring a degree of control over abnormal or absent body functions, a technique referred to as functional electrical stimulation (Ragnarsson 2008). To generate muscle contraction, the stimulus is generally applied to a peripheral nerve, anywhere along the length of the nerve from its origin to its motor point where it connects with the muscle. There is substantial scientific evidence that

shows that physical exercise of the paralysed body parts is of substantial clinical value and likely essential for maintenance of neural circuitry. It is thought that it reverse wasting, improve strength, endurance, and cardiovascular fitness; and may reduce the progression of osteoporosis (Creasey et al. 2004). In addition, there is evidence that shows that functional electrical stimulation not only stimulates production of endorphins, but contributes to the upregulation of BDNF, which may promote synaptic and functional plasticity within the brain and spinal cord (Vaynman et al. 2005). Significant achievements have been made in restoring limb function. Application of upper limb functional electrical stimulation systems is limited by the extent of LMN destruction within the injured cervical spinal cord. Useful hand grasp can be provided in C5 and C6 tetraplegia with preserved C7 and C8 neurological segments, reducing dependence on adapted equipment and assistants (Ragnarsson 2008).

1.8 Intraspinal implantation of ventral roots in humans (Brachial plexus re-implantation)

Encouraged by the findings of animal experiments, repair of avulsed roots was performed in humans following BP avulsion injury first by Carlstedt and colleagues (Carlstedt et al. 1995).

1.8.1 Operative technique of brachial plexus re-implantation in humans

The patient is placed in the lateral position with the affected side up and the head is held in a Mayfield clamp with the neck slightly flexed toward the unaffected side. The operating table is positioned head up to prevent venous congestion. A skin incision is made over the sternoclavicular joint and extended laterally and cranially into the posterior triangle of the neck, towards the C4 and C5 spinous processes. The spinal accessory nerve is identified and protected as it emerges from the dorsal aspect of the upper part of the sternocleidomastoid muscle. The BP is then identified and dissected. Occasionally, the ganglia and roots may have not been pulled out of the intervertebral foramina. They may be found in between the scalene muscles or further distally or may have even been pulled beneath the clavicle. Subsequently, the lateral masses of C5 - C7 and transverse process of T1 are approached between the levator scapulae and the posterior and medial scalenus muscles and the longissimus muscle is split longitudinally to approach the spine. The paravertebral muscles are dissected off the hemilaminae and C5 - C7 hemilaminectomy and medial facectomy is performed. The denticulate ligaments are cut and held by stay sutures and the spinal cord is, then, gently rotated to bring its ventrolateral aspect into view. The detached nerve roots are, subsequently, retrieved through the intervertebral foramina or through a small incision in the dura mater. Implantation of nerve rootlets is performed by making 2-3 mm longitudinal slits in the pia mater of the spinal cord as close as possible to the ventral root exit zone. The roots are positioned 1-2 mm deep to the pia mater in the spinal cord and the position retained using fibrin glue.

When the avulsed roots cannot be brought close enough to the spinal cord, a nerve graft is taken from the superficial radial nerve of the forearm. The graft is attached/

stitched distally to avulsed roots and proximally the nerve graft is separated into 2 or 3 fascicles and implanted into the spinal cord as described above.

Spinal cord monitoring is performed throughout the procedure to avoid an injury to the spinal cord particularly when tilted and during re-implantation of the roots.

1.8.2 Preliminary studies of functional recovery following BP re-implantation

The first human case BP re-implantation following avulsion injury was reported in 1995 (Carlstedt et al. 1995). This was a 25-year-old woman who presented with Horner's syndrome and paralysis of wrist and finger movements. In addition, there was weakness in the shoulder and elbow movements (C5-7). Sensory testing revealed normal sensation in the C6 dermatome, reduced sensation in the third finger and complete loss of sensation in the C8-T1 distribution. Open exploration of the BP revealed that there were a combination of supraganglionic rupture and avulsion injury of the C8 and T1 roots. The remainder of the roots of the BP were in continuity. The proximal ends of C8 and T1 ventral roots were reconnected to their corresponding spinal nerves via 7-8 cm long sural nerve grafts. Three years after, there was activity of the shoulder elbow and wrist, reduced flexion activity in the index finger but full power in the flexion of the three ulnar fingers. There was complete loss of power in the intrinsic muscles of the hand. Activity in the finger extensors and thumb was not reported at three years. Some activity was noted in the 18-month follow-up assessment in the finger extensors, except thumb. Electromyography showed reinnervation potentials in the flexor digitorum profundus, the ulnar wrist flexor and finger extensor muscles. Sensory activity was

reported normal in the median and radial nerve distribution but remained absent in the ulnar nerve distribution.

Subsequently, a case series of 10 cases was published (Carlstedt et al. 2000). This report included one female and seven male adult patients and two babies with obstetric injury to the BP. Two had complete BP avulsion injury, three patients had a mixture of ruptures and avulsions observed only when the dura was opened and one patient had pure ruptures of two ventral roots. The remainder four patients had incomplete injuries with avulsions of two roots supplying the BP. In one patient the dorsal roots were in continuity with the spinal cord whereas the ventral roots were avulsed. Repair was performed by re-implantation of nerve grafts apposed to two or three avulsed ventral roots. Assessment of neurological recovery was performed mainly by clinical examination. In some patients standard electromyography, central magnetic stimulation to assess muscle co-contractions and sensory function tests including thermal threshold, light touch threshold and axon reflex vasodilation were performed but only documented in illustrative cases. The first electrophysiological signs of reinnervation occurred 9 to 15 months of surgery with MRC Grade 1 power in relevant muscles. Useful function of MRC Grade 3 was reported in three patients. In 5 patients the best motor recovery was power of Grade 1-2.

A subsequent case study reported partial recovery of hand function in a pre-adolescent boy who underwent re-implantation surgery for complete BP avulsion injury (Carlstedt et al. 2004). Nerve grafts were connected distally to the upper, middle and lower trunks of the BP. Re-implantation was performed in combination with nerve transfers; the accessory nerve was transferred to the suprascapular nerve,

a cervical plexus motor branch was transferred to the upper trunk and supraclavicular sensory nerves were joined to the sensory parts of the C7, C8 and T1 spinal nerves. Proximal muscle group recovery started 8-10 months after surgery. At two years after surgery there was normal power (Grade 5/5) serratus anterior muscle, Grade 4/5 in the deltoid, biceps and forearm muscles, wrist and finger flexors, Grade 2/5 in the triceps and intrinsic muscles of the hand, but no clinical function in the wrist or finger extensors.

Other interesting observations made in studies of BP re-implantation in humans include the finding of greatest motor recovery in patients in whom surgery was performed within 1 month after injury (Carlstedt et al. 2000; Htut et al. 2007) and co-contractions between antagonistic muscles (for example biceps-triceps), which compromised function but reduced with time (Carlstedt et al. 2000). In addition, re-implantation has been shown to have effects on sensory function with return of sensation in the avulsed dermatomes (Carlstedt et al. 2000) and improvement in the intractable neuropathic pain associated with root avulsion injury (Carlstedt et al. 2000; Carlstedt et al. 2004). Interestingly, pain relief has been reported to precede restoration of muscle function (Berman et al. 1998; Kato et al. 2006). The mechanism of pain improvement in these patients is currently uncertain but it has been suggested that it may be due to recovery or regeneration of proprioceptors in reinnervated muscles, which inhibit pain transmission in the dorsal columns (Htut et al. 2007).

In the above studies, re-implantation was thought to be responsible for the functional recovery observed. However, the above studies are descriptive and lack objective

methods of assessment of neurological recovery, a comparison group and homogeneity in subjects' injury. In addition, the study of patients with incomplete BP injuries and the well-established fact that there is significant variation in the segmental innervation of individual muscles raises the question whether recovery of function could be due to reinnervation from uninjured spinal roots.

1.9 Assessment of clinical recovery and regeneration

1.9.1 Principles of Needle electromyography

The degree of injury involvement and reinnervation in a given muscle can be investigated by means of electromyography (EMG) techniques, aiming at the estimation of parameters of a motor unit action potential. The motor unit consists of an anterior horn cell, its axon, and all the muscle fibres innervated by that axon and its branches. The motor unit action potential (MUAP) is the electrical field generated by the voluntary contraction of muscle fibres belonging to one motor unit as recorded by the tip of a nearby needle electrode. An MUAP is characterized by its amplitude, duration, shape, rate of firing and number of phases. The amplitude of an MUAP is proportional to the number of muscle fibers that contract with activation of a motor neuron. The duration reveals the synchrony of firing of the muscle fibres. Under normal circumstances, muscle fibers belonging to one motor unit are all depolarized and repolarized somewhat synchronously and their MUAP has a di- or tri-phasic configuration.

Neurological recovery after transection of a nerve occurs in two forms: true axonal regeneration and the reinnervation of denervated muscle fibres by terminal collateral sprouting. Both processes show abnormal electrical configurations of increased polyphasicity, as reinnervation takes place from regenerating or sprouting axons that reach the muscle through the distal nerve stump at scattered time intervals. Two types of polyphasic potentials can form following axonal degeneration: (1) nascent potentials and (2) motor units formed from terminal collateral sprouting:

For true axonal regeneration to occur, there must be an intact anterior horn cell and an intact endoneurial tube. The axon distal to the site of injury undergoes Wallerian degeneration. The proximal axon forms a bud that begins to regenerate distally through the endoneurial tube toward the denervated muscle. This process occurs at a rate of 3–4 mm/day so axonal regeneration is length-dependent. New axons reach muscle fibres that have been denervated for varying times and belonged to different motor unit. MUAPs from such motor units are called "nascent" potentials of small amplitude (100-200 μv), short duration (3 - 5 ms), and polyphasic. With continuing maturation of the motor unit, nascent units become of longer duration, higher amplitude and less polyphasic. Eventually, they may reach normal size for the muscle being examined.

With collateral sprouting from undamaged adjacent axons, more muscle fibres are activated by the stimulation of one motor unit, resulting in high amplitude, short duration MUAPs (Lee et al. 2004).

In chronic denervation processes, surviving nerve fibres increase their motor unit territory and fibre density, producing high amplitude, long duration MUAPs. The duration is prolonged because there are more fibres to depolarise, and the increase in the number of phases is due to the lack of synchronization between the host and newly acquired fibres.

Neurological recovery is also dependent on healthy viable muscle tissue. This is necessary for the release of nerve growth factors from denervated muscle. These factors act as a catalyst to stimulate the axon to regenerate. If the denervated muscle becomes fibrotic, these factors may no longer be released. Muscle tissue must also remain viable and electrically active if a regenerating axon is going to establish a connection with a functional neuromuscular junction. Chronically denervated muscle will eventually become fibrotic and electrically inactive. This usually happens somewhere between 18 and 24 months. In myopathy, the motor unit territory and fiber density decrease because of the muscle fiber degeneration, producing small amplitude, short duration MUAPs (Lee et al. 2004).

Furthermore, observations at rest can provide further information. *Insertional activity* is the electrical response of muscle membrane to insertion of the EMG needle. Increased insertion activity, or persistent abnormal spontaneous electrical activity, is secondary to a hyperexcitable muscle membrane. Several abnormal spontaneous potentials beyond the cessation of needle insertion, including fibrillations (low amplitude, short biphasic or triphasic potentials), positive sharp waves (PSWs) (positive deflections followed by a prolonged negative wave), and fasciculations are observed with denervation within 2-3 weeks (Lee et al. 2004).

Moreover, the rate and pattern of MUAP firing or *recruitment* can also assist in evaluating disease processes. With increasing effort of contraction, the firing frequency of individual motor units increases and progressively more and larger unit are activated in normal subjects. Reduced recruitment occurs whenever a lesion results in a reduced number of functionally intact motoneurons and axons. In myopathy, the muscle fibre content of each motor unit is reduced and the number of motor units required to maintain a given force increases. This recruitment pattern is called "early or increased recruitment".

The recruitment pattern at maximal voluntary contraction is called "interference *pattern*" due to the increasing degree of superimposition of action potentials from different units. Reduced interference pattern signifies a decreased number of MUAPs being activated and is suggestive of a neurogenic lesion.

1.9.2 Principles of nerve conduction studies

The propagation of action potentials along a nerve can be recorded by using surface electrodes. A recording from a mixed nerve is referred as compound nerve action potential (CNAP). Recordings from a pure sensory nerve is referred to as sensory nerve action potentials (SNAP), whereas when motor nerves are stimulated recordings are called compound muscle action potential (CMAP). Typically SNAPs and CNAPs are measured by stimulating a peripheral nerve and recording the response a known distance away (Robinson 2000). They both are characterized by

two measures: (1) speed of conduction (latency or velocity) and (2) amplitude of response. The latency and velocity conduction is affected by temperature in normal healthy subjects and are slowed in pathological conditions involving loss of axons or demyelination. Distal lesions between the sites of stimulation and recording will decrease the amplitude of CNAP immediately, as conduction cannot traverse the lesion. Proximal lesions, such as in the BP, that separate sensory axons from their cell bodies in the DRGs, will show reduced-amplitude SNAP (Robinson 2000).

To evaluate conduction velocity along a motor nerve, motor nerves are stimulated at two places the distance between the two stimulation sites is divided by the difference in latency to cancel out the conduction time across the neuromuscular junction and muscle depolarisation. The amplitude of the response is diminished by defects of the neuromuscular junction or loss of anterior horn cells. A root lesion proximal to the DRG would diminish the amplitude of CMAP but not that of SNAP.

The F-wave is an electrophysiological artefact produced by antidromic activation of motoneurons following distal electrical stimulation of motor nerve fibres. F-waves are commonly recorded using surface electrodes from hand muscles (abductor pollicis brevis and abductor digiti minimi). Because F-waves traverse the entire length of a peripheral nerve between the spinal cord and muscle, F-waves provide a means of examining transmission between stimulation sites in the arm and the related motoneurons in the cervical cord. Because a different population of anterior horn cells is stimulated with each stimulation, each F wave has a slightly different shape, amplitude and latency. The latency of the F-wave (typically 25-32 ms in the upper extremities and 45-56 ms in the lower extremities) is the most commonly used

parameter for assessing the F-wave and reflects the conduction time between the site of the stimulation of the peripheral nerve and the spinal cord for reactivation of the motoneurons.

1.9.3 Sympathetic skin response

The sympathetic skin response (SSR) is defined as a momentary change of the electrical potential of the skin and provides a non-invasive approach to investigate the function of the sympathetic system. It reflects sympathetic cholinergic sudomotor function, which induces changes in skin resistance to electrical conduction. It is a result of polysynaptic reflex arch activation. The efferent part of the SSR reflex arch consists of myelinated sympathetic fibres of neurons from intermediolateral nucleus in T1-L2 part of the spinal cord that terminate in paravertebral sympathetic ganglia. Postganglionic fibres are nonmyelinated (type C) and innervated eccrine sweat glands (Vetrugno et al. 2003). The central part of the reflex arch presumed to be polysynaptic with a connection to the structures of hypothalamus, ventrolateral part of the brainstem, medial and basal parts of the frontal lobe and medial part of the temporal lobe (Vetrugno et al. 2003).

Response is most often biphasic in the hands with negative and positive phases. Although its use remains controversial, SSR can assist the localization of the lesion to the effector glands or nerve fibers. However, an abnormal SSR can result from abnormal autonomic efferents but also from atrophy of effector sweat glands after chronic denervation and from altered perception (afferent sensory fibers of the arc)

and therefore, simultaneous nerve conduction studies are required for interpretation of findings.

1.10 Hypothesis Formulation

The following chapter of this thesis was designed to investigate the long-term effects of a homogeneous group of patients with complete BP injury with objective experimental methods. To that end, neurophysiological tests and standardised patient-reported outcome measures as well as clinical examination were utilized to investigate these effects. Correlations of functional recovery with factors that may affect recovery were also examined to determine their contribution to functional outcomes. The central hypothesis of the following chapter is that patients with BP re-implantation after complete BP injury will demonstrate better functional recovery in clinical examination and evidence of regeneration in neurophysiological experiments compared to patients without re-implantation. With that bigger framework in mind and in view of the existing literature presented in this introduction we expect to find the following:

a) An improved functional recovery in patients with re-implantation compared to patients with complete BP injury but without surgical repair.
b) An improved functional recovery in proximal muscles compared to more distal musculature.
c) Electrophysiological evidence of reinnervation in muscle supplied by re-implanted ventral roots.

Chapter 2

The long-term outcome of brachial plexus re-implantation following complete brachial plexus avulsion injury

2.1 Introduction

This chapter presents a prospective observational study aiming at revealing the functional recovery of the affected arm in patients that have undergone BP re-implantation surgery after complete BP avulsion injury. The motor and sensory function of patients who have had re-implantation surgery are assessed with clinical, neurophysiological and patient reported outcome measures and compared to patients who were treated conservatively for their injury.

2.2 Aims and objectives:

The aims of this chapter are twofold. The first aim is to explore the clinical, neurophysiological and patient reported recovery in the patients following complete BP avulsion injury and re-implantation surgery. The second aim is demonstrate whether there is a difference in functional recovery between patients who had had re-implantation surgery and patients with complete BP avulsion injury but without re-implantation of ventral roots.

2.3 Methods

2.3.1 Patients

Potential patients were identified via evidence of BP re-implantation procedure in the surgical books and a log provided by the surgeons. To the date of data collection

for this study (2010), twenty-five patients who have had re-implantation surgery (re-implantation group) after complete BP avulsion and sixteen patients with complete BP avulsion injury who have had no surgical intervention (control group) were identified for participation in our study. The remaining patients were not assessed for one of the following reasons: (a) had been lost to follow up, (b) patients declined participation, (c) have had amputation of the affected arm or, (e) had associated lower limb weakness.

Of the above, 15 patients in the re-implantation group and 7 patients in the control group were included in the study. All 15 patients in the re-implantation group underwent BP re-implantation surgery at the National hospital for Neurology and Neurosurgery, London. Initially, hospital records were inspected for evidence of a completely paralyzed arm, complete loss of sensation from C5-T1, evidence of Tinel's sign and Horner's syndrome at presentation. Subsequently, the operation record of the exploration procedure was then inspected for evidence of complete BP injury. Diagnosis was also correlated with findings of other available investigations, including preoperative CT myelography, MRI and electrophysiological studies. Patients with evidence of brain or spinal cord injury on preoperative MRI, root rupture during the exploration procedure and any electrophysiological response in perioperative electrophysiological studies were excluded. Only patients with traumatic BP injury were included.

Seven patients with clinical, electrophysiological and perioperative evidence (as per the re-implantation group) of complete BP supraganglionic avulsion injury who did not undergo re-implantation surgery were recruited as control patients. One patient

had undergone nerve transfers for repair of the accessory nerve to the suprascapular nerve and 4^{th} and 5^{th} intercostal nerves to the musculocutaneous nerve.

2.3.2 Motor and sensory clinical assessment

All patients were assessed clinically based on the Medical Research Council (MRC) to estimate limb and axial muscle strength. A summated muscle score based on the MRC clinical scale was also used to assess global power in the affected arm ("global MRC score"). This was obtained the following way: on the affected side, seven selected upper limb muscles or muscle groups were tested and scored from 0 to 5 according to the MRC muscle strength scale. Muscles included are the deltoid (C5-6)/ supraspinatous (C4-6), infraspinatous (C5-6), pectoralis (C5-6), biceps brachii (C5-6), triceps (C6-C8), for wrist movements extensor carpi radialis (C5-6) and ulnaris (C7-8)/ flexor carpi radialis (C6-7) and ulnaris (C7-8, T1) and finger movements flexor digitorum superficialis (C7-8, T1) and profundus (C7-8, T1)/ flexor digiti minimi (C7-8, T1)/ flexor pollicis (C8-T1)/ extensor digitorum (C7-8)/extensor indicis (C7-8)/extensor pollicis brevis (C8-T1) and longus (C7-8, T1) interossei (C8-T1). The segmental muscle innervation was based on MRC UK memorandum (MedicalResearchCouncil 1976). Modifications to the MRC scale add either a minus or a plus to the score. For example, 4- represents a muscle that is slightly weaker than one with a score of 4 and equals to 3.5. MRC scores for each muscle/muscle groups were added to obtain the "global MRC score", which has a range from 0 to 35. In addition, the presence of Horner's syndrome was documented and Tinel's sign was tested.

2.3.3 Sensory examination

All patients underwent sensory testing, which included: (a) light touch using cotton wool and (b) pinprick with blunt pin. The sites of testing followed the dermatomes based on the MRC UK memorandum (MedicalResearchCouncil 1976). These were recorded as being either normal or altered. (c) Vibration sense using a 128 Hz tuning fork and (d) proprioception and (c) cold temperature sense by touching. These were tested clinically at the shoulder, elbow and wrist. Examination was performed with their eyes closed. The unaffected arm was examined first.

If a patient reported referred sensations, defined as sensations that are perceived to emanate from the other areas of the body than the body part being stimulated, a more detailed examination was conducted and patients were asked to describe the sensation and location perceived to the best of their ability. Perceived sensations were drawn on a schematic diagram of the arm. Patients were told that the sensitivity of the upper arm was assessed and were not informed of the possibility of experiencing abnormal or referred sensations. Similarly, when patients reported an insensate area within a dermatome, a more careful examination was performed in an attempt to localize the insensate region. This was, also, drawn on a schematic diagram of the arm. Lastly, observations of allodynia were also recorded, defined as pain caused by stimuli that were non-noxious in the intact contralateral limb or normal subjects.

2.3.4 Electrophysiological assessment

Neurophysiological studies were performed in all 7 of control patients and 13 out of the 15 patients (86.6%) who have had re-implantation surgery. The remainder two of the re-implantation patients refused or did not turn up for their appointment. The neurophysiological examination was performed in all patients by an experienced EMG neurophysiologist (M.K.), who was blinded to the status of the patients.

All neurophysiological tests were performed using a Viking™ NCS, EMG, EP, IOM System (CareFusion, San Diego, CA, USA; Version 12) and stimulator Digitimer DS5 (Digitimer, Welwyn Garden City, UK).

2.3.4.1 Motor nerve conduction studies

The median and ulnar nerve motor conduction data were determined using surface electrodes for stimulation at the elbow and proximal to the wrist and for recording over the abductor pollicis brevis muscle (APB) and over the abductor digiti minimi muscle (ADM). For each nerve, the following conduction data were recorded: distal motor latency (DML), conduction velocity, amplitude and F-wave latency stimulated at the wrist.

2.3.4.2 Sensory nerve conduction studies

Sensory conduction velocity (SCV) of the median, ulnar and radial nerves were assessed. SCV of the median nerve was determined orthodromically from (a) the second finger, (b) the third finger and (c) palm to the wrist. The SCV of the ulnar nerve was tested from (a) the fifth finger and (b) the palm to the wrist and the SCV of the radial nerve was tested from the forearm to the wrist.

2.3.4.3 Electromyography

Needle electromyography (EMG) was performed with TECA® Elite Disposable Concentric Needle Electrode (37 mm, 26G; CareFusion, Middleton, WI, USA) and conventional EMG recorder, Viking Select EMG machine (CareFusion, San Diego, CA, USA; Version 12). EMG was attempted in the following muscles: deltoid, biceps, triceps, infraspinatous, first dorsal interosseous (DFIO), flexor digitorum superficialis (FDS), extensor digitorum communis (EDC). After needle insertion, pathologic spontaneous activity, shown as fibrillation potentials and positive sharp waves (PSW) were first determined. These were rated as "0" no fibrillation potentials/PSWs, "+1", "+2" and "+3" with increasing severity. The patient was then asked to contract the muscle of interest to assess the presence of motor unit action potentials (MUAPs) under voluntary control and if present these were recorded. The duration, amplitude, degree of polyphasicity, recruitment and interference patterns were studied. The grading of muscle reinnervation was based on the configuration of the MUAPs. Reinnervation was graded as follows: "0" No recorded MUAPs; "1" MUAPs of increased duration/reduced amplitude/increased polyphasicity; "2"

MUAPs of increased duration/increased amplitude/increased polyphasicity; "3" MUAPs of increased duration/normal amplitude/minimal polyphasicity; "4" MUAPs of minimally increased duration and amplitude/no polyphasicity. Assessment of recruitment was made at minimal muscle contraction to determine the recruitment pattern and at maximal voluntary contraction to assess the interference pattern.

2.3.4.4 Sympathetic skin response

In addition, the sympathetic skin response (SSR) latency was determined using standard surface silver (Ag-Ag-Cl) electrodes stimulating the median nerve on the palm of the affected arm. Single square-wave electrical stimulus with intensity of 10-30 mA and duration of 0.1 - 0.5 ms was applied.

2.3.5 Outcome measures

To gain an insight into the way patients perceive their health and the impact of their disability to their quality of life, four validated patient-reported outcome measures (PROMs) were given to the patient to complete prior to their examination. Patients completed these questionnaires without any help or explanation of the questions. The validated patient-reported outcome measures used are described below:

Firstly, the visual analogue scale (VAS) was used to assess the severity of pain in BP avulsion injury patients. The VAS scale consists of a 10-cm line anchored by 2 extremes of pain, with zero representing "no pain" and 10 representing ''worst imaginable pain''. Pain was defined as every form of pain in the hand (Appendix 1).

Secondly, to assess the global function of the arm, the Disabilities of the Arm, Shoulder and Hand (DASH) questionnaire was used (Appendix 2). The DASH is a self-administered outcome instrument focused on musculoskeletal disorders of the upper extremity. It emphasizes physical function but also includes questions on social and emotional function. It consists of 30 items measuring the degree of difficulty a person has in performing various daily activities including the severity of pain symptoms, activity-related pain, tingling, weakness and stiffness (five items), and the effect of the condition on social activities (one item), work (one item), sleep (one item), and self-image (one item), measured on a 5-point Likert scale (1 to 5). The scores of all items are added to calculate a DASH score ranging from 0 to 100. Higher DASH scores reflect greater disability. The DASH questionnaire also contains two optional modules concerning the patient's ability to practice a sport or a musical instrument and to work. For each module, four items ask about the patient's physical ability to perform the activity (Beaton et al. 2001).

Secondly, the Michigan Hand Outcomes Questionnaire (MHQ) which measures a person's perception of their hands in terms of function, appearance, pain, and satisfaction (Appendix 3). It consists of 37 items on six subscales: (1) overall hand function, (2) activities of daily living, (3) pain, (4) work performance, (5) aesthetics, and (6) patient satisfaction with hand function. Items are scored on a 5-point Likert scale from 1 (very good/not at all difficult/always/ very mild/very satisfied) to 5 (very poor/very difficult/ never/severe/very dissatisfied). Raw scores are converted to a scale from 0 - 100 according to a scoring algorithm. Ranges for subscales are: hand function (5 - 25), unilateral ADL (5 - 25), bilateral ADL (7 - 35), work (5 - 25),

pain (0 - 24), aesthetics (4 - 20), and satisfaction (6 - 30). Higher scores indicate better performance in all domains except pain (Chung et al. 1998; Chung et al. 1999).

Lastly, the SF-36, a generic, multi-purpose, short-form health survey comparing the relative burden of diseases, and in differentiating the health benefits produced by a wide range of different treatments (Appendix 4). It consists of 36 items and yields an 8-scale profile of functional health and well-being scores as well as psychometrically-based physical and mental health summary measures and a preference-based health utility index (Ware et al. 1992).

2.3.6 Statistical analysis

All statistical analysis was performed using STATA statistical software Version 11 (StataCorp LP, College Station, TX). A Wilcoxon-Mann-Whitney test (z) was used to compare parameters after testing for normality. A Spearman's rank correlation coefficient (rho) was used to test for statistical correlations between two continuous variables. Statistical significance was accepted at the 5% level ($p < 0.05$), unless otherwise stated.

2.4 Results

2.4.1 Description of patients

Of the seven control patients included in the study, five were men and two women. All patients sustained their injury in motor vehicle accidents. Their average age was 43 years (sd; 8.8 years of age, range; 28-57 year of age). All control patients were right-handed from birth. Three injured their right arm (57.14%) and four injured their left (42.86%). The median period from the day of injury to assessment for this study was 156 months (sd; 95.5, range; 74-338 months). The mean of days from injury to exploration was 205 days (sd; 173.81, range 48-483 days).

All 15 patients in the re-implantation group were men with a mean age of 32 years (sd; 9.71 range; 18-48 year of age). Thirteen re-implantation patients were natively right-handed (86.67%) and two were left-handed (13.33%). Of the 13 right-handed, five injured their right arm (38%) and eight injured the left (62%). Both natively left-handed patients injured the left arm (100%).

The median period from injury to exploration was 11.9 days (sd; 8.95, range; 1-33 days). The mean period from the day of injury to the day of re-implantation was 33.3 days (sd; 30.29 days, range 4 - 138 days). Re-implantation surgery took place within 40 days from injury in all patients, except in one patient who was not fit for surgery immediately and was operated 138 days after his injury. All patients had re-implantation of roots C5, C6 and C7 via grafts obtained from the superficial radial or medial cutaneous nerve of the ipsilateral forearm as described in section 1.8.1. All patients had their avulsed dorsal roots trimmed distally to the level of a normal

looking dorsal root or the to the junction with the ventral root. The median period from the day of injury to assessment for this study was 60.6 months (sd; 50.3, range; 10-155 months).

Three out of the seven control patients (42%) analgesics and nine out of 15 re-implantation patients (60%) were on analgesic treatment consisting of different combinations of oral morphine, pregabalin, amitryptyline and Diclofenac®. All subjects of both groups not taking analgesics mentioned they had stopped taking analgesics because they suffered their side effects without pain control.

2.4.2 Clinical assessment of motor function

MRC scores are summarised in Table 2.1 and 2.2. In summary, of the seven control patients, two (28.6%) had movement in the deltoid muscle, 0 in the pectoralis muscle, one (14.3%) in the infraspinatous muscle, three (42.8%) in the biceps, two (28.6%) in the triceps and none showed wrist or finger movement. Of the 15 patients in the re-implantation group, movement was noted in 12 (80%), 10 (66.6%), 10 (66.6%), in the deltoid muscle, pectoralis muscle and infraspinatous muscle respectively and 9 (60%), 9 (60%), 1 (6.6%), 2 (13.3%) in biceps muscle, triceps muscle, wrist and finger movement respectively. No co-activation of antagonistic muscle function or co-contractions was observed.

A two-sample Wilcoxon rank-sum test revealed a statistically significant difference in deltoid ($z = -2.19$, $p = 0.028$), pectoralis ($z = -2.72$, $p = 0.007$) and infraspinatous power ($z = -2.09$, $p = 0.037$) between the control and re-implantation groups. There

was no difference between the two groups in the power of the biceps (z = -0.30, p = 0.764), triceps (z = -1.185, p = 0.236), wrist movements (z = -0.68, p = 0.494) or finger movements (z = -0.98, p = 0.323). The group mean "global MRC score" of the control group was 2.57 (sd; 3.26, range; 0-7) and significantly lower (z = -2.17, p = 0.03) then that of the re-implantation group estimated at 6.93 (sd; 4.79, range 0-14).

Table 2.1: *Results of motor examination of the affected arm; values reflect MRC grades.*

Patient	Trapezius	Deltoid	Pectoralis	Infraspinatous	Biceps	Triceps	Wrist movements	Finger movements	Global MRC score (out of 35)
Control 1	5	2	0	0	1	3	0	0	6
Control 2	5	0	0	2	2.5	0	0	0	5
Control 3	0	0	0	0	0	0	0	0	0
Control 4	4	0	0	0	0	0	0	0	0
Control 5	5	1	0	0	3.5	1	0	0	6
Control 6	5	0	0	0	0	0	0	0	0
Control 7	0	0	0	0	0	0	0	0	0
Reimplant 1	3	2	1	0	4	3	0	0	10
Reimplant 2	5	1	1	1	0	1	0	0	4
Reimplant 3	5	0	0	0	0	0	0	0	0
Reimplant 4	4	0	0	0	0	0	0	0	0
Reimplant 5	5	4	3	3	1	3	0	0	14
Reimplant 6	4	4	3	1	1	1	0	0	10
Reimplant 7	4	3	2	1	2	1	0	0	9
Reimplant 8	4	2	2	1	1	0	0	2	8
Reimplant 9	4	0	0	1	1	1	0	0	3
Reimplant 10	5	1	1	3	0	0	1	3	9
Reimplant 11	5	3	3	3	2	3	0	0	13
Reimplant 12	4	1	0	0	0	1	0	0	2
Reimplant 13	5	1	0	0	0	0	0	0	1
Reimplant 14	5	2	3	4	2	0	0	0	11
Reimplant 15	5	1	3	3	1	2	0	0	10

Table 2.2: *Mean MRC scores, SD and range for each muscle group tested.*

	Control group			Re-implantation group		
	Mean	**SD**	**Range**	**Mean**	**SD**	**Range**
Trapezius	3.43	2.37	0-5	4.46	0.64	3-5
Deltoid	0.57	0.96	0-2	1.73	1.28	0-4
Pectoralis	0	0	0-0	1.46	1.30	0-3
Infraspinatous	0.29	0.76	0-2	1.40	1.40	0-4
Biceps	1	1.44	0-3.5	1.00	1.13	0-4
Triceps	0.57	1.13	0-3	1.07	1.16	0-3
Wrist movement	0	0	0-0	0.07	0.26	0-1
Finger movement	0	0	0-0	0.33	0.90	0-3

2.4.3 Clinical assessment of sensory recovery

2.4.3.1 Dermatomal distribution

Of the seven control patients, four (57%) reported altered or reduced light touch sensation in the distribution of the C5 root, two (28%) in the C6, C7, and C8 dermatome and one in T1 distribution. On examination of pinprick sensation, three (43%) perceived sensation in the C5 territory, two (28%) in C6 and C7 distribution, one in C8 and another in T1. Horner's syndrome was present in four out of seven control patients (57 %) and six out of 15 re-implantation patients (40 %).

Of the 15 patients in the re-implantation group, 14 (93%) reported light touch and 13 (87%) pinprick in the C5 distribution. Eight (53%) had light touch sensation and seven (47%) pinprick in the C6 territory. In C7 distribution, only two (13%) reported light touch and one (7%) reported pinprick. One patient (7%) reported sensation in the C8 territory in both pinprick and light touch and eight out of 15 (53%) patients had sensation in the T1 distribution in light touch and seven (47%) in pinprick.

Reduced temperature sensation was perceived in the region of the shoulder in four controls and 13 re-implantation patients, at the elbow two controls and seven re-implantation subjects, and none at the wrist from either group.

A two-sample Wilcoxon rank-sum test revealed a statistically significant difference between the two groups in the frequency of patients with recovery in soft touch and pinprick sensation in the C5 dermatome ($z = -2.003$, $p = 0.045$ and $z = -2.100$, $p = 0.036$ for soft touch and pinprick sensation respectively). Recovery of soft touch or pinprick sensation in the remainder of dermatomes was not found to be statistically different (Table 2.3). There was no significant difference in the number of patients with temperature sensation in the shoulder or wrist. However, a two-sample Wilcoxon rank-sum test showed a statistically significant difference in the frequency of patients with temperature sensation in the region of the elbow (Table 2.3).

Vibration was perceived at the shoulder in 4 controls and 12 re-implantation patients, at the elbow in 1 control and 3 re-implantation patients, and at the wrist in one control and two re-implantation patients. Proprioception was accurate at the shoulder in four controls and 13 re-implantation patients, at the elbow in two controls but seven re-implantation patients and at the wrist none in either patient group. There was no difference between groups in the number of patients perceiving proprioception or vibration sense at the shoulder, elbow or wrist.

Table 2.3: Mann-Whitney z-scores and p values comparing the frequency of patients with return of sensory modalities tested between the two groups of patients. Asterisk (*) denotes statistical significance ($p < 0.05$). Chi^2 statistic and p values comparing the frequency of normal sensation for each dermatome and modality between groups.

Soft touch	**z-score**	**p value**	**Chi^2**	**p value**
C5	-2.003*	0.0452*	0.66	0.045
C6	-1.342	0.1797		1.66
C7	0.843	0.3991	-	-
C8	1.362	0.1731	0.35	0.55
T1	-1.695	0.0900	0.74	0.39
Pinprick	**z-score**	**P value**		
C5	-2.100*	0.0358*	3.3	0.036
C6	-0.856	0.3918	2.22	0.14
C7	1.362	0.1731	-	-
C8	1.362	0.1731	-	-
T1	-1.437	0.1508	1.66	0.19
Proprioception	**z-score**	**P value**		
Shoulder	-1.504	0.1327	3.3	0.07
Elbow	-0.786	0.4321	0.74	0.78
Wrist	-	-	0.74	0.39
Vibration	**z-score**	**P value**		
Shoulder	-1.095	0.2733	0.29	1.11
Elbow	-0.316	0.7518	-	-
Wrist	-0.990	0.3222	0.55	0.35
Temperature	**z-score**	**P value**		
Shoulder	-1.36	0.173	0.74	0.39
Elbow	-2.139*	0.0325*	3.59	0.11
Wrist	-0.990	0.3222	0.74	0.39

Furthermore, in the re-implantation group, dermatomes were not entirely innervated but often there were insensate patches within one dermatome (Table 2.4). Two patients described insensate patches in the lateral aspect of the upper arm. Another two patients reported an abrupt end of sensation at the level of the elbow and one midway the forearm but with some reduced sensation in anterior lateral aspect of the wrist.

2.4.3.2 Abnormal sensations

2.4.3.2.1 Tinel's sign

Tinel's sign on percussion in the region of the nerve roots at the base of the neck was present in four patients with re-implantation but no control patients. In all four re-implantation patients percussion over the region of the nerve roots provoked paraesthesia (pins and needles) in the whole upper arm and forearm. In addition, paraesthesia was also elicited in the dorsal central aspect of the hand in one patient and in another subject in the thumb.

2.4.3.2.2 Referred sensations

Two patients of the re-implantation group described perception of sensations in remote locations not stimulated (Table 2.4 and Figure 2.1). Specifically, one patient perceived sensation in the little finger (C8 distribution) on testing sensation at the thumb (C6) and medial aspect of the forearm (T1 dermatome). In addition, the same patient reported sensation in the thumb on stimulating at the base of the neck (C4 dermatome) and at the lateral aspect of the upper arm (C5 dermatome). A different

patient reported sensation in the medial aspect of axilla (T2) on stimulating the medial forearm (T1). Another patient reported pins and needles in the lateral aspect of the elbow on testing soft touch of C5 distribution with a cotton wool away from the region felt.

1) 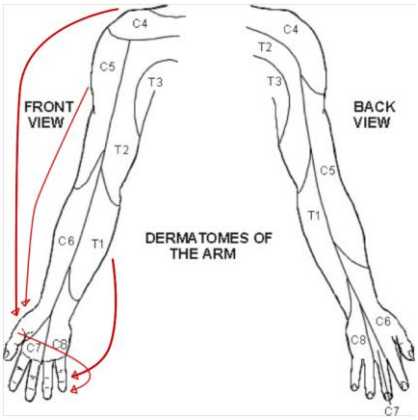

2) 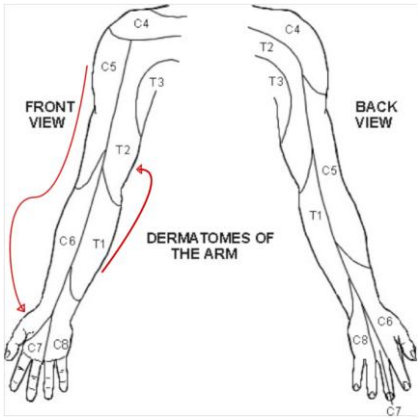

Figure 2.1: Schematic representation of referred sensation in two patients. 1.) Sensation in the thumb and index finger on stimulating at the lateral aspect of the upper arm and sensation in T2 distribution on stimulating at the medial forearm; 2) Sensation in little finger when touching the thumb, sensation in little finger when inner aspect of forearm, sensation in the thumb on stimulating at C4 distribution and sensation in the thumb on stimulating at C5 distribution.

2.4.3.2.3 Allodynia

One control patient reported hypersensitivity in what was assumed to be the T1/T2 border on light touch examination. Two re-implantation patients reported hyperesthesia in the C5 territory on soft touch and pinprick testing.

Table 2.4: Results of sensory examination

PATIENT	LIGHT TOUCH						PIN PRICK					
	C4	**C5**	**C6**	**C7**	**C8**	**T1**	**C4**	**C5**	**C6**	**C7**	**C8**	**T1**
Control 1	N	A	A	A	A	A[1]	N	A	A/R	A	A	A
Control 2	X	↓	X	X	X	X	↓	X	X	X	X	X
Control 3	N	X	↓	↓	N	X	N	X	↓	↓	N	X
Control 4	X	X	X	X	X	X	X	X	X	X	X	X
Control 5	N	N	X	X	X	X	N	N	X	X	X	X
Control 6	↓	↓/A	X	X	X	X	↓	↓/A	X	X	X	X
Control 7	X	X	X	X	X	X	X	X	X	X	X	X
Re-impl 1	N	N	X	X	X	X	N	N	X	X	X	X
Re-impl 2	N	↓	A	X	X	X	X	↓	X	X	X	X
Re-impl 3	N	↓	X	X	X	X	N	X	X	X	X	X
Re-impl 4	A[1]	A	X	X	X	↓	R[3]	A	X	X	X	↓
Re-impl 5	N	↓/ A[1]	X	X	X	R[2]	N	↓/ A[1]	X	X	X	R[2]
Re-impl 6	N	N	↓	X	X	X	N	↓	N	X	X	X
Re-impl 7	N	N*	A*	X	X	N	N	A*	A	X	X	R
Re-impl 8	N	N	N	X	X	N	N	↓	↓	X	X	↓
Re-impl 9	N	X	X	X	X	X	N	X	X	X	X	X
Re-impl 10	N	N^	N	↓	X	↓	N	N^	N	↓	X	↓
Re-impl 11	N	N*	N/↓	X	X	↓°	N	N*	N	X	X	N/↓°
Re-impl 12	N	N/A	X	X	X	A	N/A	N/A	X	X	X	A
Re-impl 13	N	N	N/R[3]	A	↓	N/R[4]	N/R[5]	R[6]	X	X	N	X
Re-impl 14	N	N	↓	X	X	X	N	N	↓	X	X	X
Re-impl 15	N	N^	N*	X	X	N/↓*	N	N^	N*	X	X	N/↓*

Table 2.4: Cont.

Abbreviations:

N = Normal

X = No sensation

A = Altered sensation: does not feel as it supposed to or pins and needles; A^1 = allodynia

↓ = Reduced sensation

- Except for a patch in the region of the *regimental badge*

^ Patch lower down the arm without sensation

* Sensation to just above the elbow, no sensation below elbow

° No sensation halfway down the forearm except patch in anterior medial aspect of the wrist with reduced sensation

R = Referred sensation

1. Sensation in the thumb and index finger on stimulating at the lateral aspect of the upper arm (C5)
2. Sensation felt in T2 distribution (medial aspect of axilla) on stimulating at the medial forearm (T1)
3. Sensation in little finger (C8) when touching the thumb (C6)
4. Sensation in little finger (C8) when inner aspect of forearm (T1)
5. Sensation in the thumb on stimulating at C4 distribution
6. Sensation in the thumb on stimulating at C5 distribution

T = Tinel's positive in re-implantation patients 5,8 (dorsal hand), 9 and 13 (thumb)

Table 2.4: Cont.

PATIENT	JOINT POSITION SENSE			VIBRATION		
	SHOULDER	ELBOW	WRIST	SHOULDER	ELBOW	WRIST
Control 1	X	X	X	X	X	X
Control 2	N	N	X	N	N	X
Control 3	↓	X	X	↓	X	X
Control 4	X	X	X	X	X	X
Control 5	N	N	X	↓	X	X
Control 6	↓	X	X	↓	X	X
Control 7	X	X	X	X	X	X
Reimplant 1	↓	X	X	↓	X	X
Reimplant 2	X	X	X	X	X	X
Reimplant 3	↓	↓	X	↓	↓	X
Reimplant 4	↓	X	X	↓	X	X
Reimplant 5	N	X	X	N	X	X
Reimplant 6	N	N	X	X	X	X
Reimplant 7	N	N	X	N	X	X
Reimplant 8	N	N	X	N	X	X
Reimplant 9	X	X	X	X	X	X
Reimplant 10	N	X	X	N	X	X
Reimplant 11	N	↓	X	N	N	N
Reimplant 12	N	N	X	↓	X	X
Reimplant 13	N	N	X	A	A	A
Reimplant 14	N	X	X	N	X	X
Reimplant 15	N	X	X	N	X	X

2.4.4 Results of Neurophysiological assessment

2.4.4.1 Results of nerve conduction studies in the control group

None of the seven control patients showed evidence of response in the motor conduction studies from either the median or ulnar nerve.

In one control patient there was a reduced SSR but absent SNAPs (Control 1). In another two patients no SNAPs or SSR were observed (Control 4 and 6). Reduced SNAPs along the median nerve, but not ulnar nerve, with absent SSR were observed on one control patient (Control 3). Reduced median and ulnar nerve SNAPs and SSR were observed in three control patients (Control 2,5,7).

2.4.4.2 Results of nerve conduction studies in the re-implantation group

Of the 15 subjects in the re-implantation group, CMAPs were recorded in one patient on stimulation of both the median and ulnar (Re-implantation 10). The median nerve demonstrated prolonged DML of 33.7 ms, decreased a CMAP amplitude of 3.5 mV and 3.1 mV when stimulated at the wrist and elbow respectively, and prolonged F-wave latency of 33.7 ms. The ulnar nerve demonstrated normal distal motor latency of 2.7 ms, decreased CMAP amplitude of 6.6 mV, 3.9 mV and 3.7 mV when stimulated at the wrist, below the elbow and above the elbow respectively, and prolonged F-wave latency of 31 ms.

Two patients of the re-implantation group showed evidence of SNAPs when stimulated at the index and middle finger and recorded at the wrist (Re-implantation 9 and 10). Five patients showed SNAPs when stimulated at the palm and recorded at the wrist (Re-implantation 3,9,10,11 and 12), including the two patients with responses from the index and middle finger (Re-implantation 9 and 10). The same two patients also showed ulnar nerve conduction velocities when stimulated at the little finger and recorded at the wrist. All SNAPs recorded were of reduced amplitude and increased latency. None of the re-implantation patients showed evidence of response to radial nerve stimulation.

There was no significant difference in SSR amplitude and latency between the re-implantation and control group (SSR amplitude: $z = 0.951$; $p = 0.3416$, SSR latency: $z = 0$; $p = 0.9158$).

2.4.4.3 Results of needle EMG studies in the control group

MUAPs were recorded from one patient in the deltoid, biceps and triceps (Control 1) and another in the biceps (Control 4). The patient with accessory nerve to the suprascapular nerve and 4^{th} and 5^{th} intercostal nerves to the musculocutaneous nerve transfers (Control 2) demonstrated MUAPs in the biceps and infraspinatous muscles.

2.4.4.4 Results of needle EMG studies in the re-implantation group

The results of the needle EMG studies for all re-implantation patients are given in Table 2.5. Evidence of innervation of upper limb muscles was observed in total of eight out of the 12 patients examined (67%). MUAPs were detectable from the deltoid muscle in six patients, from the biceps in seven subjects, from the triceps in five, infraspinatous in five and FDIO in one. In addition, distant to the needle MUAPs were observed in FDS in another patient. Furthermore, there was neurophysiological evidence of ongoing reinnervation with polyphasic nascent units in three patients in the deltoid muscle, five in the biceps, four in the triceps and infraspinatous muscle.

All patients in the re-implantation group demonstrated fibrillation potentials/PSWs. A spearman correlation coefficient did not reveal a correlation between the extent of fibrillation potentials/PSWs and time since the re-implantation procedure in the deltoid, infraspinatous, biceps or triceps (rho = -0.11; p = 0.72, rho = -0.89; p = 0.11, rho = -0.17; p = 0.59, rho = -0.17; p = 0.59 respectively). In addition, there was no significant correlation between time since the re-implantation and grade of reinnervation for deltoid, infraspinatous, biceps or triceps (rho 0.15; p = 0.63, rho = -0.08; p = 0.86, rho = 0.033; p = 0.92, rho = -0.011; p = 0.97 respectively).

Early recruitment of large units was noted in deltoid muscle in three patients, in the biceps in four patients, triceps in three and infraspinatous in one.

Of note, there was a single unit firing in the dorsal, but not the anterior, part of the deltoid when the patient tried to clench the fist, but not when trying to abduct the shoulder.

2.4.4.5 Comparison of needle EMG studies between groups

Comparison of the grade reinnervation between the two groups revealed statistically significant differences in the reinnervation of the infraspinatous ($z = -2.448$; $p = 0.0144$), biceps ($z = -2.21$; $p = 0.0264$), triceps ($z = -2.42$; $p = 0.0154$). There was no significant difference deltoid muscle reinnervation ($z = -1.58$; $p = 0.113$).

2.4.5 Outcome measures

2.4.5.1 Description of pain and correlation of pain scores to motor and sensory recovery

All 15 patients in the re-implantation group and three out of five in the control group reported experiencing severe pain in the affected arm. The description of pain was very similar in all patients; a background dull pain involving the whole arm with intermittent bursts of shooting pain down the forearm, wrist, hand or fingers. Four patients in the re-implantation group and one of the control group reported worsening of their arm pain with cold weather. No alleviating factors were reported. One patient described considerable improvement in pain soon after the re-implantation procedure.

***Table 2.5**: Raw Needle EMG data of the re-implantation group.*

DELTOID	**Fibri / PSW**	**Dur ation**	**Amplit ude**	**Polyph asicity**	**Recruitment**	**Interference**
Reimplant 1	.	.	.	.	.	.
Reimplant 2	3	↑	↑	normal	Reduced, large units recruiting early	severe decrease_single units
Reimplant 3	3	.	.	.	No MUAPs	.
Reimplant 4	2	.	.	.	No MUAPs	.
Reimplant 5	.	.	.	.	.	.
Reimplant 6	2	↑↑	normal	↑↑	nascent units, reduced	moderate decrease
Reimplant 7	2	↑↑	↑↑	↑↑	Reduced, large units recruiting early	moderate decrease
Reimplant 8	2	↑↑	↓↓	↑↑↑	nascent units, reduced	severe decrease_single units
Reimplant 9	2	.	.	.	No MUAPs	.
Reimplant 10	3	.	.	.	No MUAPs	.
Reimplant 11	3	↑	normal	↑↑	nascent units, reduced	moderate decrease
Reimplant 12	3	.	.	.	No MUAPs	moderate decrease
Reimplant 13	2	↑	↑	normal	Reduced, large units recruiting early	severe decrease_single units
Reimplant 14	2	.	.	.	No MUAPs	
Reimplant 15	0	.	.	.	No MUAPs	
BICEPS	**Fibri / PSW**	**Dur ation**	**Amplit ude**	**Polyph asicity**	**Recruitment**	**Interference**
Reimplant 1	.	.	.	.	.	.
Reimplant 2	3	↑	↑↑	↑	Reduced, large units recruiting early	severe decrease_single units
Reimplant 3	3	.	.	.	No MUAPs	.
Reimplant 4	.	.	.	.	.	.
Reimplant 5	.	.	.	.	.	.
Reimplant 6	2	↑	↑	↑	Reduced, large units recruiting early	severe decrease_single units
Reimplant 7	3	↑↑	normal	↑↑	nascent units, reduced, large units recruiting early	severe decrease_single units
Reimplant 8	2	↑↑	↓↓	↑↑↑	nascent units, reduced	severe decrease_single units
Reimplant 9	2	.	.	.	distant single units	.
Reimplant 10	3	↑↑↑	↓	↑↑↑	nascent units, reduced	severe decrease_single units
Reimplant 11	2	.	.	.	No MUAPs	.
Reimplant 12	3	.	.	.	No MUAPs	.
Reimplant 13	3	.	.	.	No MUAPs	.
Reimplant 14	2	↑	↑	↑↑	nascent units, reduced, large units recruiting early	severe decrease_single units
Reimplant 15	3	norm al	↓	↑↑	nascent units, reduced	severe decrease_single units
TRICEPS	**Fibri / PSW**	**Dur ation**	**Amplit ude**	**Polyph asicity**	**Recruitment**	**Interference**
Reimplant 1	.	.	.	.	.	.
Reimplant 2	3	↑	↑↑	↑	Reduced, large units recruiting early	severe decrease_single units
Reimplant 3	3	.	.	.	No MUAPs	.
Reimplant 4	.	.	.	.	.	.
Reimplant 5	.	.	.	.	.	.
Reimplant 6	2	↑	↑	↑	Reduced, large units recruiting early	severe decrease_single units
Reimplant 7	3	↑	↓	↑↑	nascent units, reduced, large units recruiting early	severe decrease_single units
Reimplant 8	2	.	.	.	No MUAPs	.
Reimplant 9	2	.	.	.	No MUAPs	.
Reimplant 10	3	↑↑↑	↓	↑↑↑	nascent units, reduced	.
Reimplant 11	2	.	.	.	nascent units, distant units	.
Reimplant 12	3	↑↑	↓	↑↑↑	nascent units, reduced	severe decrease_single units
Reimplant 13	3	.	.	.	No MUAPs	.
Reimplant 14	2	.	.	.	No MUAPs	.
Reimplant 15	3	.	.	.	No MUAPs	.
INFRASPINA TOUS	**Fibri / PSW**	**Dur ation**	**Amplit ude**	**Polyph asicity**	**Recruitment**	**Interference**
Reimplant 1	.	.	.	.	.	.
Reimplant 2	.	.	.	.	.	.

Reimplant 3	.	.	.	.	.	.
Reimplant 4	.	.	.	.	.	.
Reimplant 5	.	.	.	.	.	.
Reimplant 6	.	.	.	.	.	.
Reimplant 7	.	.	.	.	.	.
Reimplant 8	.	.	.	.	.	.
Reimplant 9	.	.	.	.	.	.
Reimplant 10	3	↑↑	↓	↑↑	nascent units, reduced	severe decrease_single units
Reimplant 11	2	↑	↑↑	normal	nascent units, reduced, large units recruiting early	
Reimplant 12	.	.	.	.	.	.
Reimplant 13	.	.	.	.	.	.
Reimplant 14	2	normal	normal	↑↑	nascent units, reduced	severe decrease_single units
Reimplant 15	3	normal	normal	↑↑	nascent units, reduced	severe decrease_single units

Of the 15 re-implantation patients, five patients reported pain in the hand in general, one in the palm, two in the dorsal aspect of the hand, four in the thumb or index finger (C6 dermatomal distribution), one in the 5th finger, 1 in the forearm, two in the whole arm in general and one reported very mild pain to no pain. Interestingly, of the four who reported pain in the thumb or index finger, three had normal or reduced sensation in the C6 distribution.

The average VAS score reported by patients in the control group was 6.9 (sd; 2.01, range; 5-8.5), whereas in the re-implantation group the average VAS score was 5.4 (sd; 2.03, range; 2-8) (Figure 2.2). A two-sample Mann-Whitney test did not reveal a statistically significant difference in VAS scores between the two groups ($z = 1.07$, $p = 0.29$).

Similarly, a Spearman correlation coefficient did not demonstrate a statistical significant correlation between VAS score and global MRC score *(rho = 0.42; p =0.11)* (Figure 2.3) or a correlation between VAS score and number of dorsal roots with sensory recovery (out of 5; C5 through to T1) ($z = -0.12$; $p = 0.67$) (Figure 2.4).

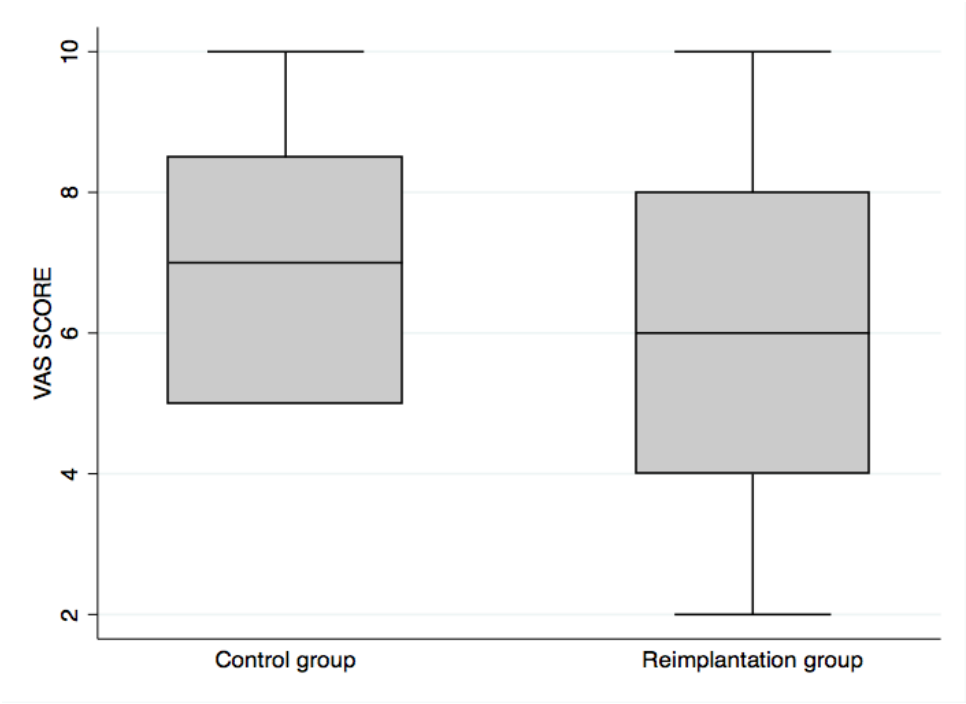

***Figure 2.2**: VAS scores for the control and re-implantation group. The line across the box represents the sample median (Control group: median; 7, Reimplantation group: median; 6). Whiskers represent the sample maximum and minimum (Control group: max; 5, min; 10, Reimplantation group: max; 2,min; 10).*

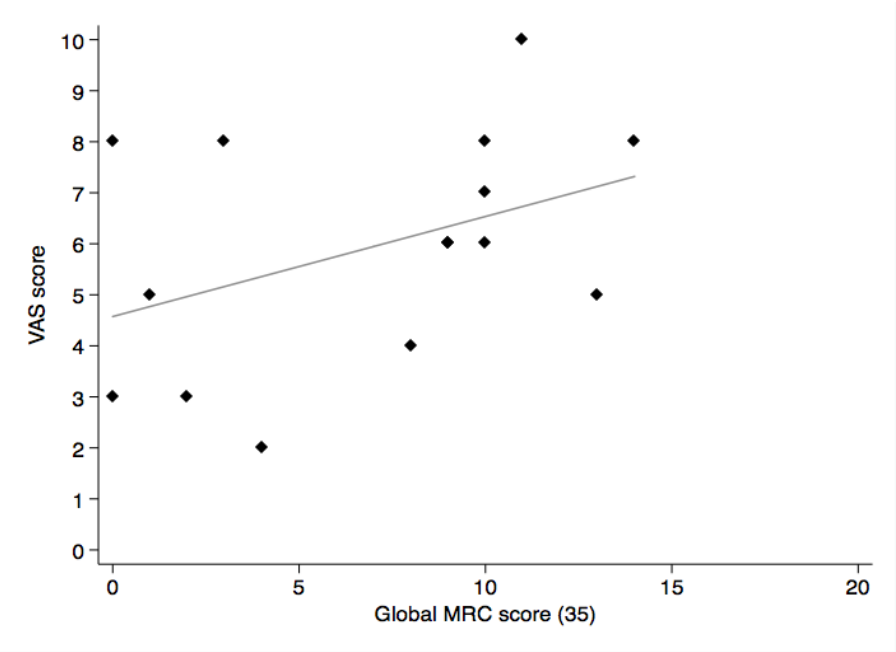

Figure 2.3: *The relationship of VAS score and MRC scale in re-implantation patients. There was no statistically significant association between VAS and MRC scale (z = 0.42; p=0.11).*

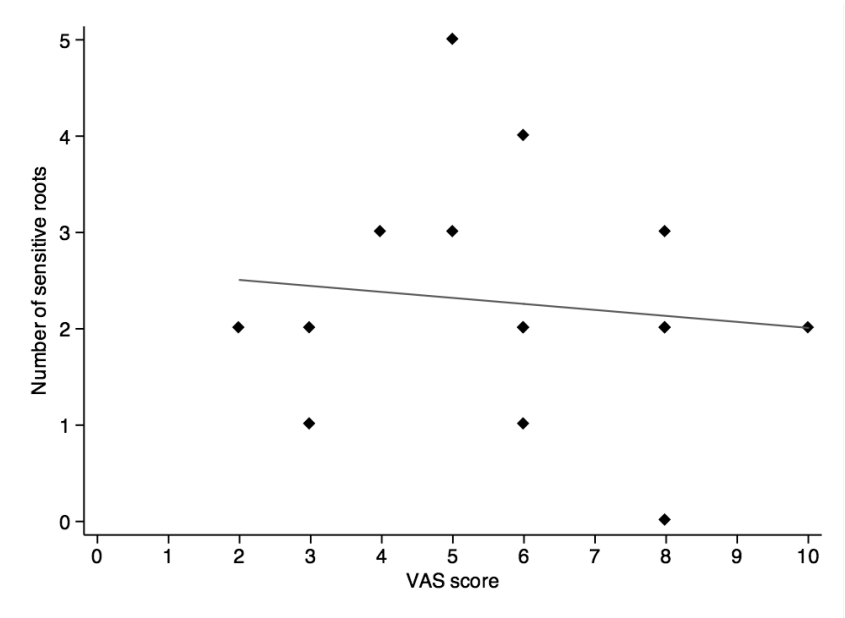

Figure 2.4: *The relationship of VAS score and number of sensitive roots in re-implantation patients. There was no statistically significant association (z = -0.12; p =0.67).*

2.4.5.2 Results of the DASH outcome measure including work and social demographics.

The mean DASH score for the control group was 31.8 (sd = 11.94; range = 11.7 – 46.7) and the re-implantation group 47.17 (sd = 22.98; range 12 - 89). There was no statistical significant difference in the DASH score between the two groups (z = -1.693, p = 0.09) as shown by a two-sample Mann-Whitney test.

At the time of the interview, 9 out of 15 patients (60%) within the re-implantation group and 3 out of 7 patients (42.86%) of the control group were working. Of the 7 control patients only 4 completed the DASH work questionnaire, which showed a mean of 31.8 (sd; 11.94, range; 11.7-46.7). In the re-implantation group, 9 out of the total 15 patients completed the DASH work questionnaire, which gave a means of 47.17 (sd; 22.98, range; 12.5-89.2). There was no statistical significant difference in the DASH work score between groups (z = -0.23, p = 0.82).

Regarding sporting activities, only one control patient played sports (14.29%), who scored 25 in the DASH sport score, whereas 6 (40%) out of 15 engaged in sporting activities in the re-implantation group. 8 (53%) out of the 15 re-implantation patients and one (14.29%) of the control group completed the DASH sport questionnaire. The group mean for the re-implantation was 53.12 (sd; 38.23, range; 12.5 - 100), whereas the one control patient scored 25 in the DASH sport questionnaire. There was no statistical difference in the DASH sport score between groups (z = -0.399, p = 0.69).

2.4.5.3 Results of the MHQ outcome measure

The mean MHQ total score in the control group was 23.89 (sd = 9.21; range 11.33 – 29.28) in the control group and 25.676 (sd = 15.17; range = 1.43 - 54.29) in the re-implantation group. A two-sample Mann-Whitney test did not reveal a statistically significant difference in MHQ total scores between the two groups (z = 0.04, p = 0.97) (Table 2.6).

Table 2.6: *Results of MHQ*

	Mean		**SD**		**Min**		**Max**	
	Control	**Reimplant**	**Control**	**Reimplant**	**Control**	**Reimplant**	**Control**	**Reimplant**
Overall score for function of affected hand	0.71	1.78	1.88	6.68	0	0	5	25
Overall ability to work	42.86	44.64	36.15	35.92	0	0	95	100
Overall score for function relative to pain	54.14	68.75	30.26	21.00	11	0	85	100
Overall score for ADL	20.72	20.59	17.68	15.76	0	25	44.64	100
MHQ total score	**23.89**	**25.68**	**9.21**	**15.17**	**11.33**	**0**	**39.28**	**48.21**

2.4.5.4 Results of the SF36 outcome measure

The mean scores for the SF36 physical health summary in the control group was 42.57 (sd = 3.1; range = 36 - 46) and for the SF36 mental health summary 42.85 (sd

= 10.53; range = 24 - 55). The re-implantation group scored 39.06 (sd = 9.69; range = 23 - 53) in the SF36 physical healthy summary and 42.27 (sd = 14,82; range = 16 - 64) in the SF36 mental health summary. There was no statistical difference between groups in the SF36 physical health summary or the SF36 mental health summary (z = 0.83, p = 0.38 and z = 0.035, p = 0.97 respectively).

2.5 Discussion

In the current study we assessed 15 patients who have had complete BP and re-implantation surgery and compared their functional and electrophysiological evidence of reinnervation a mean of 13 years after injury with patients who have had BP avulsion injury without re-implantation surgery. This is the first study to investigate the effects of re-implantation surgery in the chronic phase of recovery and compared with a control group of patients. In addition, to our knowledge, EMG data have not been correlated thus far with clinical function after reconstruction by re-implantation surgery.

2.5.1 Recovery of motor function

Patients who have had re-implantation surgery showed a significant difference in clinically examined power in the deltoid, pectoralis and infraspinatous muscles and "global MRC score". Significantly improved reinnervation by EMG criteria, when

compared to controls, was found in infraspinatous, biceps and triceps muscles. There was no significant difference deltoid muscle or muscles of the hand. Nevertheless, MUAPs from distal hand muscles were recorded only from patients of the re-implantation group, one in FDS and one in FDIO. There was neurophysiological evidence of ongoing reinnervation with polyphasic, small amplitude MUAPs (nascent units) in 3 patients in the deltoid muscle, 5 in the biceps, 4 in the triceps, and 4 in the infraspinatous muscle.

The fundamental question regarding the observed functional recovery in these patients is whether reinnervation of muscles of the upper arm has occurred via the re-implanted roots. Perhaps the first step towards answering this question is by determining whether functioning muscles were denervated due to avulsion of ventral roots supplying it. Previous studies of BP re-implantation have included on their cohorts patients with two or more avulsed roots. However, it is well known that differing opinions exist regarding the nerve supply to muscles and, therefore, one cannot exclude reinnervation from collateral sprouting of caudal or cranial uninjured nerves. To avoid this phenomenon we studied patients with complete BP avulsion involving avulsion injury to all roots supplying the BP. In theory, any reinnervation of muscles of the upper limb would have to be supplied via one or more re-implanted roots.

Furthermore, it should be determined whether the injury to the root was a true central avulsion as the pathophysiological processes that take place following root rupture differ from avulsion injury. In this thesis, we only included patients whose injury was confirmed with open exploration of the BP, the current gold standard.

Nevertheless, our study revealed patients in the control group demonstrating absent SNAPs suggesting an infraganglionic injury to the BP. This may be a result of incorrect characterization/documentation of the lesion at the time of exploration. It is important to note that in patients who do not undergo re-implantation, their dura is not opened during the exploratory procedure and, therefore, root remnants attached to the spinal cord may not have been clearly visualised. Also, it is common to see extensive scarring, and the ruptured nerve endings or damaged DRGs are difficult to identify, leading to inaccuracies in documentation. Interestingly, two of those patients showed voluntary MUAPs in the deltoid and biceps respectively. Alternatively, it suggests a combination of infraganglionic and supraganglionic injury, which is possible given the degree of mechanical force exerted to the plexus.

It is important to note here that in neurophysiological terms an avulsion injury is referred as a preganglionic injury and is paradoxically based on the presence or absence/disconnection of the DRG and, thus, neurophysiological examination better describes dorsal root lesions. The presence of a certain injury to the dorsal root does no imply a similar lesion to the ventral root. In fact, the combination of intact dorsal and avulsed ventral roots is the second most common type of avulsion injury after complete avulsion, preceding intact ventral root with avulsion of the dorsal root, which is rare (Carlstedt 2008). As a consequence, neurophysiological studies cannot differentiate ventral root avulsion from rupture post-operatively.

In the pre-operative setting, EMG studies can be used to define the location of a root lesion in relation to the intervertebral foramen. The posterior primary rami of the ventral roots that innervate the erector spinae muscles arise within the exit foramina so that in root lesions in which there is no evidence of denervation in these muscles

the lesion must be distal to the foramen (Swash 1986). In root lesions in which the erector spinae muscles show evidence of reinnervation, the injury can be localized proximal to or within the neural foramen. Nonetheless, it does not localize the injury in respect to the transitional zone. Pre-operative neurophysiological examination was not common practice at the time of these re-implantation cases studied here and thus, such data are not available. The important point however, is that even with preoperative evidence of infraganglionic injury, neurophysiological examination cannot exclude a concomitant avulsion injury.

Infraganglionic injury was suggested based on their neurophysiological studies in four patients with re-implantation in this study. During the re-implantation procedure the dorsal root is trimmed to the most distal closest normal appearing segment, most often including the DRG. As a result, we were not expecting to find any SNAPs or SSR in these patients. The likeliest possibility is that the DRG was not removed completely but injured during the trimming process. Alternatively, it may imply a combination of lesions in the absence of removal of the DRG.

Furthermore, in the re-implantation group, the extent of denervation and degree of reinnervation was not shown to correlate with time since the re-implantation procedure, as demonstrated by a lack of correlation using Spearman's rank correlation coefficient. It is well known that neurological recovery is also dependent on healthy viable muscle and the release of nerve growth factors from denervated muscle which act as catalysts to axonal regeneration. Chronically denervated muscle will eventually become fibrotic and electrically inactive within 18 and 24 months (Forman et al. 1978). The finding of MUAPs demonstrating early recruitment of

large units in deltoid muscle in three patients, in the biceps in four patients, triceps in three and infraspinatous recorded from patients with re-implantation surgery supports the suggestion that muscle fibre damage is a contributory factor to the lack of recovery in the presence of some reinnervation. This is also supported by the fact that most patients in this study, but also in the previous publications in humans and animals (Carlstedt et al. 2000; Eggers et al. 2010), demonstrate an improved recovery in the proximal muscles of the arm and poor recovery distally.

Given the prompt reduction of motor neurons and dorsal horn cells after avulsion injury and the assumption that best results are seen when prompt re-implantation occurs, we hypothesised that excluding patients who were re-implanted more than a month after the injury would perhaps show some relationship. However, excluding patients who were operated more than 30 days after the injury did not improve the statistical correlations.

Finally, observation of the data revealed that occasionally the clinical examination and neurophysiological tests did not correlate i.e. showing evidence of innervation for specific muscles in both types of examination. A number of reasons may account for these differences. Firstly, accurate clinical examination of these patients proved difficult in that when patients were asked to perform a movement they had the tendency to contract the whole arm (whether or not there are functional muscles) rather than purposefully contract the respective muscle that performs the movement asked. In addition, more than one muscle can perform a movement and it was difficult to distinguish which muscle actually works to perform that movement. Secondly, differences may be due to incorrect positioning of the EMG needle during

testing. Accurate positioning of the needle did indeed seem challenging as muscles are markedly atrophied and do not hold their usual positions. Thirdly, other factors can lead to similar results, including adaptive biomechanical changes, functional compensation and muscle substitution patterns (Feinberg 2006). For example, three patients from the re-implantation group had some power in shoulder abduction in clinical examination, which was no supported by evidence of presence of MUAPs in needle electromyography. Typically, to abduct their shoulder, patients shrug their shoulder using their trapezius muscle to either assist or achieve the intended movement. Alternatively, concomitant use of muscles not tested could produce the movement.

2.5.2 Recovery of sensory function

Sensory testing in affected dermatomes showed generally poorer recovery in the control group. In the re-implantation group there was better recovery at the C5, C6 and T1 dermatomes. The best recovery was found at the C5 dermatome with a statistically significant higher frequency in return of sensation in the re-implantation group compared to controls for both soft touch and pinprick sensation.

The return of sensory function in avulsed dermatomes is difficult to explain as only the ventral roots have been reconnected to the spinal cord. In addition, during the re-implantation procedure the DRGs are actively sought for and excised. It has been proposed that sensory recovery could be attributed to collateral sprouting of fibres from an overlapping dermatome rather than regeneration through repair (Carlstedt

2008). This could explain recovery at the C5 and T1 dermatome from C4 and T2 collateral sprouting respectively. Alternatively, new processes could extend from dorsal horn neurons along the implanted ventral root. The mechanism by which sensory recovery occurs is yet to be demonstrated.

Two re-implantation patients perceived referred sensations. Referred sensations have been described in a number of conditions including amputation, somatosensory deafferentation, and in BP injury (Berman et al. 1998; Htut et al. 2006). The pathophysiology of such sensations is also poorly understood, however, one proposed mechanism is through sprouting of primary afferent nerve fibres within the grey matter of the dorsal horn of the spinal cord. McMahon and Kett-White (McMahon et al. 1991) have shown that primary afferent nerve fibres show greatly enhanced sprouting when; 1) vacant synaptic sites are created by the degeneration of other primary afferent fibres; and 2) the peripheral branches of the axons are actively regenerating. In our two patients with referred sensations, sensation was perceived in dermatomes immediately adjacent to the dermatome examined, making it possible that recovery occurs by collateral sprouting. In support of collateral sprouting is also the fact that in two patients with positive Tinel's sign referred at the posterior aspect of the hand and thumb respectively, there was also present sensation when the dermatome to which the pain referred to was tested. However, in the absence of DRGs and SNAPs in the distribution of the median, radial or ulnar nerve as demonstrated in the relevant patients the mechanism of return of sensation remains a mystery.

2.5.3 Pain

Neuropathic pain associated with BP avulsion injury has been well described (Berman et al. 1998; Htut et al. 2007) and can be very severe, persistent and resistant to treatment.

Initial clinical observations have suggested that pain in the affected arm is related to the number of avulsed roots (Berman et al. 1998). It is, therefore, unsurprising that our patients in whom all five dorsal roots of the BP are avulsed, are experiencing severe pain in the whole arm. Initial clinical observations also suggested that successful surgical repair was associated with relief of avulsion pain and that improvement in pain severity was correlated with the return of muscle activity (Berman et al. 1998; Carlstedt et al. 2000; Htut et al. 2006). In this study, a statistical significant correlation between pain and motor recovery or a temporal relationship from the time of surgery was not demonstrated. In addition, there was no statistically significant difference in the pain severity between the re-implantation and control group. There are some fundamental differences between this study and previous investigations of pain phenomena in BP injury. Firstly, subjects studied in the previous reports included patients with any type of BP injury including ruptures and avulsions of only two or more spinal roots involved which, consequently, resulted in a greater number of patients. In this study, to avoid variability we studied a more homogeneous group of patients, including patients with complete BP injury alone. It is, therefore, logical to assume that differences in assumptions made could be due to either the inclusion of more modest injuries, where there is more room for synaptic plasticity or to a failure to demonstrate such correlations in our small group of patients.

2.5.4 Outcome measures

The use of patient-reported outcomes as primary measures in clinical trials has become increasingly popular over recent decades. The use of condition-specific instruments has great potential for evaluating domains of physical functioning and health-related quality of life commonly affected by a specific pathology. Since there are no such measures specific to brachial plexus injuries, a literature review of all outcome measures focusing on conditions of the upper limb was performed and the DASH and MHQ were thought to be most adequate in assessing function recovery following brachial plexus avulsion injury. These scores have been shown to demonstrate reliability and reproducibility in other conditions affecting the upper limb (Chung et al. 1998; Beaton et al. 2001). Construct validity refers to the extent to which scores on a questionnaire relate to other measures in a manner that is consistent with theoretically derived hypotheses concerning the constructs that are measured (Kirshner et al. 1985) - by examining its correlation to other generic instruments such as SF36 (SooHoo et al. 2002). However, no differences in the mean scores of the upper limb outcome measures used between patient groups were demonstrated. One reason for this is that although both DASH and MHQ focus on the upper limb, they do not have content that exclusively relevant to the population studied and do not concentrate on specific disease-associated impairments. In addition, it is noted that most patients in both groups scored the worst possible score in both instruments indicating that the scale used is not sensitive enough to measure improvement in a substantial proportion of patients and that some actual variation in the data is not reflected in the scores obtained from that instrument. This reduced

limited variability in the gathered data may have reduced the power of statistics on correlations between variables.

2.6 Limitations

The present study is subject to a number of limitations. An important limitation in the current study is the small number of patients assessed both in the control and re-implantation group. However, given the uncommon type of injury including more patients was not feasible, particularly in the control group who sustained their injury more than 10 years ago, making it difficult to trace.

Another limitation of the present study is the identification of patients retrospectively making it necessary to rely on documentation of others for the confirmation of diagnosis of complete avulsion injury, which may not always be accurate. Ideally, patients studied should have their diagnosis confirmed with both open exploration and neurophysiological evidence of complete BP avulsion, including paraspinal muscle EMG to best localize the lesion. Great effort was made to ensure that only patients with explicitly complete avulsion injury were included in this study by correlating clinical notes, neurophysiological tests at the time of the injury where available and findings of the exploratory procedure.

Moreover, there are a number sources of bias. First, it has been suggested that these patients sustain significant concurrent brain injury as demonstrated by neuropsychological assessment even in the absence of brain parenchymal

abnormalities on imaging. Secondly, the rehabilitation received by each patient varies significantly. All patients receive an intensive 2-week rehabilitation program in the immediate post-operative period with highly specialized rehabilitation specialists, physiotherapists and neuropsychologists at the National Hospital for Neurology and Neurosurgery. The program aims to increase and maintain range of movement, mobilize tight scar tissue, maintain good joint position, adjust analgesia, improve posture and encourage return to activities. Subsequently, patients are referred to their local services, which vary significantly depending on the knowledge and skills of the responsible physiotherapists. These factors are thought to significantly affect clinical recovery and clinical outcome. In addition, differences in age, sex and length of time from injury to assessment for this study are further factors that may have influenced results. Similarly, the clinical assessment was performed by the author who was not blinded to the status of patients, introducing observer bias.

Furthermore, the examination of the sensory system proved to be more difficult than anticipated and results were too complicated to be able to make accurate assumptions. It would be useful to use a more quantitative method of sensory system examination with thermal, noxious and mechanical thresholds, as opposed to examining clinically. This would, perhaps, reveal small differences between groups not evident with clinical examination.

2.7 Future directions

The present study has been important in providing a more robust assessment of functional improvement in patients with BP re-implantation surgery after complete

avulsion injury. Nonetheless, unanswered questions and room for improvement in study design still remain. There are no studies in the literature that compare functional recovery of these patients with a control group or with patients who had had alternative surgical procedures for repair such as nerve transfers. Given the results presented within the present thesis, it would be fruitful to perform a prospective study comparing the three aforementioned groups of patients, those without re-implantation, those with re-implantation and those with nerve transfers using clinical, neurophysiological tests and outcome measures at varying time points during their recovery. This would also eliminate confounding factors and also assist in better determining the mechanism of regeneration. Moreover, the use of imaging methods, as suggested in Chapter 5 and 6 of this thesis, could further provide a more robust outcome measure and add to our knowledge of the mechanisms of repair.

2.8 Conclusion

In closing, the present study set out to investigate the effects of BP re-implantation after complete BP avulsion injury. Patients that have undergone BP re-implantation surgery after complete BP avulsion injury were discovered to have better neurological recovery in the proximal arm muscles. Nonetheless, they were not found to have significant difference when compared to control subjects in the outcome measures assessing the function of their arm and activities of daily leaving. Neurophysiological findings are vast and complicated demanding a structured assessment protocol to be used in the future in order to further understand mechanisms of recovery. The subtle differences in clinical and neurophysiological tests revealed in this study point out to the need for additional work to determine

whether additional strategies such as the use of growth factors or cellular therapies may produce further improvement.

Chapter 3

Olfactory ensheathing cells: properties, effects on axonal regeneration and clinical strategies

3.1 Introduction

The failure in achieving greater functional connectivity with peripheral nerve grafts alone, partly centers on the cellular nature of the graft-host interface and the inhibitory molecular properties of the CNS. The interaction of Schwann cells and astrocytes is not favourable. In co-culture Schwann cells and astrocytes occupy distinct and non-overlapping areas and there is evidence suggesting that Schwann cells may even promote gliosis and the deposition of nonpermissive extracellular molecules, such as chondoitin sulphate proteoglycans (Lakatos et al. 2000).

The olfactory mucosa has attracted the interest of neuroscientists due to the observation that olfactory neurons present in the olfactory epithelium are able to exhibit continual turnover and project axons into the central nervous system (CNS) throughout adulthood and after injury to the primary olfactory system. Olfactory neurogenesis takes place in the basal cell layer of the olfactory epithelium (Graziadei et al. 1979). Newly generated unmyelinated olfactory neurons extend a single dendrite that arises from the apical pole and projects into the luminal surface of the epithelium, and a basal axon that joins other axons in the lamina propria to form bundles (fila olfactoria). These grow through the underlying basal cell layer, cross the cribriform plate of the ethmoid bone, traverse the pia mater, enter the CNS and navigate within the olfactory nerve and glomerular layers of the olfactory bulb (OB). There, they establish new functional connections with mitral, tufted and periglomerular neurons in the glomeruli of the OB (Graziadei et al. 1979; Doucette 1990). Similar processes have also been observed after injury or transection of the fila olfactoria in experimental models (Graziadei et al. 1980). The permissiveness of

the OB to axonal regeneration was unexpected compared to other mature CNS lesions where axonal regeneration is abortive primarily due to the presence of an unfavourable glial environment and the formation of a glial scar after injury (Silver et al. 2004). The permissiveness the OB to axonal elongation has been attributed to the presence of a different glial cell type supporting olfactory axons; the olfactory ensheathing cell (OEC).

3.2 Olfactory ensheathing cells

OECs have been characterized from neonatal and adult rodent olfactory tissues. Different populations of OECs have been described in terms of morphologic and antigenic characteristics. It has been suggested however, that OECs belong to a single, malleable cell type that expresses a variety of phenotypic characteristics with both similarities, as well as, differences to astrocytes and Schwann cells.

OECs originate from the olfactory placodes, which are two ectodermal thickenings in the rostrolateral region of the embryonic head (Cuschieri et al. 1975; Valverde et al. 1991) unlike Schwann cells, which are derived from the neural crest. They ensheath olfactory axons through their pathway from the olfactory epithelium guiding olfactory axons to the OB and preventing from coming into contact with other glial cells types (Doucette 1984; Doucette 1993). Within the OB, in which OEC processes do not invade, olfactory axons are devoid of glial covering (Raisman 1985). Unlike Schwann cells, OECs enfold densely packed bundles of unmyelinated axons. Their internal surface of their fine glial processes faces directly the nerve

bundles dividing them into interconnected fascicles. Their outer surface is apposed to a basal lamina in those regions where they contribute to form the external glia limiting membrane (i.e. the junction between the olfactory nerve axons and the protoglomeruli in the olfactory bulb) (Ramon-Cueto et al. 1998). Consequently, in contrast to other PNS-CNS transitional zones, the plasma membranes of ensheathing cells and astrocytes are not separated by a basal membrane (Doucette 1984; Doucette 1991).

Morphologically, OECs have characteristic morphological appearances both in development and in the adult. During development ensheathing progenitor cells can be distinguished by their scanty cytoplasm containing a lobulated electron dense nucleus with patchy chromatin and one or two nucleoli. Mature rodent OECs are distinct owing to their indented nuclei with uniformly distributed, but slightly clumped chromatin, and an electron dense cytoplasm with scattered filaments. SC have electron dense nucleus with chromatin clumped throughout and more electron dense cytoplasm compared to OECs. Astrocytes have ovoid nuclei with an electron-lucent cytoplasm. OECs can form end-feet junctions with blood vessels in a manner comparable to astrocytes.

3.3 Immunocytochemical properties of OECs

Extensive work has been done to fully characterize OECs. The immunocytochemical profile of OECs remains to be determined. Specific antibodies or battery of antibodies that uniquely identify this group of cells has not been defined yet.

As shown in both in vivo and in vitro studies, OECs express proteins associated with both Schwann cells and astrocytes. Differentiating them from astrocytes, OECs are immunoreactive for the low-affinity nerve growth factor receptor p75 ($p75^{NTR}$) (Gong et al. 1994), laminin, the cell adhesion molecule L1, and the neurofilament vimentin (Miragall et al. 1988; Ramon-Cueto et al. 1998; Kawaja et al. 2009). They both express GFAP (Barber et al. 1982). Positive immunostaning has also been shown for the calcium binding protein S100β (Takahashi et al. 1984) and the cell adhesion molecule NCAM (Miragall et al. 1988). Schwann cells are also immunoreactive to S100β, but they can be differentiated from OECs due to their expression of the myelin protein P0. OECs lack immunoreactivity against A2B5, Ran2, and MAP 2, all of which mark astrocytes and do not share expression of O-24, HNK-1, GD-3, A2B5, which characterize oligodendrocytes. An extensive description of the immunocytochemical profile of OECs can be found in the review article of Kawaja et al., (Kawaja et al. 2009).

3.4 Olfactory ensheathing cells as candidates for promoting CNS repair in the olfactory system

3.4.1 Experimental models of OEC-mediated repair

The first experiment to demonstrate the effects of OECs on regenerating axons was performed by Ramon-Cueto and Nieto-Sampedro (Ramon-Cueto et al. 1994) who demonstrated that transplants of adult olfactory bulb OECs mediate the re-entry of

regenerating dorsal root axons into the dorsal spinal gray matter following T10 dorsal rhizotomy and anastomosis. The dorsal root entry zone (DREZ) marks an abrupt transition from SC cells to astrocyte and oligodendrocyte ensheathment and has been the prototype lesion paradigm for determining the regeneration promoting properties of OECs. After injury to a dorsal root, primary afferent fibers within the root are able to grow back to their normal region in the spinal cord but arrest there and are unable to enter the CNS environment of the spinal cord (Ramon Y Cajal 1928). In Ramon-Cueto's and Nieto-Sampedro's experiment, regenerating sensory axons were noted to traverse the glial scar and innervate the correct laminae of the spinal cord. The transplanted OECs appeared to accompany the regenerating DRG axons into the dorsal horn, beyond the area of the lesion. This work was extended by Nieto-Sampedro and colleagues, who reported that the regenerating fibres were also able to re-establish functional connections with spinal cord neurons (Navarro et al. 1999; Pascual et al. 2002).

Thereafter, regeneration-promoting capacity of OECs has been studied in various in vitro and acute and chronic lesion paradigms. In lesions of the corticospinal tract, transplanted OECs have been shown to migrate and align themselves with the host astrocytes. In addition, they induce axonal branching, which wander and elongate through the lesion and into the denervated caudal host tract with evidence of associated functional restoration demonstrated using directed forepaw retrieval tasks in rats. (Li et al. 1997; Keyvan-Fouladi et al. 2003). OECs were also shown to be highly angiogenic and to induce the formation of a dense plexus of microvessels (Li et al. 1998).

Furthermore, Pascual et al., (Pascual et al. 2002) performed bilateral section of identified dorsal roots receiving bladder innervation to demonstrate dorsal root afferent regeneration, as well as, bladder activity restoration after unilateral injection of OECs in the sacral parasympathetic nucleus of adult rats. L6 to S2 dorsal roots were sectioned bilaterally close to the dorsal root entry zone and reattached to the cord with fibrin glue. The interruption of bladder sensory innervation led to an atomic, unresponsive and distended bladder. Approximately 30,000 purified OECs were injected in each of the three sectioned roots. Anatomic regeneration of bladder primary afferents was demonstrated by the presence of labeled wheat germ agglutinin-horseradish peroxidase fibers in the dorsal horn and sacral parasympathetic nucleus. In the olfactory ensheathing group the proximal stump of the dorsal root contained labeled fibers that entered the spinal superficial laminae but transganglionic transport of the tracer was not identified in any of the control animals. Cystometrography demonstrated recovery of bladder activity in the transplanted group six weeks after surgery.

Moreover, OEC transplantation has been shown to stimulate the return of supraspinal control of breathing and major improvements in climbing after unilateral knife cuts to sever the entire spinal gray and white matter at the level of the second cervical segment in adult rats abolishing ipsilateral phrenic nerve and diaphragm function (Li et al. 2003). In addition, severed adult retinal ganglion cells where also used to show the growth promoting effect of OECs (Li et al. 2003). Anterograde labeling with cholera toxin B showed that at 2 weeks postoperatively axons penetrated the transplants, entered the distal stump and elongated for 10 mm together with the transplanted cells.

The intimate relationship with astrocytes has been explored in both in vivo and in vitro experiments demonstrating that when co-cultured with astrocytes, OECs intermingle with astrocytes, do not induce astrocytic hypertrophy and elicit less chondroitin sulphate proteoglycan and GFAP expression after transplantation (Lakatos et al. 2000; Lakatos et al. 2003; Andrews et al. 2007). In addition, Li et al., (Li et al. 2004) examined the cooperation between the transplanted OECs and the host astrocytes following a single lumbar dorsal rootlet transection and re-implantation with OECs smeared at the cut surface of the root. A characteristic ladder-like arrangement of parallel bridging structures aligned in the orientation of dorsal roots was identified. Immunostaining showed that these structures were made up of intimately intermingled fine fascicles of astrocytic processes recruited from the spinal cord and peripheral tissue processes recruited from the peripheral nerve. Axons projected through the dorsal OEC formed fascicles into the dorsal horns and formed long straight unbranched fibres that traveled for at least 10mm caudally as well as rostrally.

In addition, although OECs do not myelinate olfactory axons in their natural environment, their ability to assemble peripheral like myelin has been well demonstrated. OECs co-cultured with neurons enfold, myelinate and provide a favourable substrate for dorsal root ganglion neurite outgrowth (Ramon-Cueto 2000). In vivo, they have been shown to remyelinate axons after transplantation into an ethidium bormide/x-irradiated demyelinated area of the adult rat spinal cord (Franklin et al. 1996). OEC remyelination of axons in the posterior columns has also been shown to enhance axonal conduction across the previously demyelinated area, thus demonstrating a functionally significant degree of remyelination (Imaizumi et

al. 1998). Li et al., (Li et al. 1998) provided evidence that OECs also remyelinate corticospinal axons that have regenerated into and through the site of an OEC graft subsequent to an electrolytic lesion in one-cell-to-one axon myelinating fashion.

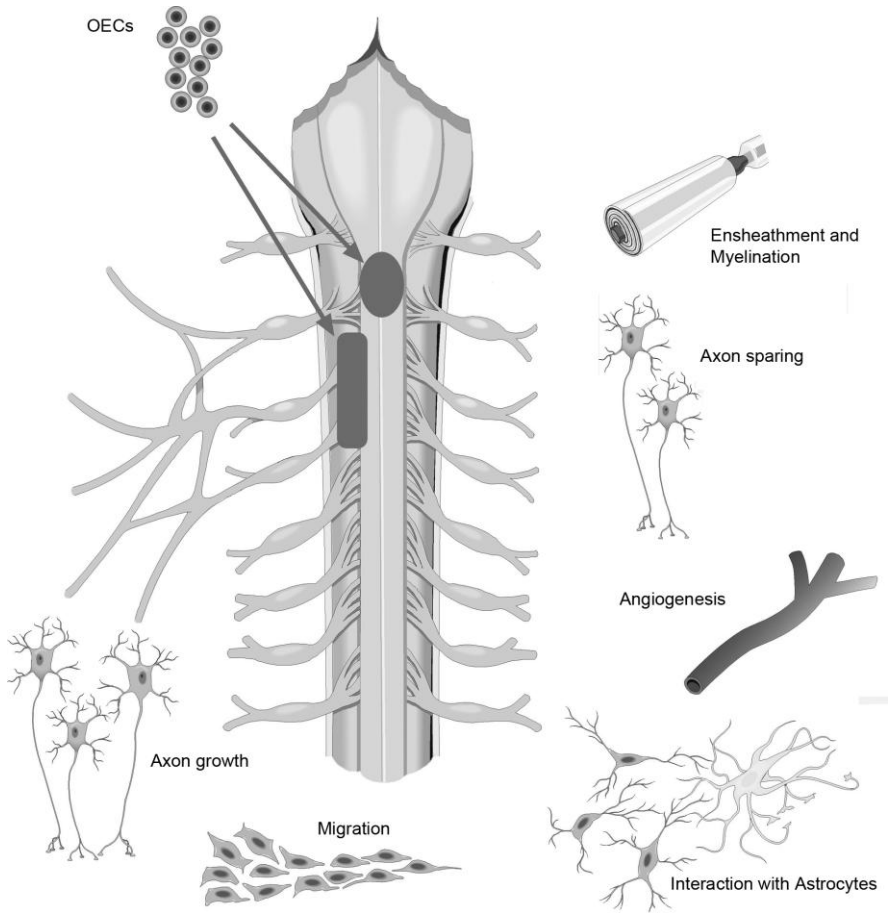

Figure 3.1: Putative neuroregeneration-promoting effects of OECs after transplantation into a spinal cord injury (from Kachramanoglou et al., (Kachramanoglou et al. 2011). Permission to reproduce this image has been granted by Informa Healthcare).

Despite the advances in our understanding of the functional properties of OECs, there is still little known about the molecular mechanisms through which OECs mediate axonal repair. Cultured OECs have been shown to secrete neurotrophins to have implications in axonal regrowth. These include BDNF, GDNF, NGF and glial growth factor 2 (GGF2), neurotrophin 4/5 and neuregulin (Chuah et al. 2000; Boruch et al. 2001; Woodhall et al. 2001; Pastrana et al. 2007). OECs axonal-promoting properties have also been attributed to their expression of membrane surface associated molecules. Such growth-associated molecules include laminin, N-CAM and L1 (Chuah et al. 1991; Whitesides et al. 1996). Another hypothesis states that OECs assist by mechanical means by restoring pathway via which growing axons can cross the area of injury (Keyvan-Fouladi et al. 2002; Li et al. 2005). OECs have been observed to form tunnel-like structures with their processes within the transection lesion site through which groups of previously transected axons are grow suggesting that OECs provide a permissive environment through which transected spinal cord axons could regenerate across the lesion site (Li et al. 1997). A table with all OEC transplantation studies in the spinal cord is provided in the Appendix 5.

In summary, the principal beneficial effects of OECs by which they contribute to regeneration and increased functional recovery include: (a) stimulation of axonal growth, (b) reduction in astoglial response and decrease scar tissue, (c) promotion of angiogenesis, (d) restoration of myelin, (e) free migration within the CNS parenchyma and coexistence with astrocytes (Figure 3.1). Consequently, OECs are currently considered one of the most promising candidates for cell-mediated repair of nervous system injury. Considerable attention has now shifted towards obtaining human OECs and testing them in experimental and clinical studies.

3.4.2 Clinical studies of OEC transplantation

Despite the incomplete characterization of OECs, clinical trials with OECs have already taken place in China, Portugal and Australia. The majority have taken place in China using olfactory bulb-derived OECs from aborted foetuses in patients with spinal cord injury. Data published involved 171 patients who ranged from 2 to 64 year of age and received transplants at post injury times extending as much as 30 years (Huang et al. 2003). Follow-up examinations were performed only 8 weeks after transplantation. Analysis was made by grouping patients according to time from injury only. No clear clinical or anatomical selection requirements for the surgical procedure, either inclusion or exclusion criteria, were apparent for this series of participants (Dobkin et al. 2006). Subjects who had incomplete SCI and retained functional movements below the lesion were eligible, along with those with a complete traumatic SCI. In addition, there were no strict criteria about the anatomical location for injection of OECs; for example, one patient had cells placed at the rostral C-3 level of an asymptomatic syringomyelia, but the spinal cord injury had caused paraplegia at T7 spinal level. Another patient had cells placed bilaterally into the frontal lobes of the brain (Dobkin et al. 2006). For the above reasons, no definitive conclusions can be drawn from this study based on its experimental design.

There have been another four case series describing intraspinal implantation of olfactory tissues in patients with SCI. The first autotransplantation paradigm was reported by Feron et al., (Feron et al. 2005) This was a Phase 1 study of three adult males at 6–36 months after spinal cord injury who received OECs harvested from the

nasal septum, dissociated and expanded in culture and transplanted an injector/micromanipulator into both normal and damaged spinal cord tissue. No peri-operative complications were reported, and at 1 year after implantation, there was no clinical deterioration in motor, sensory or pain symptoms (Feron et al. 2005).

A subsequent pilot study aimed at determining the safety and feasibility of transplanting whole olfactory mucosa autografts from the patients' nasal septum into the spinal cord cavity (Lima et al. 2006). Seven patients ranging from 18 to 32 years of age in American Spinal Injury Association (ASIA) Class A were treated at 6 months to 6.5 years after injury. Lesions were present at C4–T6 levels and ranged from 1–6 cm in length. Patients were followed from 18 months after surgery. No perioperative complications were reported. One patient reported increase in pain, which was controlled with medication. Another patient reported decrease in sensation following the surgery. Authors attributed this to the fact that they had difficulties in localizing the lesion at the time of surgery. Furthermore, this study also reported preliminary advantageous effects of their treatment; two patients had a significant functional improvement from ASIA class A to class C (Lima et al. 2006).

Lastly, the same group Lima et al., (Lima et al. 2010) published an unblinded, non-randomised study of seven paraplegic and 13 tetraplegic subjects (19–37 years old) who sustained a traumatic SCI 18–189 months previously and received pieces of whole olfactory mucosa in addition to a very aggressive rehabilitation regimen. This study reported improvements in 11 of 20 patients from an ASIA Impairment Scale score of A to C (motor/sensory complete to motor and sensory incomplete). Unfortunately, this study lacked a control group receiving rehabilitation alone.

3.5 The human olfactory mucosa cellular composition and architecture

In most OEC transplantation paradigms, cells have been obtained from the olfactory bulbs of experimental animals. OECs have also been isolated from human olfactory bulbs resected during neurosurgery (Barnett et al. 1993), from olfactory bulbs and olfactory mucosa of cadavers (Miedzybrodzki et al. 2006) and aborted foetuses (Huang et al. 2003). If OECs are to be used clinically, a readily accessible source needs to be identified which allows collection of OECs with low risk and inconvenience to the patient. Ideally, cells should be obtained from the same patient for autologous transplantation to avoid the problems of immune rejection or transmission of viral or prion disease. To overcome these ethical and practical problems, researchers are now focusing on how to obtain sufficient amounts of OECs from the human olfactory mucosa.

The olfactory mucosa consists of a pseudostratified columnar olfactory epithelium resting on a highly cellular lamina propria, separated by it by a basal lamina. The lamina propria contains axon fascicles, blood vessels, connective tissue and Bowman's glands. The olfactory neuroepithelium consists of four major
cell types, the olfactory receptor neurons (ORNs) and glial-like sustentacular cells, microvillar cells and basal cells.

The axons of the 10-20 million olfactory receptor neurons ensheathed by OECs cross the basement membrane of the epithelium into the lamina propria, join together to form bundles or fascicles of axons and pass through the 15-20 foramina of each cribriform plate to synapse within the olfactory bulb.

Sustentacular cells are large columnar cells that surround olfactory receptor neurons. They are presumed to contribute to regulating and maintaining the appropriate ionic milieu around the receptor neurons for olfactory transduction to occur (Morrison et al. 1990).

Basal cells do not project to the epithelial surface and rest on the basement membrane. It is a current belief that basal cells are the stem cells in the olfactory epithelium that divide to give rise to new neural and supporting cells (Roisen et al. 2001; Schwob 2005)

Microvillar cells are flask-shaped cells that extend axon-like cytoplasmic processes into the mucus layer of the epithelium and hypothesized to be a second morphologically distinct class of chemoreceptors. However, their putative role in olfaction has not been definitively demonstrated (Montani et al. 2006).

3.6 Localization of the human olfactory mucosa

Unlike the rodent olfactory mucosa which is easily recognizable by its yellow colour and easily excised from the nasal cavity, in the human, there is no clear delineation between olfactory and respiratory tissue (Kolmer 1927). Both light microscopic and

scanning electron microscopic observations have shown that the olfactory epithelium is intermittently distributed across the nasal mucosa, interspersed with patches of respiratory epithelium (Morrison et al. 1990; Lane et al. 2002). The exact distribution of human olfactory neuroepithelium, however, is not yet known. There is general agreement that it is located high in the nasal cavity, predominantly on the dorsal aspects of the nasal vault, the septum and superior turbinate. It occupies approximately 1.25% of the nasal mucosa with a total of approximately 1-2 cm^2 (Smith 1941; Moran et al. 1982). More importantly, the olfactory mucosa has been shown to decrease with age in 55% of adults and to be completely absent in 13% of elderly patients (Smith 1941). The olfactory ability of these 13% was not measured.

A number of studies have attempted to map the distribution of the human olfactory mucosa. Feron et al. (Feron et al. 1998) first obtained mucosa biopsies from patients undergoing routine nasal surgery. They reported that olfactory tissue is more likely to be found in the posterior nasal cavity, septum, and turbinates; 20% of their specimens contained pure olfactory mucosa and 31% contained mixed olfactory with respiratory mucosa. The greatest proportion of pure olfactory epithelium was detected in the posterior area of the middle turbinate. The highest chance of finding any olfactory tissue however was by taking specimens from the superior turbinate.

In another study, healthy individuals were recruited to investigate the distribution of the olfactory epithelium in humans by means of the electro-olfactogram using vanillin, which specifically excites olfactory receptor neurons and anatomically located biopsy specimens (Leopold et al. 2000). The largest responses were recorded from the olfactory cleft. Histological examination showed olfactory tissue in 47%

specimens from the septum and 41.6% of biopsies from the lateral wall, dorsal to the anterior insertion of the middle turbinate and up to 22 mm anterior to the olfactory cleft on either the lateral or medial walls of the nasal cavity. Notably, tissue without olfactory mucosa was also obtained from the same areas.

Lane et al. (Lane et al. 2002) examined the inferior portion of superior turbinate following resection. It was demonstrated that olfactory mucosa exists only in its medial aspect. Other studies have demonstrated the presence of olfactory mucosa in the anterior septum (Jafek et al. 2002), septum opposite the superior portion of the middle turbinate and superior and inferior portions of the middle turbinate (Rawson et al. 1995; Rawson et al. 1997; Nibu et al. 1999), and replicated the initial observations of the patchy distribution of the olfactory epithelium interspersed with respiratory epithelium in histological analyses (Jafek et al. 2002; Lane et al. 2002).

3.7 Olfactory mucosa biopsy technique

The first study focusing on biopsies of the human olfactory mucosa was published in 1975 by Douek et al. (Douek et al. 1975) who attempted to correlate clinical **m**anifestations with the light and electron microscopic pathologic findings of the olfactory epithelium in selected patients with disorders causing smell abnormalities. The authors took biopsies from the most upper septal surface, using a long thin pair of toothed dissecting forceps, a self-retaining speculum and the operating microscope, but recognized the limitations of the procedure, resulting from the indistinct margins and variable size of the olfactory epithelium.

In 1982, Lovell et al. (Lovell et al. 1982) designed the "olfactory biopsy instrument" (OBI), to avoid crushing artefacts caused by biopsy forceps. It had a 1 mm diameter, 120 mm long shaft ending in a 1 mm long U-shaped trough, designed to collect 3 mm^3 specimens and worked by cutting through the lamina propria and leaving the epithelial surface undistorted. The procedure was performed blindly under local anaesthesia and vasoconstriction, and the septum was the preferred biopsy site because of its vertical orientation and smooth surface. Another study proposed a new technique using the more widely available 3 mm, 70 degree upturned, vertical opening cupped giraffe forceps (Lanza et al. 1993). The success rate was improved when biopsies were performed under endoscopic guidance (2:3.5 as opposed to the success rate of 1:4 to 1:6 with the OBI), and no adverse effect was detected in the sense of smell after olfactory biopsy with this technique. Other researchers have described the use of cupped (Trojanowski et al. 1991) or other special forceps (Nakano's forceps) (Yamagishi et al. 1988) to obtain olfactory tissue. Regardless of the design, forceps can obtain large specimens and also avoid the occasional loss of the tissue that can occur with the OBI. However, all types of forceps crush the specimens resulting in loss of tissue.

Biopsy of the olfactory region carries some inherent theoretical risks, including anaesthetic complications, loss of smell and leak of cerebrospinal fluid (CSF). CSF leak is the most serious potential complication as it may be complicated by intracranial infection and meningitis. The skull base in the region of the olfactory niche is the thinnest in the nasal cavity and can be fractured easily. Because the dura is adherent to the cribriform bone, it is prone to tearing when the bone fractures,

potentially causing a leak of cerebrospinal fluid and an associated risk of meningitis. Particularly high risk areas are, firstly, where the anterior ethmoid artery enters the anterior skull base at the lateral lamella of the cribriform plate and secondly where the middle third of the middle turbinate starts to attach more laterally from the skull base to the lateral nasal wall. To date, there have been no instances of severe complications related to olfactory biopsy reported in the literature. It is important to note however that, as described above, biopsies were taken from lower portions of the nasal cavity, avoiding the more risky region of the olfactory niche, which potentially can result in better success rates.

3.8 OEC yield

Culture of OECs from the OB of rats (Ramon-Cueto et al. 1992; Li et al. 1997), primates (Rubio et al. 2008), dogs (Krudewig et al. 2006; Techangamsuwan et al. 2008) and humans (Barnett et al. 2000) has been achieved in relatively large numbers. However, laboratories culturing OECs agree that it is more difficult to derive a sufficiently large population of cells for human transplantation. Cultured OECs from the olfactory mucosa of dogs constituted of approximately 40% OECs at 7 days and approximately 25% at 21 days, whereas those cultures from the OB of dogs yielded 50% OECs at 7 days and approximately 75% at 21 days (Ito et al. 2006). These changes are accompanied by corresponding increases in the population of fibronectin positive cells (fibroblasts) (Ito et al. 2006). This poses an additional difficulty to the culture of OEC from human olfactory mucosa, in addition to, the small surface of the nasal cavity area covered olfactory mucosa and its relatively unknown location within the nasal cavity.

The aforementioned studies in Section 3.5 investigated the acquisition of olfactory mucosa alone in an attempt to study olfactory neurons. Only two studies have concentrated on the yield of OECs from the obtained biopsy specimen to date. Firstly, Bianco et al. (Bianco et al. 2004) mapped the yield of OECs in different regions. However, their study included only three patients. Choi et al. (Choi et al. 2008) studied the submucosal septal approach of 23 patients who where biopsied with ethmoid forceps during transphenoidal surgery. The authors attempted to "map" of the septal olfactory mucosa to identify rich areas for biopsy. They found better results from postero-superior biopsies and suggested that location is more important than specimen size. However, authors reported that biopsies did not provide sufficient OEC yield for transplantation.

3.9 Conclusion

The presence of ongoing human clinical trials of OEC transplant mediated repair following spinal cord injury may imply that the issues regarding the harvest and culture of human OECs have been resolved and that open issues only refer to details of the clinical application. However, as described in this introductory Chapter, this is not the case. The harvest of human olfactory mucosa and yield of OECs from biopsies remain a hindrance. Alternative culture and biopsy methods using different instruments and from different regions should be investigated to further improve the likelihood of successful clinical applications. In the next Chapter, we investigate the yield of OECs from biopsies of human olfactory mucosa using a new surgical

technique and focusing on the superior turbinate. Factors leading to better cell proportions are also examined.

Chapter 4

Translating basic research in to clinical practice: Harvesting human Olfactory Ensheathing Cells

This chapter presents a study investigates methods by which OECs can be harvested from the human nasal cavity and features that would lead to a better yield. The study describes a new reproducible surgical approach for biopsies of the superior turbinate and correlations between OEC yield and specimen- and patient-related features are performed to assess conditions that would lead to a higher yield of OECs from human specimens of the superior turbinate. Given the finding of previous studies investigating the location of the human olfactory mucosa, it was decided to focus to the cranial portions of the superior turbinate where it is believed that OECs are more closely packed as olfactory axons coalesce to cross through the cribriform plate.

4.1 Aims

The aims of this chapter are threefold. The first aim is to describe a safe and reproducible surgical technique for obtaining human olfactory mucosa biopsies. Our second aim is to determine the areas within the olfactory mucosa of the superior turbinate that systematically provide sufficient OEC yields to enable a more targeted biopsy. Thirdly, we aim to identify factors within the patients' medical history that may affect the yield of OEC cultures from the human olfactory mucosa.

4.2 Materials and Methods

4.2.1 Patients

Consecutive patients who presented to the Royal National Throat Nose and Ear Hospital and the National Hospital for Neurology and Neurosurgery for functional endoscopic sinus (FES) surgery were invited to participate in this observational study. The majority of patients required nasal surgery for symptoms of nasal obstruction, reduction of sense of smell and excessive secretions, pain and pressure, caused by inflammatory polyposis and infective rhinosinusitis refractory to medical therapy or benign or malignant tumours. The aim of the operation was to improve the ventilation of the sinuses and restore mucociliary clearance.

The patients' medical history was documented including age, sex, presenting complaint, past medical and surgical history, drug history including use of topical and/or oral steroids, allergies and smoking status.

4.2.2 Surgical Procedure - Endoscopic Method

The surgical technique for our biopsies was developed by the principal surgeon (PA). Another three surgeons provided specimens according to the principal surgeon's directions and technique (Table 4.2). All surgeons are Consultants in ear, nose and throat surgery with special interest in FES surgery under general anaesthesia.

All patients were operated under general anaesthesia. Patients received topical treatment with either Cophenylcaine spray (Lignocaine hydrochloride 50mg/ml and Phenylephrine hydrochloride 5mg/ml) or Moffatt's solution (2 ml of 6% cocaine, 1 ml of 1:1000 epinephrine, 2 ml of 8% sodium bicarbonate, made up to 10 mls with 5

mls of normal saline) placed on a thin ribbon gauze in the nasal airway for approximately 10 minutes to maximize vasoconstriction and anaesthesia. Ribbon gauzes soaked in 1:10,000 epinephrine are placed into the middle and superior meati by the operating surgeon, so as to maximize vasoconstriction. Patients were placed supine in 20° head-up position to reduce the venous pressure and anaesthetic hypotensive technique was used keeping the mean blood pressure between 65 and 75 mmHg. Surgery was performed using the 0° 4 mm endoscope.

For each patient, we aimed to obtain a specimen from the superior turbinate, as close to the olfactory cleft as possible avoiding the risk of a CSF leak but also enabling reproducibility. Particular effort was also made to include the whole thickness of the mucosa to ensure that the lamina propria is not left behind. The olfactory biopsy specimen was obtained as follows: The superior turbinate was gently medialised and inspected. A portion of the middle third of the superior turbinate was resected using endoscopic microscissors. Two cuts were made through the superior turbinate, perpendicular to the skull base using endoscopic microscissors. A third incision was made joining the two parallel incisions using curved microscissors. Using Blakesley forceps, the resected middle section was gently retrieved. Biopsies of 3 to 4 mm in size were obtained. The position of the specimen was recorded on a diagram of the nasal cavity and a snap shot image or movie of the procedure was taken.

The specimen was immediately placed in ice-cold (4°C) complete culture medium consisting of Dulbecco's Modified Eagle Medium/Ham's Nutrient Mixture (Logan, UT) F-12 (DMEM/F12) (1:1 DMEM/F12 with GlutaMAX [Invitrogen]), 1% insulin-transferrin-selenium (1.0 mg/ml insulin, 0.67 mg/ml transferrin, and 0.55 mg/ml

selenium) (insulin-transferrin-selenium; Invitrogen), 10% deactivated foetal calf serum (Invitrogen) and transferred to the laboratory. Postoperatively patients were nursed 30° head-up position. An epinephrine (1:10 000) soaked pack was placed for more than minor oozing.

4.2.3 Processing of olfactory mucosa biopsies

On arrival to the laboratory, the specimen was transferred in Hanks' Balanced Salt Solution (HBSS) (calcium and magnesium free; Invitrogen Ltd., Paisley, UK) supplemented with 100 U/ml of penicillin and 100 μg/ml of streptomycin (Invitrogen). Blood clots, debris and bone were removed from the specimen. The specimen was then photographed and its greatest diameter recorded. Subsequently, the specimen was divided into 2 pieces, one for histology and one for culture.

4.2.4 Culture Procedure

After removal of the excess solution, the portion of the specimen for culture was weighed on an analytical balance (Precisa 262SMA-FR, readability 0.1–0.01 mg; Precisa Balances, Ltd., Milton Keynes, UK). Specimens were then transferred to 35 mm dishes filled with growth media (as described above), cut into small pieces to approximately 1-2 mm^2 in size, transferred to 2 ml of digestion mixture containing 2.4 U/ml Dispase II (Roche) and 0.25% collagenase (Type H; Sigma) in DMEM/F12 incubated in at 37°C for 30 min and triturated to remove lumps using a flame-polished Pasteur pipette. The enzymatic reaction was stopped by adding 8 ml of

Hanks' Balanced Salt Solution. After centrifuging at 300 x *g* for 5 minutes the supernatant was discarded and the tissue pellet was further triturated into cell suspension in the complete culture medium, and penicillin and streptomycin to a cell density of 2 to 2.5 x 104/cm2. The resulting cells were plated down in 35 mm culture dishes (Nunclon) coated with poly-L-lysine 50 ug/ml (Sigma) and maintained in a humidified incubator enriched with 5% CO_2 for 10-14 days at 37°C. The culture medium was replaced every 3 days. The cell cultures were observed with daily inverted light microscopy under aseptic conditions. Beyond 14 days of culture, fibroblast proliferation outstripped the growth rate of OECs, and at 14 days, the number of OECs was felt to be optimum.

4.2.5 Immunocytochemistry

After 10-14 days in culture, cells were rinsed in 0.01 M phosphate-buffered saline (PBS), fixed in 4% paraformaldehyde in PBS at 4°C overnight, rinsed in PBS, permeabilised and blocked with 2% skim milk (Merck KGaA, Germany) in PBS containing 0.1% Triton X-100 (TAAB) for 30 minutes. They were then incubated in primary antibody solution at 4°C overnight, washed in PBS three times with 10 minute intervals and incubated with appropriate species fluorescent secondary antibody solutions at room temperature for 2 hours. After washing three times, cells were counterstained with 4', 6-diamidino-2-phenylindole (DAPI; Invitrogen), mounted using ProLong® Gold Antifade (Invitrogen) and coverslipped. The primary antibodies used to identify OECs were mouse anti-human low-affinity neurotrophin receptor (anti-$p75^{NTR}$; 1:500; Sigma, N5408) and rabbit anti-S100β Ig (1:500; Dako,

Z0311) and, for olfactory nerve fibroblasts, rabbit anti-human fibronectin (1:1000; Dako). The secondary antibodies used for simultaneously visualizing anti-p75 and anti-fibronectin were Alexa-488 goat anti-mouse and Alexa-546 goat anti rabbit, and for anti-S100β, Alexa-488 goat anti-rabbit. All antibodies were diluted in PBS containing 2% milk and 0.1% Triton X-1000.

4.2.6 Histology procedure and immunohistochemistry

The pieces of specimens reserved for histology were fixed in 4% paraformaldehyde in PBS overnight. They were then cryoprotected in 10% followed by 20 % sucrose in PBS solution at 4°C until the specimen sunk. 12 µm sections were cut on a cryostat (Leica CM3050), mounted on MAS coated slides (S-9441, Matsunami Glass Ind., Ltd.) and allowed to dry at room temperature for 24 hours. The sections were washed in PBS several times, blocked with 2% skim milk (Merck KGaA, Germany) in PBS containing 0.1% Triton X-100 for 30 minutes, incubated in primary antibody solution at 4°C overnight, washed in PBS several times and incubated with appropriate species fluorophore-conjugated secondary antibody solutions as above. The primary antibodies used to identify OECs were anti- $p75^{NTR}$ (1:500), anti-S100 (1:500) anti-tubulin (beta III isoform, 1:500, Chemicon) and background staining using sytox orange nucleic acid stain (1:500, Invitrogen, CBL412). The secondary antibodies used were the same as for immunocytochemistry.

4.2.7 Methods of data interpretation and Statistical analysis

4.2.7.1 Confocal Microscopy, Digital Image analysis and estimation of OEC yield

Fluorescent microscopy and image acquisition were carried out using a confocal laser scanning microscope (TCS SP1, Leica Microsystems, UK Ltd). Confocal z-planes were captured for the complete thickness of the culture and the two dimensional images were generated by projecting the z-stack using the Leica software. Image Pro Plus Version 6.0 (Media Cybernetics, Inc. Bethesda, MD, USA) was used to calculate the pixel density of red and green channels representing fibroblasts and OECs respectively, which was then converted to surface area of dish covered by red and green.

OEC yield was estimated indirectly by calculating the surface area of the culture dish covered by red and green of five representative images of each dish. Each image covered 1 mm^2 of each 35 mm culture slide. Representative images captured included the area of the dish covered with the worst and best green pixel densities and another three randomly selected locations. The proportion of the area covered by OECs (green pixels) over the total area covered by cells (red plus green pixels) was subsequently calculated and converted to a percentage of the area imaged, representing OEC yield.

4.2.7.2 Correlation between cell yield and specimen- and patient- related factors

The relationship between OEC and fibroblast yield with patient characteristics and specimen factors were assessed using Spearman's rank correlation coefficient (rho) after testing for normality. To compare the OEC yield among different surgeons, a one-way ANOVA was used correcting with Bonferroni, Scheffe and Sidak multiple comparison tests.

Patients' perception of sense of smell was graded in a scale of 0 to 4; "0" = complete absence of sense of smell, "1" = severe loss of smell, "2" moderate loss of smell and "3" = mild loss of smell and "4" = normal sense of smell.

To grade the degree of mucosal disease in the region of the superior turbinate, we used the validated Lund-MacKay endoscopic appearances score (Annamalai et al. 2003) but modified to include only the side of the nasal mucosa the biopsy was taken from (Table 4.1). The region the biopsy was assigned a grade according to the modified Lund-MacKay endoscopic appearances score by the operating surgeon and researcher at the time of surgery.

Table 4.1: Modified Lund – MacKay scoring system: endoscopic appearance (scores for side the biopsy was taken from only)

Characteristic	Grade			
Polyp	0 = absence of polyps	1 = polyps in middle meatus only	2 = polyps beyond middle meatus but not blocking the nose completely	3 = polyps completely obstructing the nose
Oedema	0 = absent	1= mild	2= severe	-
Discharge	0 = no discharge	1= clear, thin discharge	2 = thick, purulent discharge	-
Scarring	0 = absent	1 = mild	2 = severe	-
Crusting	0 = absent	1 = mild	2 = severe	-

4.2.7.3 Distribution of olfactory mucosa in the superior turbinate

To systematically map the position of olfactory mucosa within the superior turbinate, we devised a reproducible method by which the position of the biopsies were recorded at the time of the biopsy. A grid was placed on a schematic representation of the superior turbinate dividing the surface area of the superior turbinate in 24 positions (6 columns in the antero-posterior dimension and 4 rows in the cranio-caudal dimension) as shown in Figure 4.7 A and B. Spearman's rank correlation coefficient (rho) was used to correlate OEC yield and olfactory mucosal positions.

All statistical analysis was performed using STATA statistical software Version 11 (StataCorp LP, College Station, TX). Statistical significance was accepted at the 5% level ($p < 0.05$).

4.2.8 Comparison of OEC yield from the superior turbinate versus septal biopsies using blind endonasal approach

Twenty-six consecutive patients who presented to the National Hospital for Neurology and Neurosurgery for pituitary surgery were asked to participate in this observational study. Informed consent was obtained, and all procedures were performed with the approval of the hospital's research ethics committee.

Specimens of septal mucosa were obtained using an endonasal approach to the sphenoid sinus as described in our laboratory's previous study (Choi et al. 2008). In brief, 3-4 mm biopsies were taken from the superioroposterior aspect of the nasal septal mucosa using an Angel-James or Williams rongeur. A radiograph was obtained using an intraoperative image intensifier to plan and document the position of the biopsy. Processing, culture, immunocytochemistry and digital analysis were performed as described in the previous sections of this thesis chapter for the superior turbinate specimens. A Student's t-test (t) was used to compare OEC yields achieved by the two different methods.

4.3 Results

4.3.1 Description of specimens

In total, 43 superior turbinate specimens from different patients were included in the statistical analysis. Thirty-seven specimens (86%) were obtained by the primary

surgeon (PA), PC obtained 3 (6.97%), CE 2 (4.65%) and MP 1 (2.32%) (Table 4.2). An analysis of variance conducted to compare the effects of different surgeons performing the surgical procedure on OEC yield, which demonstrated no statistically significant differences among the four surgeons ($F(3,39) = 2.86$; $p = 0.049$). Posthoc analyses using Bonferroni, Scheffe and Sidak post hoc criteria confirmed that the mean of OEC yield for each surgeon was not significantly compared with other surgeons'. The mean average weight of the specimen used for culture was 26.53 μm with a range of 3.8 -143 μm (sd; 26.2). A Spearman correlation coefficient showed no significant correlation between the OEC yield and weight of specimen cultured (rho = 0.25; p = 0.14; 95%CI = -0.05 to 0.51).

Table 4.2: *Number of specimens obtained by each surgeon, mean and standard deviation of the proportion of OECs for each surgeon.*

Surgeon	**Frequency No (%)**	**Average proportion of OEC yield per surgeon (%) Mean (Sd)**
PA	37 (86.05)	0.21 (0.23)
PC	3 (6.97)	0.47 (0.66)
CE	2 (4.65)	0.62 (0.39)
MP	1 (2.32)	0.13 (0)

4.3.2 Histology of human olfactory mucosa and human OECs in culture

There were 34 out of the total 43 available specimens (79.1%) for immunohistochemical analysis. The remaining 9 were not analyzed for one of the following reasons: a) the culture specimen was not large enough for both culture and

histological analysis, b) the specimen was lost, c) the specimen was destroyed due to technical errors.

Figure 4.1 shows the histological organization of the human olfactory mucosa. The olfactory mucosa is composed of two distinct tissue layers: the outer epithelium and the deeper lamina propria. The primary olfactory axons penetrated the basal lamina of the epithelium to enter and traverse the underlying lamina propria. The lamina propria is composed of numerous olfactory nerve fascicles of varying sized as well as arterioles, venules and serous glands. OECs form conduits through which bundles of olfactory axons pass during their course in the lamina propria to the olfactory bulb.

Within the human LP the olfactory nerve bundles are immunoreactive for neurofilament. OECs were easily distinguished within the lamina propria by their immunoreactivity to $p75^{NTR}$ and S100. $p75^{NTR}$ and S100 immunopositive olfactory bundles were identified in 32 out of the 34 (94.1%) specimens analysed.

(A)

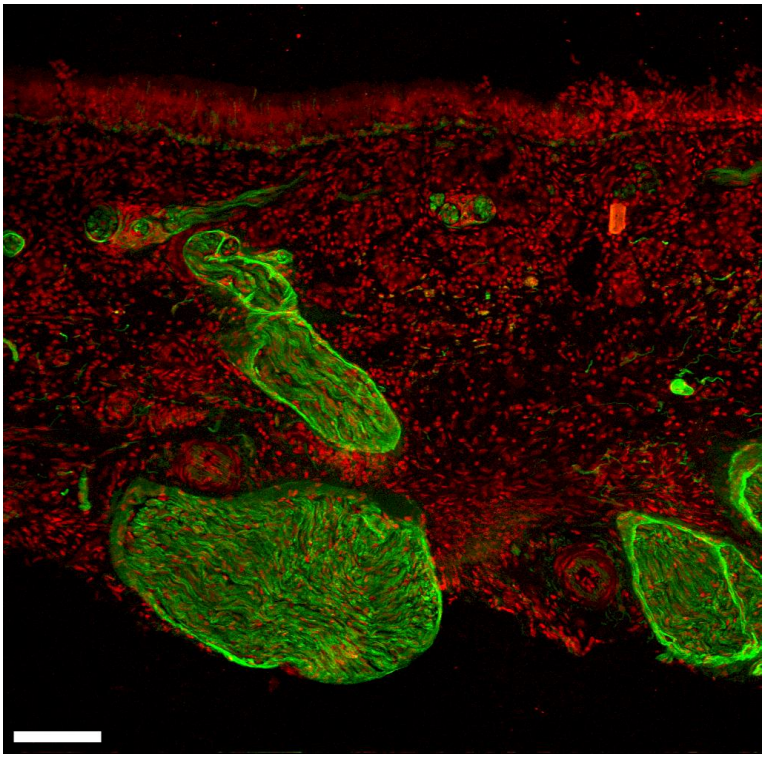

(B)

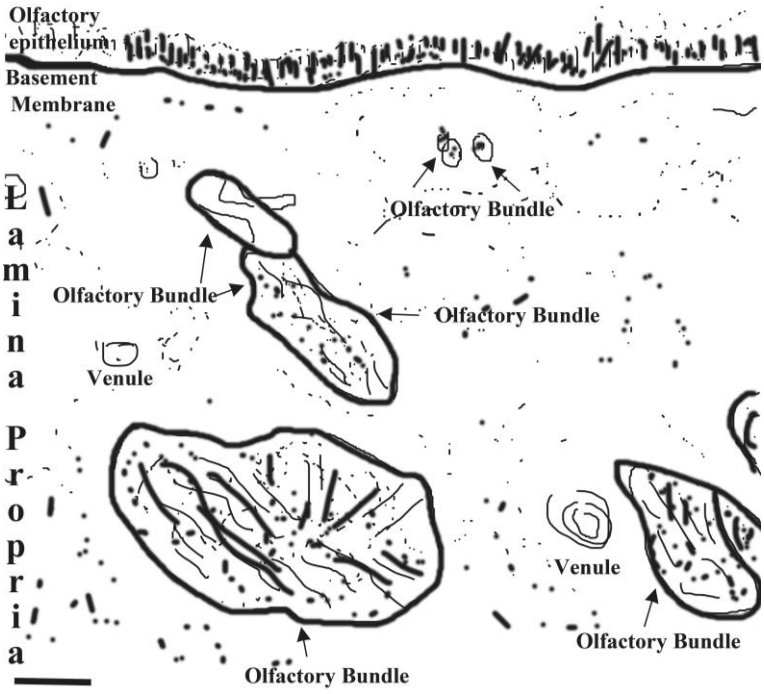

Figure 4.1: (A) *Section of human olfactory mucosa from the superior turbinate stained with anti-p75^{NTR} antibody to label OEC (green) and sytox antibody to label cell nuclei. Olfactory axons coalesce to form bundles within the lamina propria;* ***(B)*** *Schematic representation of the components of the olfactory mucosa; scale bar = 100 μm; (Kachramanoglou et al. 2012) Permission to reproduce this image has been granted by Wolters Kluwer Health.*

(C)

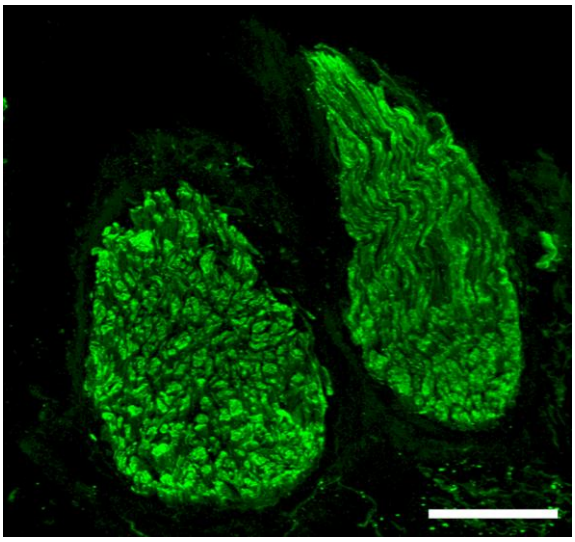

(D)

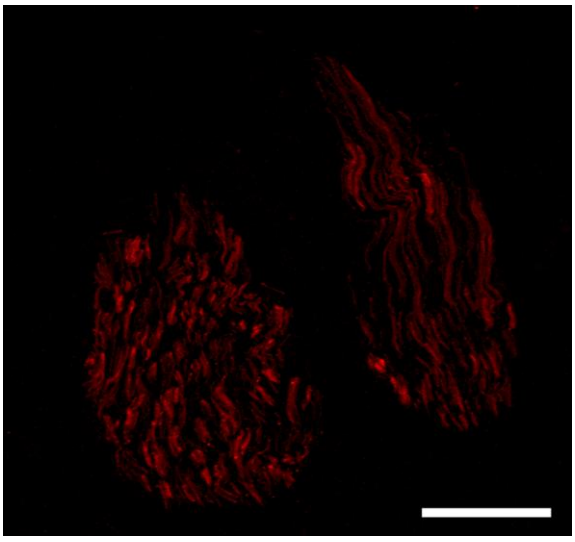

(E)

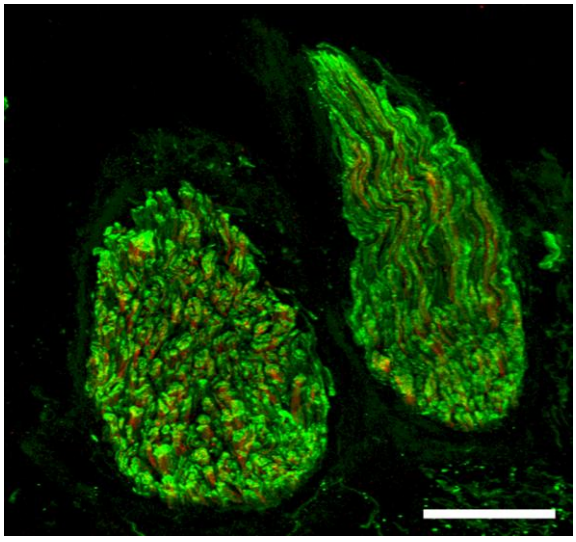

Figure 4.1 cont.: (C) *Magnified view of a cross section through an olfactory bundle consisting of OECs within the lamina propria**,** immunostained with anti-S100β antibody (green)* ***(D)*** *The same magnified image (A) of an olfactory bundle showing olfactory axons stained with anti-tubulin antibody (red), (E) Overlay of images C and D demonstrating close association and ensheathment of olfactory axons by OECs; scale bar = 100 μm; (Kachramanoglou et al. 2012) Permission to reproduce this image has been granted by Wolters Kluwer Health.*

(F) 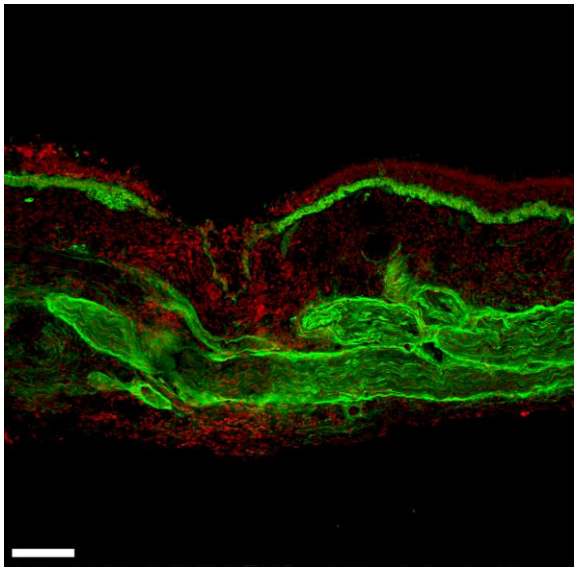

Figure 4.1 cont.: (F) *Longitudinal section of an olfactory bundle, OECs are stained with anti-p75^{NTR} (green), background stain with sytox orange (red) staining all nuclei; scale bar = 100 μm; (Kachramanoglou et al. 2012) Permission to reproduce this image has been granted by Wolters Kluwer Health.*

4.3.3 Morphology of human OECs in Culture

OEC culture was attempted in all 43 specimens collected. At least one p75^{NTR} immunoreactive cell with the characteristic morphology of OECs was identified in 42 out 43 biopsies assessed (97.7%).

A representative image of OEC culture from the superior turbinate is shown in (Figure 4.2). p75^{NTR} labeling demonstrates elongated, triangular, spindle or stellate shaped cells bearing long and thin tapering processes which become segregated into swathes of cells. Fibronectin positive cells (fibroblasts) formed a layer beneath the

p75^{NTR} positive cells and were not seen to extend long processes as the p75^{NTR} positive cells.

(A)
(B)

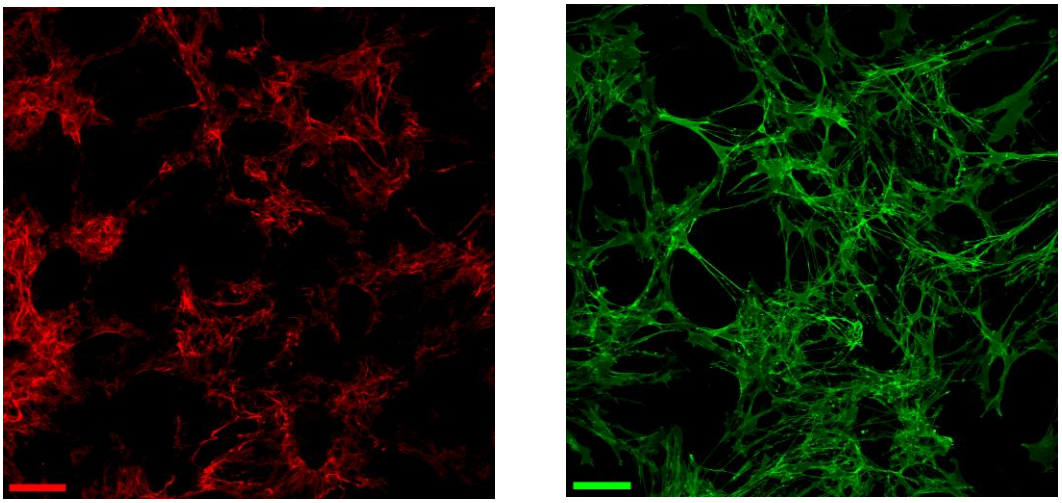

(C)

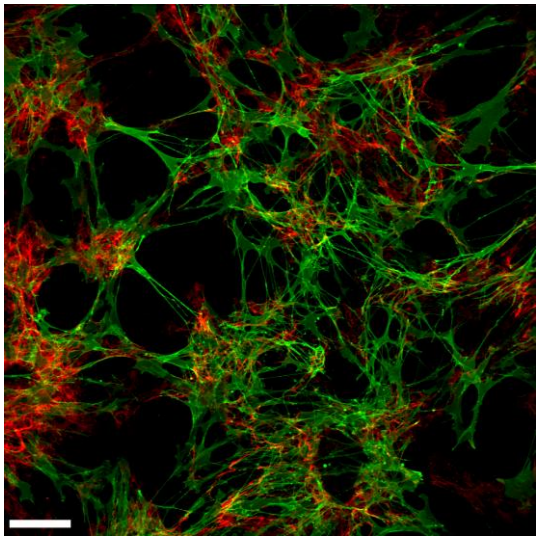

Figure 4.2: *Photomicrograph of human OEC culture; (A) fibroblasts labeled with anti-fibronectin antibody (red) (B) OECs labeled with anti-p75^{NTR} antibody (green); (C) superimposed images; scale bar = 100 μ (Kachramanoglou et al. 2012) Permission to reproduce this image has been granted by Wolters Kluwer Health.*

4.3.4 OEC yield

Analysis of OEC cultures obtained from the superior turbinate showed a mean surface area stained red of 37.12% (sd; 26.22, range; 0.09-90.60), representing fibroblasts and a mean surface area stained green of 7.94% (sd; 9.72, range; 0-42.45), representing OECs. The mean proportion of the surface area stained green (OECs) over the total amount of surface area stained by cells was 0.25 (sd; 0.28; range; 0-0.97) (Table 4.3). The proportion of OECs and fibroblast for each specimen analysed is given in Figure 4.3.

Table 4.3: *Mean and standard deviation of surface area stained green (*$p75^{NTR}$ *labeling) and red (fibronectin labeling).*

	Mean	SD
Surface area stained red (%)	37.12	26.22
Surface area stained green (%)	7.94	9.72
Proportion of surface area stained green/red+green (%)	0.25	0.28

4.3.5 Description of Patients and influence of patient-related factors on OEC yield

Of the 43 patients included in the study, 25 were men patients and 18 were women. The mean age was 44 years, ranging from 18 to 81 years of age. A Spearman correlation coefficient did not reveal a statistical significant correlation between

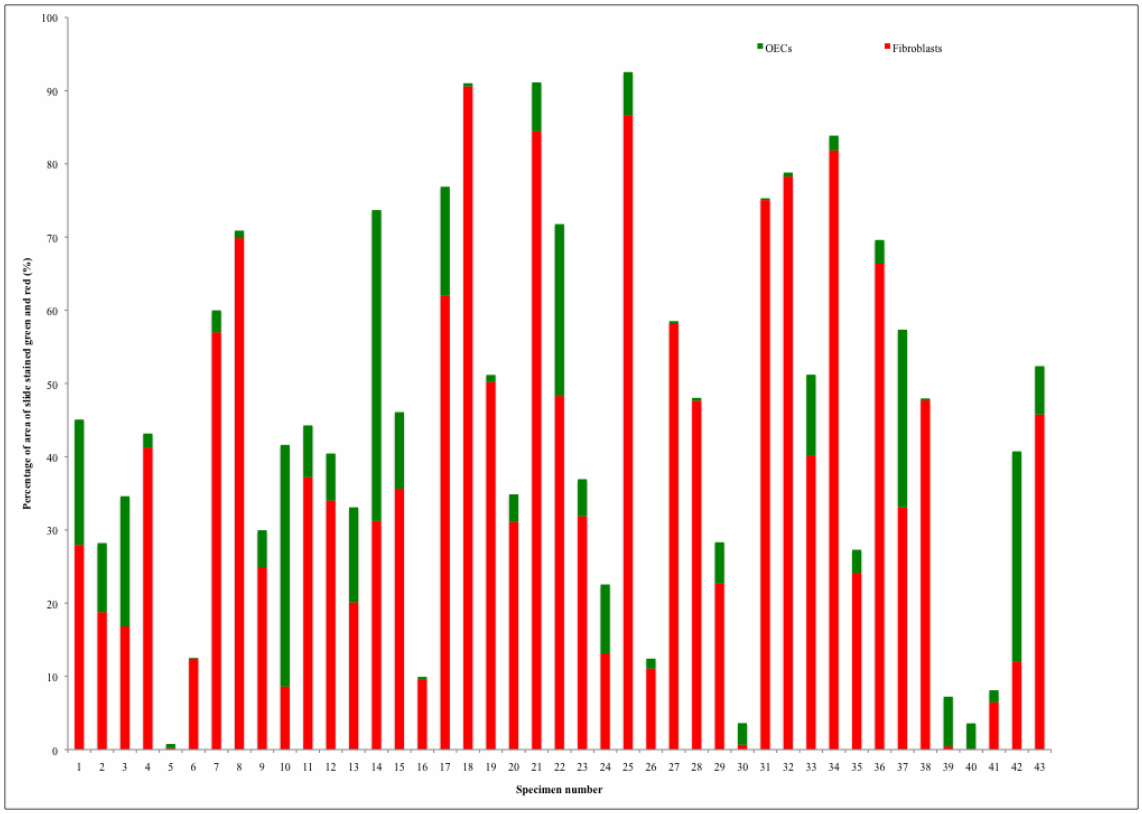

***Figure 4.3**: Graph showing the percentage of surface area per 1mm^3 surface area of the each slide covered by OECs (Green; anti-p75 labeling) and fibroblasts (Red; anti-fibronectin labeling) for each biopsy specimen of the superior turbinate. (Kachramanoglou et al. 2012) Permission to reproduce this image has been granted by Wolters Kluwer Health.*

donor gender and OEC yield (rho = -0.02; p = 0.90; 95%CI = -0.32 to 0.28). In contrast, OEC yield was found to be negatively correlated with donor age; greater OEC yields being achieved with decreasing age of donors (rho = -0.32; p = 0.034; 95%CI = -0.569 to -0.026) (Figure 4.4).

Of the 43 patients included in the study, 7 (17%) reported no sense of smell, 6 (14%) reported severe loss of sense of smell, 13 (31%) reported moderate loss of sense of smell and 15 (36%) reported only mild loss of sense of smell. Eleven (25.6%) were smokers and 32 (74.4%) were non-smokers at the time of the biopsy. Thirty-five out of the 43 patients (81.40%) received topical steroids in the pre-operative period and 8 (18.6%) patients were administered oral steroids. In 11 out of 43 donors (25.6%), the nasal cavity was treated with Cophenylcaine and 32 patients (74.4%) were treated with Moffatt's solution.

Spearman correlations did not demonstrate correlation of between OEC yield and sense of smell (rho = - 0.06; p = 0.68; 95%CI = -0.41 to 0.36), steroid use (rho = -0.11; p = 0.48; 95%CI = -0.40 to 0.2 for topical steroids and rho = 0.12; p = 0.43; 95% CI = -0.18 to 0.41 for oral steroids), smoking (rho = -0.25; p = 0.11; 95%CI = -0.51 to 0.06), or preparatory solution used (rho = 0.22; p = 0.16; 95%CI = -0.09 to 0.49).

4.3.6 Influence of nasal mucosal disease on OEC yield

Histological analysis of specimens included in this study revealed that out of 43 patients, 20 patients (46.51%) had confirmed benign nasal polyposis, 15 patients (34.88%) suffered with rhinosinusitis, 5 (4.65%) showed infections including 1 fungal infection, 1 (2.33%) showed a simple cyst and 2 showed no evidence of mucosal disease (11.63%) (Table 4.4). Of the 20 patients with the diagnosis of nasal

polyposis, 5 (11.63% of total 43 of patients) had grade 1, 6 (13.95%) had grade 2 and 9 patients (20.93%) had grade 3 (Table 4.5).

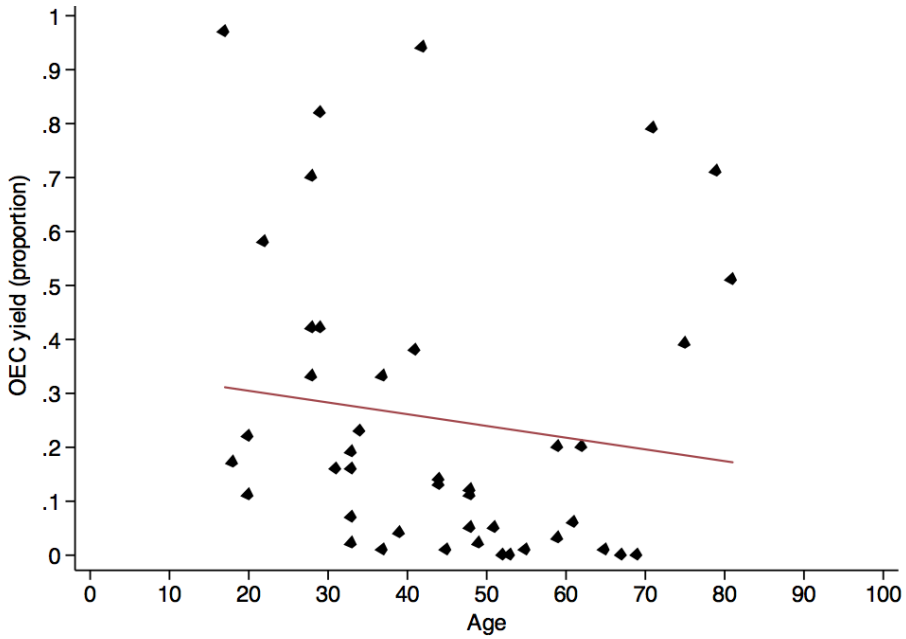

Figure 4.4: *Graph showing the association between age of patients and OEC yield; rho = -0.32; P = 0.034; 95%CI = -0.569 to -0.026 (Kachramanoglou et al. 2012) Permission to reproduce this image has been granted by Wolters Kluwer Health.*

Table 4.4: *Histological diagnoses for the 43 olfactory mucosa specimens analysed*

Nasal Pathology	**Frequency (Number)**	**Percent (%)**
Polyposis	20	46.51
Rhinosinusitis	15	34.88
Infection	5	11.63
Cyst	1	2.33
No nasal disease	2	4.65

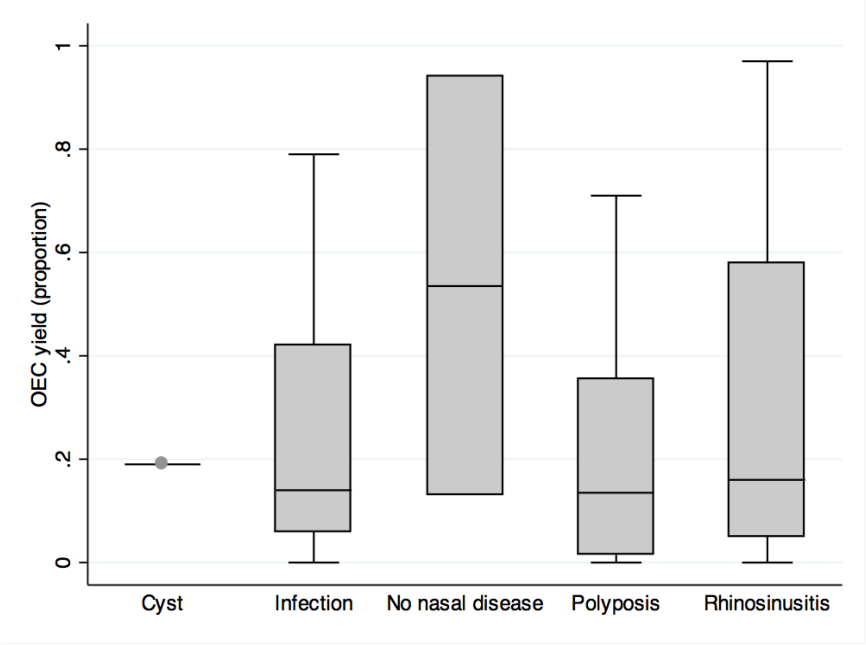

Figure 4.5: *Box plot showing the average proportion of OEC yield for each histological diagnosis. (Kachramanoglou et al. 2012) Permission to reproduce this image has been granted by Wolters Kluwer Health.*

Table 4.5: *Grading of polyposis and average OEC yield for each grade.*

Grade of polyposis	Frequency (Number)	Percent (%) of total 43 patients
Grade 1	5	11.63
Grade 2	6	13.95
Grade 3	9	20.93

4.3.7 Influence of mucosal disease on OEC culture yield

The average of OEC yields for each histological diagnosis is given in Figure 4.5. There was no significant correlation between OEC yield and histological diagnosis or grade of polyposis. The yield of OECs, however, was negatively correlated to the modified Lund-MacKay endoscopic appearance score, such that patients with worse

mucosal disease yielded poorer cell cultures (rho = -0.52; p = 0.0003; 95%CI = -0.71 to -0.26) (Figure 4.6). Greatest yields were found in patients with absence of mucosal disease (Figure 4.6).

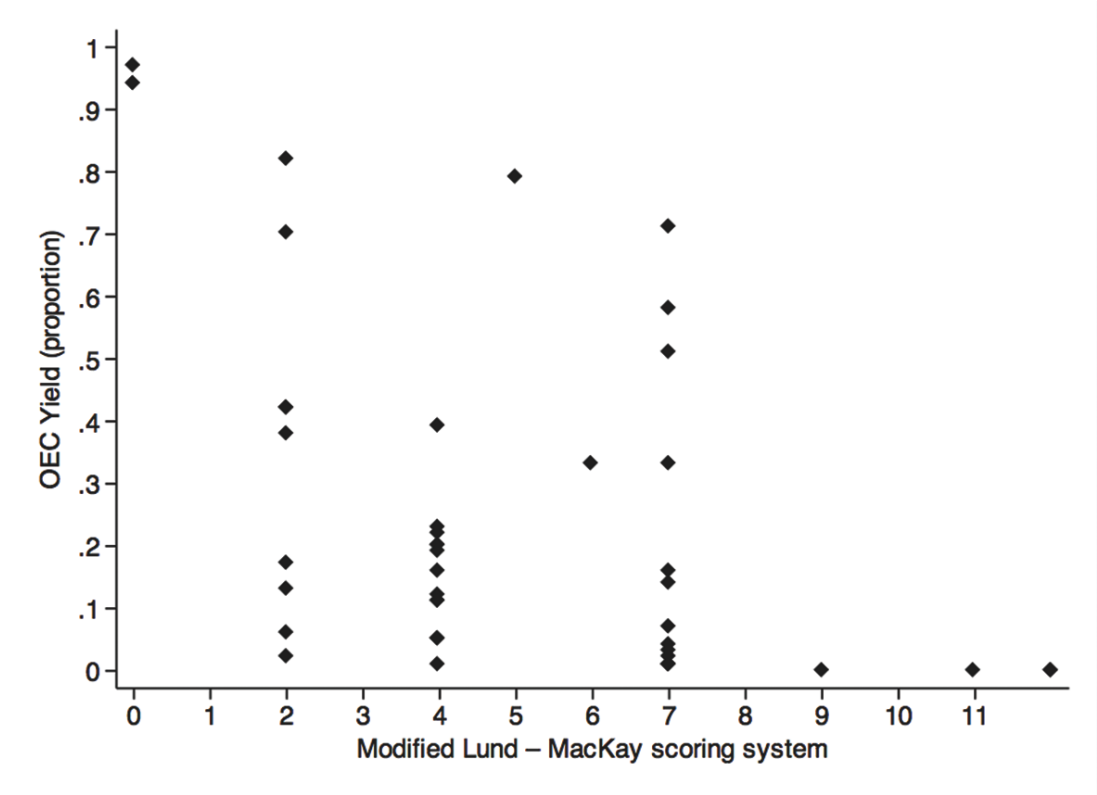

Figure 4.6: *Graph showing the association between the Modified Lund – MacKay endoscopic appearance scoring system and OEC yield; rho = -0.52; P = 0.0003; 95%CI = -0.71 to -0.26. (Kachramanoglou et al. 2012) Permission to reproduce this image has been granted by Wolters Kluwer Health.*

4.3.8 Distribution of human olfactory mucosa and influence of biopsy position on OEC culture yield

Thirty-eight specimens were included in the statistical analysis of the biopsy distribution. The remaining 5 positions were not recorded.

Larger OEC yields were positively correlated with biopsies harvested from the more cranial portions of the superior turbinate (rho = -0.61; p = 0.000; 95%CI = -0.78 to -0.37) (Figure 4.7 and 4.8). OEC yield did not correlate with the ventro-posterior location of the biopsy (rho = -0.01; p = 0.0.94; 95%CI = -0.33 to 0.31) (Figure 4.9).

(A)

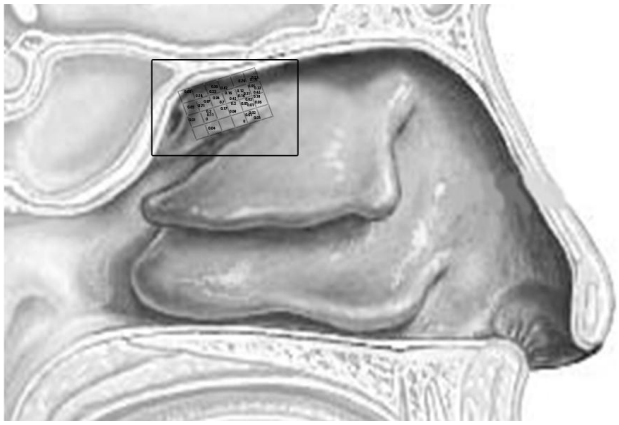

(B)

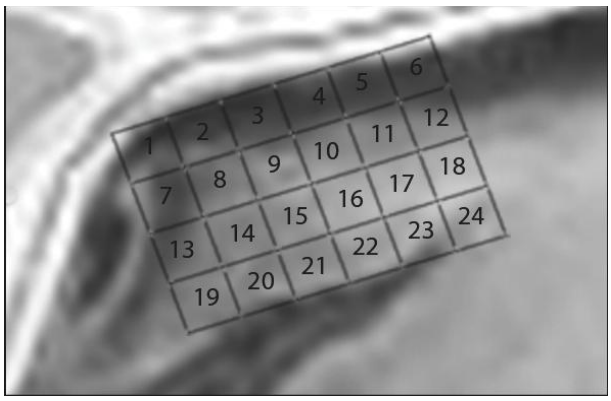

(C)

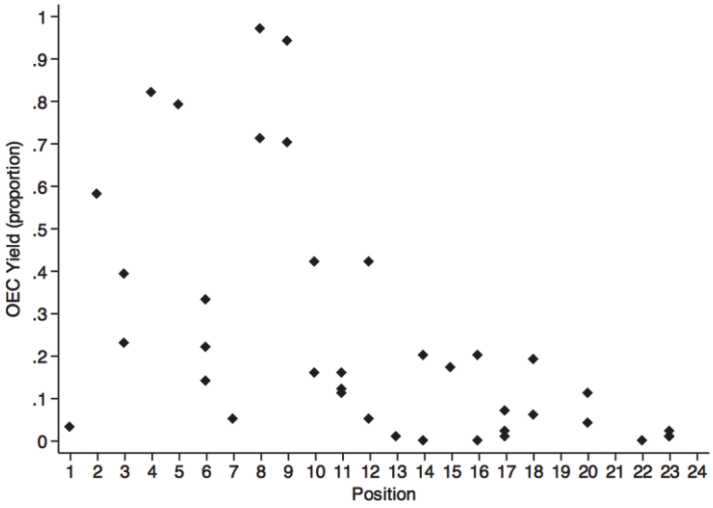

Figure 4.7: *(A) Schematic representation of olfactory mucosa biopsy location; (B) Magnified image of the superior turbinate. The superior turbinate was divided in 24 locations to determine locations within the turbinate that result in higher OEC yields; (C) Graph showing the average proportion of OEC yield for each location in B. (Kachramanoglou et al. 2012) Permission to reproduce this image has been granted by Wolters Kluwer Health.*

(A)

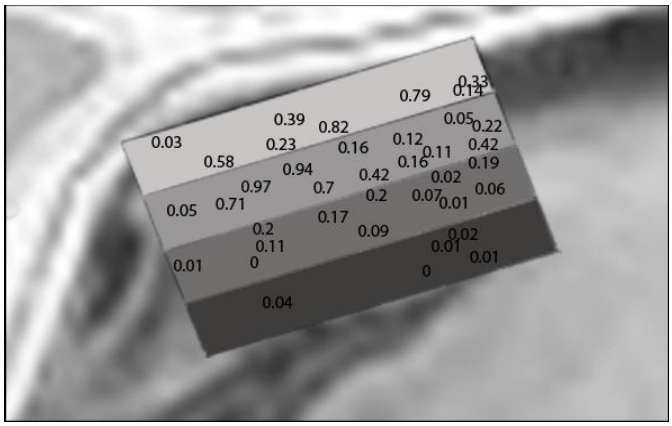

(B)

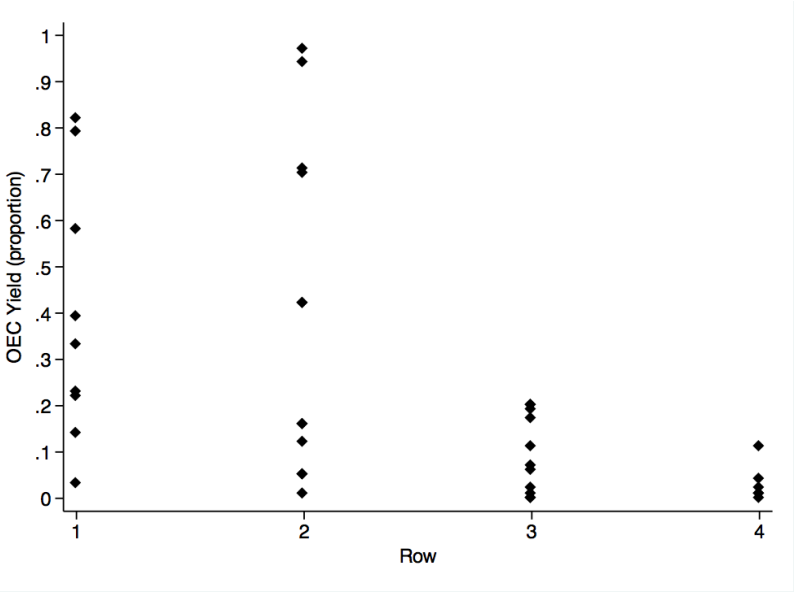

Figure 4.8: (A) *Schematic representation the superior turbinate divided in four rows to determine whether biopsies from more cranial locations result in higher yields. (B) Graph showing the association of location of OEC biopsy relative to its proximity to the cribriform plate and OEC yield; rho = -0.61; p = 0.000; 95%CI = -0.78 to -0.37. (Kachramanoglou et al. 2012) Permission to reproduce this image has been granted by Wolters Kluwer Health.*

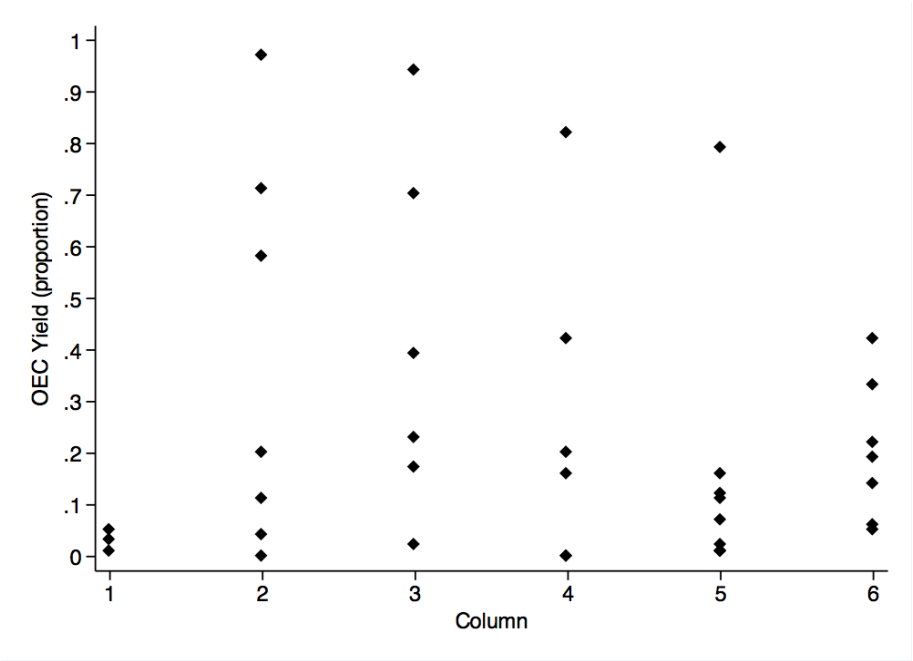

Figure 4.9: *Graph showing the association of location of OEC biopsy relative to its antero-posterior location and OEC* yield; rho = -0.01; p = 0.0.94; 95%CI = -0.33 to 0.31. *(Kachramanoglou et al. 2012) Permission to reproduce this image has been granted by Wolters Kluwer Health.*

4.3.9 Comparison of OEC yield from the superior turbinate versus septal biopsies using blind endonasal approach

OECs were cultured from all 26 specimens of the septal mucosa. The proportion of OECs and fibroblast for each specimen analysed is given in Figure 4.10. Analysis of OEC cultures obtained from the septal mucosa showed a mean surface area stained red of 28.04% (sd; 26.25, range; 0.08 - 87.03), representing fibroblasts and a mean surface area stained green of 9.86% (sd; 19.69, range; 0.02 - 83.88), representing OECs. The mean proportion of the surface area stained green (OECs) over the total amount of surface area stained by cells was 0.25 (sd; 0.29; range; 0 - 0.99).

The yield of OECs was found not to show a statistically significant difference between specimens from the superior turbinate and septum when compared using a Student's t-test (t (67) = -0.009; 95%CI = - 0.19 - 0.31; p = 0.993)

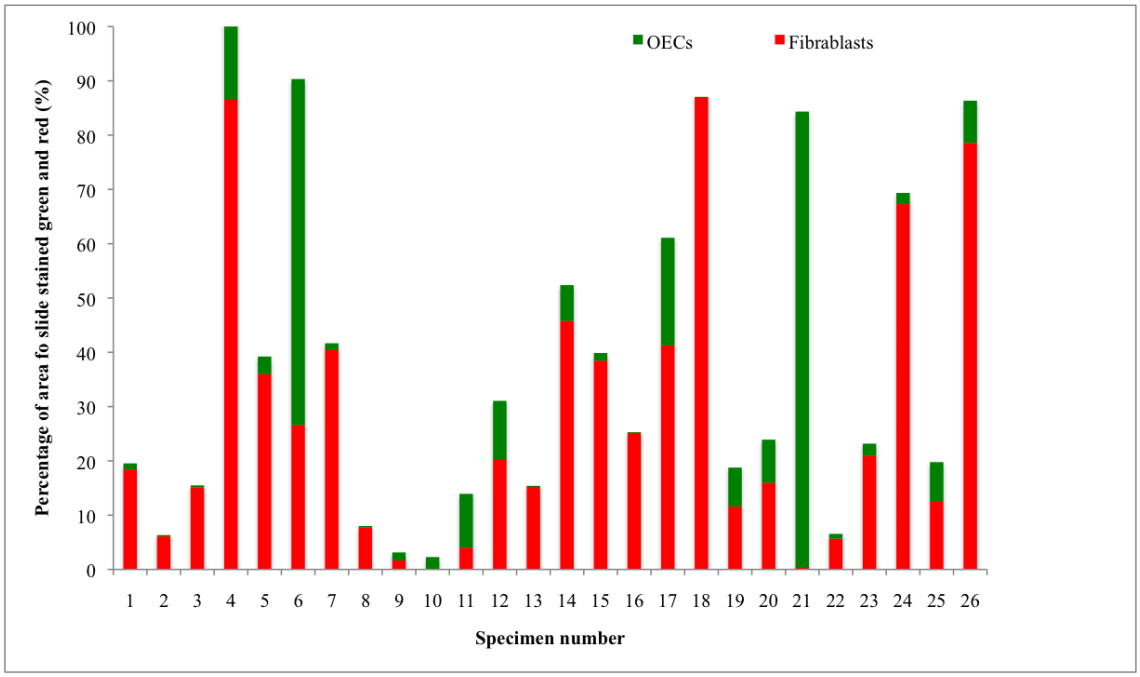

Figure 4.10: *Graph showing the percentage of surface area per 1mm^3 surface area of the each slide covered by OECs (Green; anti-p75^{NTR} labeling) and fibroblasts (Red; anti-fibronectin labeling) for each biopsy specimen of the septal mucosa.*

4.4 Discussion

In the current study we cultured OECs from 43 specimens obtained from the superior aspects of the superior turbinate using an endonasal approach and correlated OEC yield with patient and specimen related factors. This is the first study to investigate

OEC yield from superior turbinate, as opposed to, purity of olfactory mucosa obtained and the first study to assess factors that affect yield.

4.4.1 Olfactory biopsy surgical technique and effects of specimen-related factors on OEC yield

In this study, we describe a new surgical approach for the harvesting of human olfactory mucosa using endoscopic microscissors and the general principles of FES surgery. The biopsy success in obtaining olfactory mucosa from the nasal cavity was 97.7% and in histological analysis and 79.1% in culture. This is significantly higher when compared to previous reports. Feron et al., (Feron et al. 1998) obtained olfactory mucosa tissue in 59.1 % of specimens from healthy subjects and 34.6% from specimens of patients with nasal disease.

As previously suggested (Lanza et al. 1993) and demonstrated in this study, the use of endoscopic guidance assists in the localization of the target mucosal location and increases the success of olfactory mucosa harvest. Equally importantly, it allows the assessment of the quality of the regional mucosa at the time of biopsy and the avoidance of diseased areas resulting in higher OEC culture yield. Nonetheless, the significant increase may be solely due to the fact that specimens were taken from regions closer to the olfactory cleft.

A review of the literature has revealed that most commonly olfactory mucosa biopsies are performed using forceps of different design. Here, we used microscissors to dissect the tissue and Blakeley forceps to collect it. This minimized the crushing artefact caused by biopsy forceps, regardless of design, and avoids the

loss of the tissue obtained which has described with the "olfactory biopsy instrument" described in the introductory chapter (Lovell et al. 1982). In addition, instruments used are commercially available and commonly present within the standard FES surgery surgical pack.

Furthermore, it has been previously suggested that the size of the specimen may improve the success rate in obtaining olfactory mucosa (Feron et al. 1998; Leopold et al. 2000; Choi et al. 2008). In contrary, in this study it is demonstrated that the size (or weight) of the mucosal specimen was not predictive of OEC yield. It can therefore, be inferred that location and quality of mucosal tissue is more significant.

One would assume that such a procedure would have a significant learning curve and, thus, significant differences in OEC yield among biopsies obtained by different surgeons. To investigate whether there are any differences in OEC yield among surgeons, multiple comparison tests were conducted which showed no significant differences among surgeons. Nonetheless, multiple comparison tests are known to reduce the likelihood of type I errors and increase the likelihood of not rejecting the null hypothesis (type II error) and therefore, the absence of difference may be due to chance. In fact, the p-value of ANOVA was only just significant at 0.49, whereas, the difference between surgeon PA and surgeon PC was close to significance with a p-value of 0.07.

The most sinister complication of the surgical techniques described is disruption of the cribriform plate resulting in CSF leak. CSF leak was not reported in this cohort of patients indicating that meticulous technique can avoid serious complications.

Another important concern is the loss of smell. The effects of the surgical procedure in olfaction could not be investigated in this thesis. This is because the majority of patients requiring sinus surgery for polyposis or rhinosinusitis have reduced olfaction and surgery most often causes an improvement. It would therefore seem unlikely that any subtle loss of sense of smell would be revealed.

4.4.2 Effects of patient-related factors on OEC yield

The yield of OECs was compared to specimen and patient-related factors. Most satisfactory yields were obtained from younger patients. This is in accord with previous suggestions that the olfactory epithelium is replaced with respiratory epithelium with advancing age (Morrison et al. 1992). Patients with brachial plexus avulsion injury tend to be of younger age and therefore, the above finding is favourable if OEC-meditated repair is to be used in such patients (Kachramanoglou et al. 2011).

In addition, it is demonstrated that nasal mucosal disease is a negative predictor of OEC yield with best yields achieved from patients without evidence of mucosal polyposis, oedema, discharge, scarring or crusting. These findings also suggest that although chronic rhinosinusitis with or without polyposis is a disease of the respiratory epithelium, the inflammatory changes that occur affect the neighbouring olfactory epithelium (Arnold et al. 1997). Nonetheless, the degree of polyposis and obstruction was not found to correlate with OEC yield.

Smoking was not found to affect the yield of OECs. Smoking has been shown to cause an increase in olfactory sensory neuron apoptosis (Vent et al. 2004) but

whether it also causes an increased loss of OECs remains unknown. Statistical analysis is complicated by the fact that many patients included in this study had been smokers previously, but had ceased for a number of years prior to this study and, therefore, the effect of smoking on their olfactory mucosa is difficult to assess.

4.4.3 Changes OEC yields from biopsies of different location in the superior turbinate

This study is the only study which has attempted to map the olfactory mucosa in a more systematic approach, except a previous study of the same laboratory group in which the septal mucosa was studied.

Our goal is to achieve the best possible yield of OECs from mucosal biopsies obtained. Since there is a general agreement that the olfactory axons converge in the olfactory cleft on their way to the olfactory bulb through the cribriform plate, it seems logical to focus on mapping the cranial portions of superior turbinate. The success of finding olfactory mucosa from more caudal regions of the superior turbinate, middle and inferior turbinate (Feron et al. 1998; Leopold et al. 2000; Lane et al. 2002) and septum (Jafek et al. 2002; Choi et al. 2008) has already been studied with less than satisfactory results. Consequently, targeting such areas would not add significant information in our current knowledge and the likelihood of achieving adequate cell cultures for transplantation is low. We, therefore, studied the yield of OECs from several locations on the superior turbinate and confirmed that the most promising areas of the superior turbinate are those of immediate proximity to the olfactory cleft.

Contrary to previous reports (Feron et al. 1998; Choi et al. 2008), we did not find a significant difference of OEC yield in the anteroposterior position of the biopsy. Again, this is not surprising as the superior turbinate extends along the length of the cribriform plate.

4.4.4 OEC culture protocol

Despite improvements in surgical technique and localisation of olfactory mucosa, this cohort of biopsies still resulted in low yields of OECs. The mean proportion of OECs per 1 mm of the dish was 7.94 % with the majority of biopsies (48%) resulting in OEC yields of less than 5% and only 23% (10 specimens) with OEC proportion of more than 50%. Given the finding that mucosal disease affects the yield of OECs, it is not unreasonable to assume that low yields may be attributed to the presence of mucosal disease. Low OEC proportions were also obtained from cranial portions of septal mucosa. Historically OEC culture has proven difficult primarily due to the predominance of fibroblasts over OECs in culture (Li et al. 1997). It is a common observation that evolution of cultures involves a time-dependent decrease in OECs and corresponding increase in fibroblasts (Nash et al. 2001; Au et al. 2003; Jani et al. 2004). Hence, cell culture is bound to be a limiting factor in OEC yield. Our prior observation of rat OEC cultures with daily light microscopy has demonstrated that there is an initial bust of cell growth in the first week, which is attributable to fibroblast proliferation, whereas the OECs tend to multiply in the second week. Li et al., (Li et al. 1997) reported that OEC cultures acquire their optimal reparative properties at around 14 days, during which time the proportion of OECs to fibroblasts was close to 50:50; fibroblasts predominate again thereafter. In our

human OECs cultures, we applied the principles of our rat culture protocol with a view to adjust and further improve based on our findings. We, therefore, cultured cells for 10-14 days and did not include any expansion or purification methods to obtain a baseline of the natural human OEC growing capabilities. We are currently exploring new methods by which to improve culture and yield of OECs, further discussed in Section 4.7. Furthermore, we avoided over-purification methods because animal data have demonstrated that treatment with OEC transplantation is only effective when both OECs and olfactory fibroblasts are transplanted (Li et al. 1997). However, it remains to be demonstrated whether this is due to the interaction of the two cell types during co-culture, whether purified OECs are adequate in stimulating regeneration or whether a mixture of the two cell lines after separate bioprocessing of each line would be adequate.

The number of OECs required for transplantation is currently unknown and depends on the size of the lesion. It has been suggested that approximately 10^7-10^8 of pure OECs may be adequate for transplantation of human spinal cord injury resulting in paraplegia (ASIA A) (Feron et al. 2005) although the effects of such regime has not yet been published.

4.5 Limitations

The present study is subject to a number of limitations. In what will follow I will expose these limitations and explain their implications for our findings.

One of the main limitations of the current study is the relatively small number of biopsies included in the study. Given the fact that we were limited by the number of patients presented for FESS procedure and that ability to collect only one sample per patient for ethical reasons, collection of a greater number of biopsy specimens was not feasible. Nonetheless, the group of biopsies included in this study is a representative sample of common nasal mucosal disease, which may be encountered in patients presenting with spinal cord injury and need for OEC transplant mediated repair. In addition, the number of biopsies assessed in this study is considerable greater when compared to most other publications in this field.

Another limitation of the present study the inability of collecting specimens directly from the cribriform plate which could potentially result in higher OEC yields. This limitation is unavoidable as a biopsy directly from the cribriform plate would invariably cause a CSF leak and lead to potentially serious complications for the subjects' health.

An additional limitation may be considered the indirect method of counting OEC number in culture as opposed to more robust methods such as Fluorescence Activated Cell Sorting (FACS). Unfortunately, this technology was not available in our laboratory and therefore not viable. However, it is known that with such manipulation of cell cultures a significant number of cells is lost, an undesirable feature, given the difficulty of human OEC culture expansion. Furthermore, our research group holds the belief that olfactory nerve fibroblasts an essential component of the cell suspension for intraspinal implantation that plays a role in the growth promoting ability of OEC grafts (Jani et al. 2004).

Last but not least, a well recognised difficulty, experienced by all laboratories investigating OECs, has been the lack of antibodies that uniquely identifies OECs. The same antibodies including $p75^{NTR}$, GFAP and S100β can be used to immunolabel Schwann cells (Kawaja et al. 2009). The presence of Schwann cells from peripheral nerves in olfactory mucosa biopsies clearly necessitates the identification of antibodies or a battery of antibodies that uniquely identify OECs. Until this issue is resolved, it is impossible to confirm whether cells grown are OECs, a subgroup of Schwann cells or specialized fibroblasts.

4.6 Future Directions

The present study has been important in determining some of the factors, which affect the yield of human OEC cultures. Nonetheless, we are still left with many unanswered questions. With respect to OEC cultures, there is need for further improvement in the current human OEC culture protocol. We are currently exploring new methods by which to improve the yield. These include explant cultures, suppression of fibroblast proliferation leaving a higher purity population of OECs, and the use of growth factor Neurotrophic 3 to encourage growth of OECs.

Furthermore, analysis of biopsies of normal healthy subjects without mucosal disease would be useful in confirming the effects of age, mucosal disease and other patient-related factors affecting yield. Perhaps cadaveric specimens would enable this to avoid ethical issues. Lastly, we will attempt to derive an allogenic OEC line that can proliferate indefinitely upon activation a transgene by tamoxifen and is subsequently arrested when removed from culture.

With respect to the safety of the procedure, we are already investigating the effects of olfactory mucosa biopsy with the surgical procedure described in this thesis to olfaction with standardized olfactory tests before and after surgery.

4.7 Conclusion

In sum, the present thesis set out to describe a biopsy technique of human olfactory mucosa biopsy and to investigate the effects of specimen- and patient-related factors on human OEC yield. Biopsies closer to the olfactory cleft were discovered to produce larger yields of OECs, and increasing age and nasal mucosal disease adversely affect the culture yield. Contrary to held belief, specimen position in the antero-posterior direction was not revealed to affect OEC culture yield. Similarly donor gender, smoking, loss of smell, grade of polyposis, preparatory solutions for the FES procedure and weight of specimen were not shown to affect OEC yield.

Chapter 5

An introduction to the principles of magnetic resonance and magnetic resonance spectroscopy

5.1 Magnetic resonance spectroscopy

Proton magnetic resonance spectroscopy (^{1}H-MRS) is a valuable non-invasive technique which is increasingly used to evaluate the metabolic profile of the central nervous system. The history of magnetic resonance spectroscopy (MRS) is traced back to the first, independent observations of a nuclear magnetic resonance (NMR) signal in bulk matter by Block and Purcell in 1946. Two important applications of the NMR phenomenon in both clinical and research use are Magnetic Resonance Imaging (MRI) and Magnetic Resonance Spectroscopy (MRS). In MRI, the protons present predominately in tissue water are detected and used to generate structural images. In MRS, it is the protons present in metabolites and macromolecules other than water that are of particular importance.

Basic understanding of the fundamental principles of magnetic resonance is crucial for appreciating the role of MRS in the clinical setting. This chapter outlines the basic principles of magnetic resonance (MR) and MRS, to introduce the clinical application that is reported in the subsequent chapter of this thesis.

5.1.1 Nuclear magnetic resonance

NMR and NMR spectroscopy are techniques that depend on the magnetic properties of the atomic nucleus. Nuclei that have a net charge and are spinning acquire nuclear magnetic moments corresponding with spin ½ and are most suitable for detection by magnetic resonance. Important examples of such nuclei present in living systems are

^{1}H, ^{31}P, ^{13}C, ^{15}N, and ^{19}F. Hydrogen is the most abundant nucleus in the human body that possess a nuclear spin, its single proton gives it a relative large magnetic moment and is the preferred choice of proton in used in clinical applications.

5.1.2 The NMR phenomenon

When magnetic active spin ½ nuclei are placed in a homogeneous static magnetic field (B_0) the nuclei populate two energy states. A lower energy state, which is parallel to the external magnetic field (spin-up) and higher energy state, which is aligned almost opposite to the external field (spin-down) (Figure 5.1). There is a statistical distribution of protons between the two states, so that there are slightly more protons in the parallel state. The ratio is proportional to the main magnetic field strength and inversely proportional to temperature. Although both states are stable, protons can swap between the two states by gaining or losing a certain amount of energy in the form of a photon (a packet of electromagnetic radiation). The energy gap (ΔE) between the two quantum states is proportional to the strength of the magnetic field, and increases with increasing field strength. The energy required to be absorbed for the nucleus in the lower energy state to jump in the high energy state must match exactly ΔE (Equation 5.1).

$$\Delta E = h \times f = (h \gamma B_0) / 2\pi \qquad \text{(Equation 5.1)}$$

where h is Planck's constant and f is the frequency of the energy to be supplied to the photon for it to jump in the spin-up state. This frequency is equal to the *Larmor*

frequency. This orientation yields a *net nuclear magnetization* and a *net magnetization vector* M_z parallel to B_0.

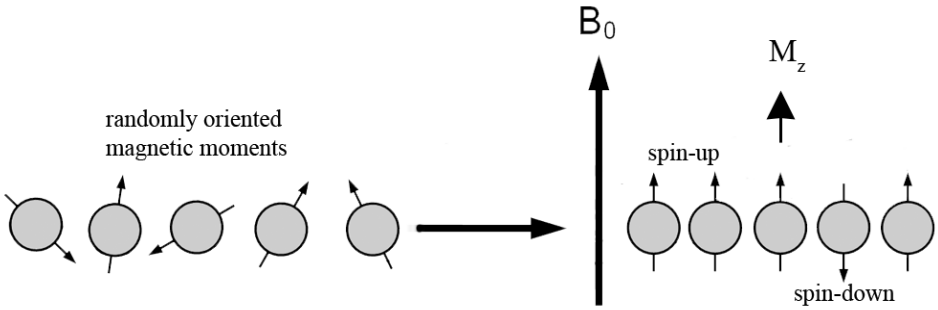

Figure 5.1: Protons possess a magnetic moment, or "spin". When placed in an external field B0, the low energy spins align parallel to B0 (along the z-axis), resulting in a magnetization vector Mz.

Furthermore, when protons are placed in B_0, they try to align themselves with the external field resulting in a circular motion around the axis of B_0 (commonly the z-axis), called *precession*. The precessional frequency of the protons is proportional to the external magnetic field, given by the *Larmor equation* (Equation 5.2):

B_0 (Equation 5.2)

where γ is the gyromagnetic ratio, a natural constant specific for a particular nucleus and is the precessional frequency (the "Larmor frequency") in Hertz (Hz). For protons equals 42.576 MHz Tesla^{-1}. The resultant longitudinal magnetization can be represented as the vector sum, the net magnetization (M_z) of the ensemble of nuclei in the magnetic field. It is virtually impossible to measure the magnetization while at

equilibrium when lying parallel to B_0. If a second, time-dependent magnetic field (B_1) is applied perpendicular to B_0, by using a radiofrequency (RF) pulse at the Larmor frequency, the magnetization vector M_z will rotate away from the z-axis towards the xy-plane. The angle of rotation (α), or flip angle, of M_z around B_1 is defined as:

$$\alpha = B_1\tau \qquad \text{(Equation 5.3)}$$

where τ is the duration of the RF pulse field B_1. After application of a 90° pulse the magnetization vector will be in the xy-plane, and the spins will be in phase coherence; M_z will be zero and M_{xy} will be at a maximum (Figure 5.3). This process is commonly referred to as pulse excitation. After the RF pulse is switched off, the net magnetization vector will start reverting back to its equilibrium state as a result of a process, which is called relaxation. The recovery process along the longitudinal axis is called *T_1 relaxation or spin-lattice relaxation*. The dephasing process in the transverse plane is referred to as *T_2 relaxation or spin-spin relaxation*.

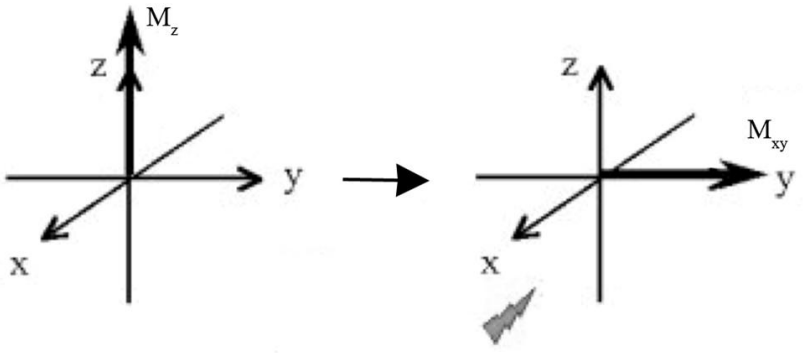

Figure 5.2: *Application of a 90° RF pulse flips M_z into the xy-plane (perpendicular to B_0), resulting in magnetization vector Mxy and phase coherence between spins.*

An RF coil placed in the transverse plane will detect the transverse component of the net magnetization vector as it precesses around B_0. The amplitude of the signal in the receive coil will decay exponentially to zero in a few milliseconds as the protons rapidly dephase with respect to each other. The rate of signal decay is dependent of T2 and the process is described as:

$$M_{xy}(t) = M_{xymax}\, e^{-t/T2} \qquad \text{(Equation 5.4)}$$

In practice, however, the signal will decay at a faster rate than T2 due to field inhomogeneities and magnetic susceptibility differences. This shorter relaxation rate is known as T_2^*.

The decaying sinusoidal signal detected in the transverse plane after a single RF pulse is known as *free induction decay* (FID). The time domain signal is uninterpretable to the human eye. The FID signal can be subjected to a fast Fourier transformation (FFT) to convert the signal as a function of time (time domain) to a plot of intensity as a function of frequency (frequency domain) (Figure 5.3). The obtained spectrum has one peak for each resonant frequency in the sample. Variations in resonant frequencies provide information on the molecular structure in which the atom resides. The relative proportion of such molecule can be also then be estimated.

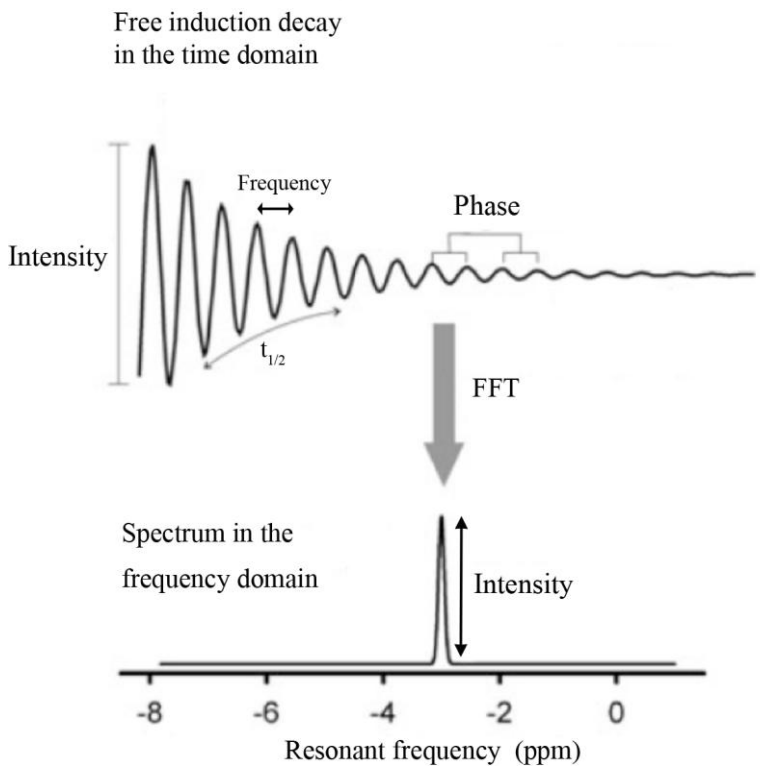

Figure 5.3: *Free induction decay; after a single RF pulse the signal detected in the transverse plane is sinusoidal in shape and decays to zero over time under influence of the transverse relaxation. The FID signal is then subjected to a FFT to convert the signal as a function of time (time domain) to a plot of intensity as a function of frequency (frequency domain; Abbreviations: FFT = fast Fourier transform, ppm = parts per million.*

5.1.3 Chemical Shift

Nuclei in different molecular environments resonate at slightly different frequencies. This occurs because the bonding electrons create their own small magnetic field that

modifies the external magnetic field (B_0) in the vicinity of the nucleus. Thus a nucleus that is shielded from the static field experiences a smaller net field than that which is actually applied (effective field at the nucleus; B_{0eff}) (Equation 5.5) and as a result, has a lower precession frequency. The effective field at the nucleus can be expressed in terms of a shielding parameter (σ) and its effect is known as the *chemical shift*. While the shielding parameter is constant and stated in parts per million (ppm), the chemical shift increases linearly with field strength (Equation 5.5) and is measured in Hz.

$$B_{0eff} = B_0 (1 - \sigma) \qquad \text{(Equation 5.5)}$$

Many resonances at a given chemical shift are split into two or more subpeaks (doublet, triplet, multiplet). These arise through the phenomenon of spin-spin coupling; the interaction between the atomic nuclei of neighbouring groups. The spacing between these peaks has a fixed frequency value (Hz) called the *J-coupling constant*. The J-coupling constant is independent of magnetic field amplitude. Molecules have characteristic number and pattern of subpeaks, which further allows identification of metabolites in a sample.

The results of MRS are displayed as a spectrum of resonances (peaks) over a range of frequencies distributed along the x-axis, which is centered on the fundamental resonant frequency of the nucleus of interest, labeled in parts per million (ppm) (Figure 5.4). The signal intensity or amplitude of the resonances is measured on the y-axis using an arbitrary scale. The line width provide the “area” which can be used

to quantitate the amount of the observed chemical. The width of the peak is inversely proportionate to T2* relaxation time.

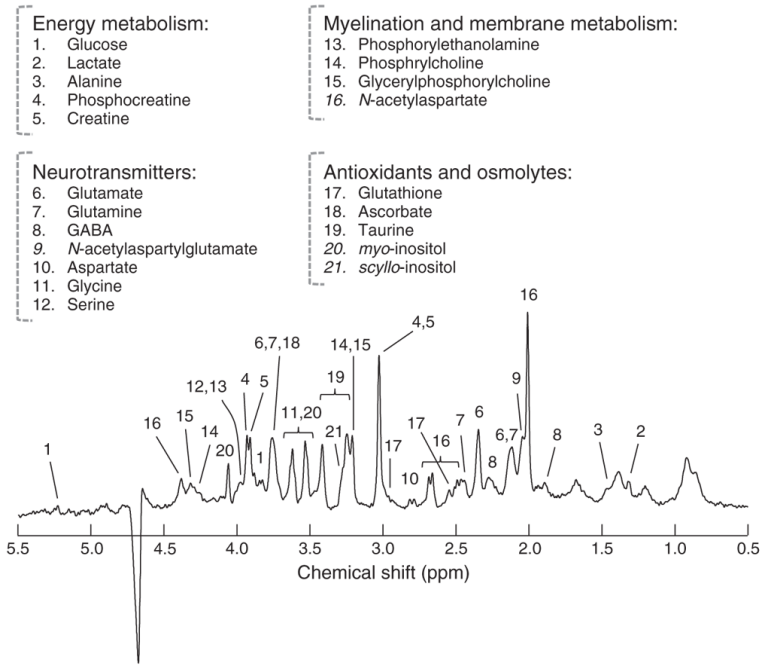

Figure 5.4*: Compounds detected in the brain with in vivo ^{1}H NMR spectroscopy. Spectrum was acquired from the rat hippocampus at 14.1 T. Image from Duarte et al., 2012 (Duarte et al. 2012). Permission to reproduce this image has been granted by Elsevier Limited).*

5.1.4 Basic *in Vivo* localization techniques

Basic in vivo MRS uses multiple RF pulses to localize on a given region of the body. Spatial localization techniques fall into two general categories: single voxel techniques where a spectrum is recorded from a single region and multi-voxel or otherwise called MR spectroscopic imaging (MRSI) or chemical shift imaging (CSI) where multiple regions are acquired simultaneously.

Single voxel techniques generate a cubic or rectangular based volume element (voxel) for a region to be sampled with MRS. The analyzed volume is selected by a succession of three selective radiofrequency pulses (accompanied by gradients) in three different directions in space (G_x, G_y, and G_z). These pulses determine three orthogonal planes whose intersection corresponds to the volume studied. Only the signal of this voxel will be recorded, by selecting only the echo resulting from the series of the three-radiofrequency pulses (Figure 5.5a). The two most common methods, used in single-voxel spectroscopy (SVS), are stimulated echo acquisition mode (STEAM) (Frahm et al. 1989) and point-resolved spectroscopy (PRESS) (Bottomley 1987). For the work presented here, the PRESS sequence is used.

PRESS generates a cubic or rectangular voxel by using slice-selective excitation in combination with two slice-selective refocusing pulse (Figure 5.5b). The initial 90˚ pulse is followed by an 180˚ pulse after a time period t_1, which is subsequently followed by another 180˚ pulse at $2t_1$. The 90˚ pulse will affect spins in a particular slice. The first 180˚ pulse applied in the presence of a magnetic field gradient that is orthogonal to the first selection gradient will refocus spins only in the second slice, and will diphase spins outside that slice. The second 180˚ pulse is combined with a magnetic field gradient orthogonal to the other two gradient directions will result in a spin-echo signal from the intersection of all three slices which will appear at a time $2t_1 + 2t_2$, equal to the echo time of PRESS. The signal originates only from the rectangular box, the dimensions of which are determined by the width of the three selected slices. Signal outside of the volume of interest (VOI) is either not excited leading to rapid dephasing of the signal by the “crusher” magnetic field gradients. The block of 90˚-180˚-180˚ pulses is successively repeated. The time to echo time

(TE) refers to the time between the 90˚ pulse and signal sampling. The repetition time (TR) refers to the interval between successive 90˚ pulses. The PRESS technique can be used with short TE (15 – 20 ms) or long TE (135 – 270 ms). PRESS is less susceptible to motion, diffusion, and quantum effects and has a better SNR than STEAM.

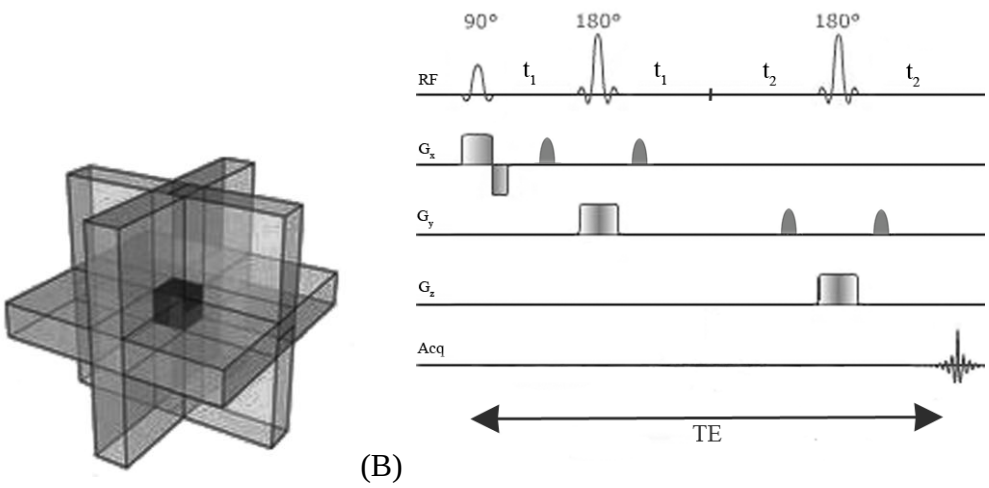

Figure 5.5: *(A). The slice selective pulses along orthogonal axes define three orthogonal slices, with the volume of interest (voxel) located at the intersection of the slices. (B) Schematic overview of the PRESS sequence consists of a slice selective 90° and two refocusing 180° pulses. The 90° RF pulse rotates the spins in the yx-plane, followed by the first 180° pulse (spin rotation in the xz-plane) and the second 180° pulse (spin rotation in the xy-plane), which gives the signal. The use of crusher gradients on either side of the 180˚ pulses diphase unwanted magnetization outside the selected voxel. The entire sequence is preceded by water suppression schemes.*

5.1.5 Water Saturation

The concentration of water exceeds the concentration (mmol/l) of metabolites of interest by a factor of 10,000 or more. If MRS were applied without suppressing the signal from water, the dominant resonance (the resonance peak) in a hydrogen spectrum will represent protons from the water molecule at 4.7 ppm, obscuring the millimolar concentration of other metabolites. Hence, suppression of the water signal is critical for proton spectroscopy in order to reliably observe the much smaller metabolite signals.

The most common approach is Chemically Selective Saturation (CHESS) (Haase et al. 1985), which is applied prior to the localization technique. It involves three short RF pulses of high amplitude applied along with a dephasing gradient to suppress the water (Figure 5.6). This allows for frequency selective excitation by permitting the metabolite resonances to rotate into the transverse plane, for signal detection, while the water is returned to the longitudinal axis, rendering it unobservable.

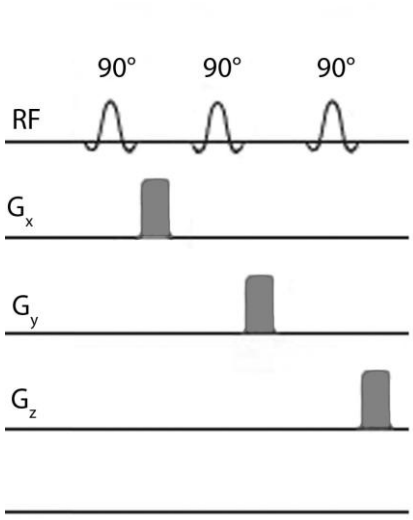

Figure 5.6: Schematic overview of the CHESS water suppression technique; the water signal is pre-saturated using frequency selective, 90° prior to the localization pulse sequence. By using more than one pulse and with correct choice of pulse flip angles, good suppression can be achieved.

5.1.6 Shimming

Optimization of the magnetic field homogeneity is an absolute requirement for obtaining high quality ^{1}H-MRS spectra. A sample brought into the main magnetic field of the scanner distorts the magnetic field. The need for maximal field homogeneity is that due to the fact that the resonance frequency of the sample depends on the magnetic field strength. Spins experiencing the same field strength will resonate at the same frequency and thus produce a resonance with narrow line and low FWHM. Narrow resonances will also result in stronger signal as the FWHM is inversely related to T_2.

^{1}H MRS requires using a process known as shimming to improve the global and/or local magnetic field. Shimming on the individual patient enhances the quality of *in vivo* spectra. The bigger the region, the harder it is to homogenize the magnetic field throughout. These effects need to be corrected as much as possible before starting the spectroscopy examination. When human subjects are concerned, one is limited by the total examination time and thus a fast and reliable method is required.

It is common practice to monitor the MRS signal of the water resonance from the region of interest (ROI), and then optimize the magnetic field on the basis of that signal. While there are many different approaches to *in vivo* shimming, the common overall goal is to compute the desired corrective fields over the ROI and apply the necessary corrective currents as offsets to the imaging gradient or to the higher-order shim coils. The advent of automatic 'shimming' programs have greatly improved the ease of acquisition. Voxel homogeneity is usually measured as the *linewidth* (the full-width at half height) of the water resonance and may be quoted in Hz or ppm.

5.1.7 Physiological movements

Movement of the patient or desired volume of interest relative to the magnet during the total acquisition period can result in the signal coming from outside the selected voxel leading to underestimation of the metabolite concentrations. In the brain and with short scanning times this may not pose a problem. However, in the spinal cord and particularly in the cervical region, the flow cerebrospinal fluid around the subarachnoid space, dominated by the cardiac cycle, translates into actual cord movement in the craniocaudal dimension (Mikulis et al. 1994). Cardiac gating techniques prospectively gate the acquisition to periods when the cord is within a specific location. 15% loss in signal and 25% increase in linewidth have been demonstrated in ungated data compared to gated acquisition. A gating delay of 400 ms after cardiac systole has been found to provide the most stable spectra (Cooke et al. 2004). New methods are being developed including motion tracking with

dynamic feedback to adjust volume selection frequencies accordingly (Kozerke et al. 2002).

5.1.8 Post-processing

Common post-processing of SVS spectra, before or after the application of the FFT, includes multiplication with a filter in the time domain, zero-filling, FT, phasing, and baseline correction (van der Graaf 2010) to improve MRS data obtained.

In addition, in localized MRS gradient switching may cause eddy current artifacts. Eddy currents are small, transient currents induced in the magnet structure after the application of a pulsed field gradient resulting in small time-varying change in the magnetic field strength and, consequently, artifacts in the spectral lineshape. Such artifacts can be removed with a reference water signal obtained without water suppression using the same sequence and from the same VOI. This so-called eddy current correction (ECC) is applied as a first post-processing step, and it results in line-shape corrections in the metabolite spectrum together with the removal of offsets in zero-order phasing and frequency (van der Graaf 2010).

5.1.9 Quantification of metabolites

Quantitative analysis of MRS spectra either requires the determination of peak areas in the frequency domain or direct time-domain analysis to estimate the amplitude of the first data point of the different frequency components that comprise the FID.

The most sophisticated and most widely software used is the co-called Linear combination model (LCModel), which fits the frequency domain data to a linear combination of the pure compound spectra known to exist in the spectrum (Provencher 1993). The model spectra in the database may be obtained from in vitro measurements of metabolite solutions using the same pulse sequence and timings as the *in vivo* measurement or by computer simulations (van der Graaf 2010). The advantage of the LCModel program is that the entire spectral pattern associated with each metabolite is used for the fitting.

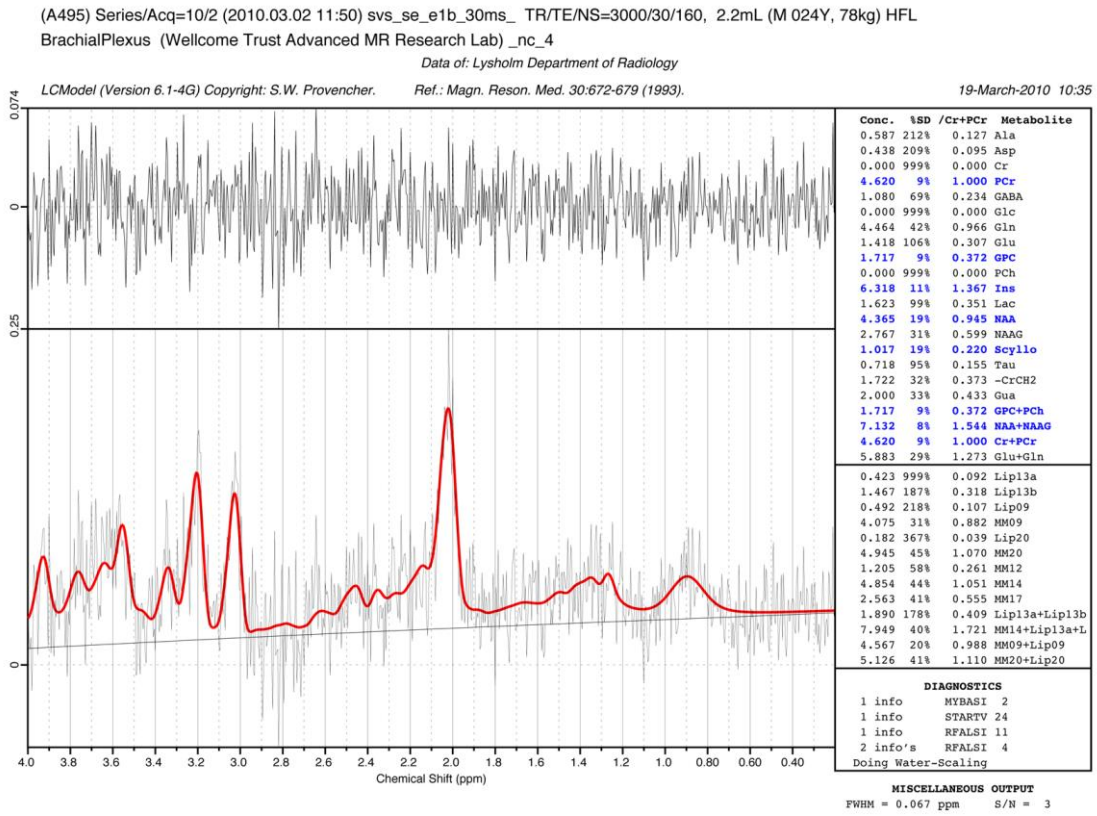

Figure 5.7: *An example of LCModel analysis method. The LCModel analyzes an in vivo spectrum as a Linear Combination of Model in vitro spectra from individual metabolite solutions. Automated baseline and phase-correction is performed and an estimate of metabolite concentrations is provided using the water reference signal for quantitation. In this example a 2.2 ml PRESS spectrum recorded at 3.0 T from a normal control subject (TR/TE/number of averages = 3000/30/160), the difference between the original experimental data and the results of the curve fit is shown in the top trace. Metabolite concentrations highlighted in blue correspond to those with an estimated uncertainty (Cramer-Rao lower bounds (CRLB) of less than 20%.*

This quantification method results in signal intensities in arbitrary units, with ratios often used in clinical diagnosis. For brain spectra, the intensity of the methyl resonance of creatine is commonly used for normalization. Although this normalization removes differences, for example in volume and coil loading, a change in a ratio can be caused by changes in both numerator and denominator (Li et al. 2003).

5.1.10 Quality of MRS spectra and signal-to-noise ratio

In MRS applications, it is generally not the signals of water and fat that are of interest, but rather the smaller metabolite signals, thus a magnetic field of sufficient strength is required. Therefore, most clinical MRS measurements are performed using MR systems with field strengths of 1.5 T or higher. Even with such magnet strengths, metabolites with concentrations of 0.5 mM or more can only be recognised in *in vivo* MRS.

In an NMR experiment, the ability to detect a signal depends not only on the signal amplitude, but also on the amount of noise in the spectrum i.e. the signal-to-noise ratio (SNR). Noise is generated by the presence of the patient in the magnet and the background electrical noise of the system produced by random, thermal motion of electrons in the receive coil. Noise occurs at all frequencies and is random in time and space, but is constant for a specific patient.

SNR and chemical shift dispersion are expected to increase approximately linearly with increasing magnetic field strength (B_0) and so *in vivo* MRS is expected to be superior at higher field strengths (Equation 5.2). Furthermore, increasing the voxel size enables the signal to contain more spins to contribute towards the signal. On the other hand, large voxels introduce partial volume effects, which may not be desirable. Moreover, to accumulate sufficient SNR most *in vivo* studies require averaging of usually hundreds of acquisitions (*n*) in order to achieve the desired spectral quality. This result in an increase in scan time, the scan time being proportional to *n* and TR.

5.1.11 Limitations of MR

There are several limitations to MRS regardless of the technique used. It is difficult to perform MRS in or adjacent to tissue with high differences in magnetic susceptibility compared with brain tissue, such as bone, air, fat, and hemorrhage. This is due to the artifacts arising from these structures and the resultant difficulty in obtaining a homogeneous magnetic field, essential for a good MRS study. Hence, spectra of good quality are difficult to obtain near the skull base, calvarial bone, paranasal sinuses, and mastoid air cells. The artifacts can contribute to so much spectral broadening that the spectra obtained from these regions may contain no discernible metabolite resonances, often rendering them useless. As a result, characterization of lesions in these challenging areas has generally relied on SVS, which is less prone to susceptibility artifacts.

5.2 Major metabolites in the central nervous system and their significance

The first high resolution proton magnetic resonance spectroscopy (^{1}H-MRS) studies of the animal brain were performed in 1983 (Behar et al. 1983). These studies demonstrated that ^{1}H-MRS allows *in vivo* observation of a number of brain compounds, including different aminoacids, phosphocreatinine, trimethylamine resonances, myoinositol and lactate. A series of experiments followed, in which ^{1}H-MRS has been applied to examine different aspects of nervous system metabolism under various conditions. The bulk of work of ^{1}H-MRS has been performed on brain tissue because technical factors favour ^{1}H-MRS on this organ; motion is a relatively smaller problem, shimming is less disturbed by the mass of nearby tissue as well as by motion, and lipids interfere less in the normal state they are part of myelin or other large molecules that are not mobile enough to give narrow signals.

In the following sections, the major metabolites identified in the brain and potential roles are discussed.

5.2.1 N-acetylaspartate (NAA)

The most prominent signal observed in brain ^{1}H-MRS acetyl group of N-acetyl aspartate resonates at 2.01 ppm, with contribution from N-acetyl aspartyl glutamate (NAAG) at 2.04 ppm (Frahm et al. 1991; Pouwels et al. 1997). Its detailed physiological role is yet unknown. NAA is synthesized in neuronal mitochondria and is speculated to be a source of acetyl groups for lipid synthesis, a regulator of protein

synthesis, a storage from of acetyl-CoA and aspartate, a breakdown product of NAAG and an osmolyte (Barker 2001). More importantly, in the nervous system NAA is a putative neuronal marker due to its exclusive intraneuronal distribution and expression demonstrated with immunocytochemical staining techniques (Simmons et al. 1991).

Reductions in NAA have been noted in conditions associated with neuronal loss or axonal degeneration. Reduced NAA levels have demonstrated in acute and chronic lesions cerebral multiple sclerosis (MS) plaques and in normal appearing white (Tourbah et al. 1996) and gray matter in patients with MS (De Stefano et al. 2001; Chard et al. 2002), providing evidence that NAA may be a marker of neuroaxonal damage. Furthermore, the relative NAA concentrations have been shown to correlate with the neurologic disability in MS patients (De et al. 1998) and, in fact, the NAA deficit correlated with MS-related clinical disability better than the traditional MR imaging radiologic markers (De Stefano et al. 2001).

In experimental models of spinal cord injury, prolonged decreases in NAA have been noted in rostral, epicenter and caudal segments of the spinal cord, which were correlated with histological confirmation of neuronal cell death in the grey matter and axonal degeneration in the dorsal lateral and ventral white matter columns (Qian et al. 2010).

In addition, NAA levels are found to be absent in tumors of glial origin (Sibtain et al. 2007) and to decrease in neuropathological conditions, correlating with the degree of

degeneration in humans and rodents (Kantarci 2007; Tkac et al. 2007; Horska et al. 2009).

Moreover, Bates et al. (Bates et al. 1996) have shown that NAA is a mitochondrial product related to oxygen consumption and adenosine triphosphate (ATP) synthesis and that inhibition of electron transport leads to reduced NAA synthesis by isolated rat brain mitochondria. In addition, after transient ischemia and brain injury without neuronal death, and in longitudinal studies of MS, NAA levels have been shown to recover (Brulatout et al. 1996; Audoin et al. 2006; Tiberio et al. 2006). Thus reduced NAA can be more generally interpreted as neuronal dysfunction rather than decrease in neuronal density or axonal structural integrity (Cader et al. 2007).

5.2.2 Creatine (Cr)

The creatine methyl resonance (Cr) is a composite peak consisting of both creatine and phosphocreatine (total Cr) and resonates at 3.03 ppm. Creatine is involved in energy metabolism via the creatine kinase reaction generating ATP, hence, is a measure of global cellular metabolic activity and a marker for brain cell density in glial and neuronal cells. Total Cr is used as an internal reference in reporting relative concentrations of other metabolites because it is considered to be a relatively stable compound. Cr has been shown to have large regional variations with lower levels in white matter than grey matter in normal brain (Jacobs et al. 2001) Cr may also increase as a hyperosmolar response to craniocerebral trauma, or be absent as in the case of creatine deficiency, a rare congenital disease (Zimmerman et al. 1997).

5.2.3 Myo-Inositol

Another prominent signal visible at 3.61 ppm in spectra obtained at 3 Tesla with short TE is myo-inositol (m-Ins). M-Ins is pentose sugar involved the inositol triphosphate intracellular second messenger system, primarily synthesized in glial cells and postulated to be a glial marker (Brand et al. 1993). The concentration of m-Ins increases with glial proliferation or with glial cell-size increase, both of which occur in inflammation (Brand et al. 1993; Flogel et al. 1994; van der Graaf 2010). It is suggested that this may be related to a difference in m-Ins/Na co-transporter activity that appears to play a key role in astrocyte osmoregulation (Strange et al. 1994). This would explain chronic disturbance in m-Ins in both degenerative and inflammatory disease. Alternatively, m-Ins may represent a breakdown product of myelin. Levels have been found reduced in hepatic encephalopathy (Singhal et al. 2010) and increased in Alzheimer's dementia (Miller et al. 1993), demyelinating diseases (Ciccarelli et al. 2007; Marliani et al. 2010) and HIV infection (Laubenberger et al. 1996).

Following complete transection of the spinal cord of rodents, conspicuous increases of m-Ins in the pericontusional zone below the level of injury in the acute (3 days post injury) and chronic period (4 months post injury) have been observed below the level of injury (Erschbamer et al. 2011). These increases correlate with the well known increases in glial fibrillary acidic protein (GFAP) immunoreactivity in histological examination, confirming an association of m-Ins and astrogliosis (Erschbamer et al. 2011).

5.2.4 Choline

The choline (Cho) signal resonates at 3.2 ppm and is a composite peak consisting of contributions from the trimethyl amine groups ($N(CH_3)_3$) of glycerophosphocholine (GPC), phosphocholine (PC) and a small amount of free choline (Barker et al. 1994). Choline-containing compounds are essential for membrane lipid synthesis. Choline is released from the breakdown of phosphatidylcholine found in membranes, salvaged and reused by the action of choline kinase, converting it to phosphorylcholine. It is then converted to phosphatidylcholine and incorporated into new membranes (Daly et al. 1987). Therefore, fluctuations of this marker are considered an indicator of cellular turnover related to both membrane synthesis and degradation (Carpentier et al. 2006) and increased Cho/Cr ratios have been observed with demyelination (Cecil et al. 1998), inflammatory reactions (Friedman et al. 1999; Brooks et al. 2000), and glial proliferation (Garnett et al. 2000).

Elevations in Cho/Cr ratio have, also, been observed in human ^{1}H-MRS studies after traumatic brain injury in normal-appearing gray matter, which correlated with injury severity and outcome and were attributed to pathological alterations in membrane turnover (Friedman et al. 1999; Brooks et al. 2000; Garnett et al. 2000). In experimental brain studies, elevations have been observed in the pericontusional brain regions (Schuhmann et al. 2003) following an initial decrease in Cho/Cr compared to controls.

Furthermore, brain tumors generally show an increase in the Cho signal, and the Cho level is believed to correlate directly with proliferative potential and malignancy (Herminghaus et al. 2002). Therefore, an increase in the total choline signal is often used in the diagnosis of a brain tumor.

5.2.5 Lactate

Lactate (Lac) is a doublet and resonates at 1.31 ppm. It indicates anaerobic metabolism and an alteration in the normal cellular biochemical oxidative process (Veech 1991). It is undetectable in most brain studies due to its low concentration within the brain under normal conditions. It may, however, be increased and detected in pathological conditions involving inflammation, local hypoxia or ischaemia and/or neuronal mitochondrial dysfunction with the resultant production of excess Lac (Petroff et al. 1992; Simone et al. 2001; Holly et al. 2009). Lactate may difficult to detect in MRS studies due to overlapping lipid resonances. Special editing techniques or long TE is required to achieve detection (Kelley et al. 1999).

5.3 MRS of the spinal cord

In vivo ^{1}H-MRS of the spinal cord is challenging because of the technical difficulties that limit the quality of the spectroscopic data. The main obstacles encountered are the strong magnetic field inhomogeneities around the cord, physiological movements and the small cross sectional size of the spinal cord. Therefore, it is no surprising that relatively few ^{1}H-MRS studies of the spinal cord have been performed to date.

The first human study of ^{1}H-MRS in the spinal cord was performed in a cohort of 6 healthy patients, which demonstrated the feasibility of ^{1}H-MRS of the spinal cord using a 1.5 Tesla system. Satisfactory spectra were acquired and the major metabolic peaks could be accurately identified and quantified (Gomez-Anson et al. 2000). The development of 3 Tesla systems with increased SNR allowed a good compromise between the size of the acquisition volume and the number of repetitions required to obtain a total acquisition time that is feasible in a clinical environment. Marliani et al, (Marliani et al. 2007) first devised an acquisition and post-processing single-voxel MRS protocol on the cervical spinal cord of healthy subjects on a 3 Tesla system with standard equipment and successfully evaluated the mean relative concentrations of the main normal metabolite concentrations and ratio in respect to Cr, including NAA (mean = 1.4, sd; 0.3), Cho (mean = 0.5, sd; 0.1) and M-Ins (mean = 1.7, sd; 0.2).

The majority of human spinal cord ^{1}H-MRS studies have been performed on patients with MS plaques since the commonly used T1- and T2-weighted MR sequences provides poor specificity and sensitivity in detecting pathophysiologic MS changes and correlation with clinical disability. These studies demonstrated changes in metabolites ratios that were in accord with the metabolic abnormalities already described in brain plaques of patients with MS, confirming that ^{1}H-MRS allows examination of spinal cord integrity at a biochemical level and may be sensitive to subtle changes occurring during the course of MS disease. Significantly reduced levels of NAA in respect to Cr compared to healthy controls are shown in all studies (Kendi et al. 2004; Blamire et al. 2007; Ciccarelli et al. 2007; Marliani et al. 2010),

which correlated with neurological assessment measures (Blamire et al. 2007; Ciccarelli et al. 2007; Marliani et al. 2010). Furthermore, increases in m-Ins/Cr and Cho/Cr levels in comparison with healthy cervical spine tissue have also been shown (Marliani et al. 2010), suggesting an increase in the activity or number of glial and inflammatory cells and attacks of demyelination and remyelination respectively. M-Ins levels have also been correlated to MS-specific disability scores further supporting that ^{1}H-MRS spectroscopy is sensitive to metabolic changes in the spinal cord in these patients.

Moreover, ^{1}H-MRS studies in patients with amyotrophic lateral sclerosis have demonstrated 40% and 38% reductions in NAA/Cr and NAA/m-Ins respectively (Carew et al. 2011) with significant correlations with forced vital capacity (FVC).

A methodologically interesting study of volume selective 2T ^{1}H-MRS of the spinal cord in healthy subjects Cooke et al. in which concentrations of NAA, Cr and m-Ins of the cervical spine were compared with data from the brainstem, cerebellum and cortex of the same individuals provided important technical information (Cooke et al. 2004). Firstly, it demonstrated that the distortion of the B_0 field was dominated by the interfaces between the vertebral spinous processes and interspinous connective tissue and that the atypical anatomy of the first two cervical vertebrae allowed slightly larger voxel to be adequately shimmed. The ideal voxel size was shown to be 9 mm in the transverse direction by 7 mm in the anteroposterior by 35 mm in the craniocaudal direction, resulting in a voxel volume of 2.21 ml. This was placed aligned with the spinal cord at the level of C2 vertebral body. Secondly, it showed a 15% increase in signal and 25 % decrease in linewidth by varying the trigger delay

such that the acquisition period occurred 400 ms after cardiac electrical systole, therefore, reducing the effects of physiological movements.

5.4 MRS of traumatic spinal cord lesions

Only two studies have been performed in traumatic conditions of human spinal cord. Holly et al. (Holly et al. 2009) compared patients with cervical spondylotic myelopathy on a 1.5 T scanner and demonstrated significantly lower NAA/Cr ratios (mean = 1.27, sd; 0.52) than the controls (mean = 1.83, sd; 0.18). No significant difference was seen in the Cho/Cr ratios. In addition, 7 of the 21 patients had demonstrable Lac peaks, which were not present in the control group. There were statistically significant differences in the NAA/Cr ratio in patients with or without Lac peaks compared with the controls. However, there was no significant correlation between the NAA/Cr ratio and neurological status within patient group. M-Ins levels were not quantified.

In a study of whiplash injury(Elliott et al. 2011), metabolite ratios were quantified in 5 patients and 7 controls. Significant reductions in NAA/Cr ratio was found in patients when compared with healthy controls (mean = 1.3, sd; 0.5 and mean = 2.0, sd; 0.7 respectively). No differences were demonstrated in Cho/Cr ratio and m-Ins was not studied.

5.5 Proton MRI in brachial plexus avulsion and re-implantation

In the previous sections, the principles of magnetic resonance imaging and major metabolites and their function were discussed. In addition, the limited number of studies in the human spinal cord affected by different conditions were described. In the next chapter, we present a study of ^{1}H-MRS of the spinal cord in patients with brachial plexus re-implantation surgery compared with control subjects.

Chapter 6

^{1}H-MRS as a diagnostic and prognostic tool in brachial plexus avulsion injury and re-implantation surgery

This chapter investigates the application of spinal cord ^{1}H-MRS and its usefulness in revealing metabolic changes occurring in the spinal cord following re-implantation surgery for complete brachial plexus avulsion.

6.1 Aims

The present study applies ^{1}H-MRS of the spinal cord in an attempt to reveal abnormalities in patients with spinal cord pathology and provide information regarding neuronal viability, cellular composition and thus provide diagnostic and prognostic insights. We aim to assess whether ^{1}H-MRS of the upper cervical cord (i.e. above the site of injury) detects pathological changes in patients with complete brachial plexus root avulsion who have received re-implantation surgery and patients with complete brachial plexus root avulsion who have not had any surgical intervention when compared with healthy subjects. In addition, we aim to explore the relationship between metabolite concentrations and clinical disability in patients.

6.2 Methods

6.2.1 Patient recruitment

For the purposes of this study we have recruited a population of patients with complete brachial plexus avulsion injury from the surgeons' complete database of

brachial plexus avulsion injury and list of re-implantation cases. In order for this cohort to be uniform we have included only patients that have had a diagnosis of complete avulsion injury by open exploration of the brachial plexus by TC. Patients in whom, at the time of exploration, the diagnosis of complete brachial plexus avulsion could not be confirmed (for example when there was suspicion of intradural rupture rather than avulsion or rootlets of one or more root remained attached) were excluded. The important findings described in Chapter 2 were not known at the time of recruitment of these patients.

This study was approved by the National Hospital for Neurology and Neurosurgery and Institute of Neurology Research Ethics Committee. Once informed consent was obtained, we collected clinical data and performed MR spectroscopy.

6.2.2 Participants

To the date of data collection for this study, twenty-five patients who have had re-implantation surgery (re-implantation group) and sixteen patients with complete brachial plexus avulsion injury who have had no surgical intervention (control group) were identified for participation in our study. From these, 10 patients from the re-implantation group and five patients from the control group were scanned. The remaining patients were not assessed for one of the following reasons: (a) had been lost to follow up, (b) patients declined participation, (c) patient had MRI-incompatible metal implants or tattoos (d) have had amputation of the affected arm

or, (e) had associated lower limb weakness. Nineteen age- and sex-matched healthy subjects (healthy group) recruited from the community were also studied.

6.2.3 Clinical assessment

On the day of the scan, patient disability was assessed using the following scales: (i) Disability for Arm, Shoulder and Hand (DASH) (Beaton et al. 2001), which is a 30-item self-report questionnaire designed to measure physical function and symptoms in people with musculoskeletal disorders of the upper limb. A higher score indicates greater disability; (ii) Visual Analogue Pain Scale (VAS), a widely used tool for measuring pain by asking the patient to indicate his/her perceived pain intensity by marking a point along a 100 mm horizontal line (Flaherty 1996); (iii) Michigan Hand Outcomes Questionnaire (MHQ) (Chung et al. 1998; Chung et al. 1999), which is a hand-specific questionnaire including six subscales: overall hand function, activities of daily living (ADL), pain, work performance and patient satisfaction with hand function and aesthetics. Higher scores indicate better hand function, except for the pain subscale on which higher scores correspond to more pain (13).

A summated muscle score of the MRC grade of 7 upper limb muscles of the affected arm was used to assess global power in the affected arm ("global MRC score") as described in Chapter 2 (Section 2.3.2).

6.2.4 MR protocol and spectroscopy

All MR data were collected on a Magnetom Tim Trio 3T system (Siemens AG, Erlangen, Germany), using the posterior half of a 12 channel head coil, the posterior part of a neck array coil, and the upper element of the spine array coil.

All subjects underwent conventional T2-weighted sagittal and coronal images (sagittal-oblique: turbo spin echo with effective TE = 96ms; TR = 3s; parallel imaging with acceleration factor 2; field of view (FoV) = 220mm^2, in-plane resolution 0.69 x 0.92 mm^2, slice thickness = 1.5 mm, gap = 0.15 mm; coronal-oblique: 3D-HASTE with TE = 247 ms; TR = 3 s; parallel imaging with acceleration factor 2, FoV = 200mm^2, in-plane resolution = 0.78 x 0.78 mm^2, 52 partitions, slice thickness = 0.8 mm), which confirmed the normal radiological appearance of the spinal cord in all patients. These scans were acquired aligned with the main axis of the spinal cord, essential for correctly positioning the spectroscopy voxel.

Single-voxel spectra were obtained by cardiac-gated point resolved spectroscopy (PRESS) sequence with TR ≅ 3000 ms (depending on the cardiac cycle), TE = 30 ms and 160 averages, with chemical-shift-selective (CHESS) water suppression (Haase et al. 1985). We used the PRESS sequence provided by the manufacturer, and no additional saturation bands were used. The excitation frequency was -2.3 ppm, with respect to the water reference frequency, i.e. 2.4 ppm. Readout bandwidth was 1200 Hz (1024 points collected). Our longer TR compared with previous studies reduced sensitivity to metabolites T1 changes. A non water-suppressed spectrum (2 averages) was also acquired for eddy-current correction. The spectroscopic voxel

was placed along the main axis of the cord, centered at C2 spinal level with its prescription boundaries completely contained within the cord on the T2-weighted images in all three planes (Figure 6.1). Optimal shim currents for all first-order (*X*, *Y* and *Z*) and second-order (Z^2, *ZX*, *ZY*, X^2-Y^2 and *XY*) shim gradients were calculated off-line with in-house software based on: i) acquisition of field maps (gradient-recalled sequence generating two images with TE = 4.92 ms and TE = 7.38 ms respectively, 2 mm isotropic resolution, 1 min. acquisition time); ii) minimisation of the magnetic field variation within the prescribed MRS voxel using calibrated field maps for each shim coil (Webb et al. 1991; Kim et al. 2002).

All MRS spectra were analysed by means of the user-independent frequency-domain fitting software LCModel 6.1 (Provencher 1993) within the 0.2 - 4.0 ppm range. Ratios of the following metabolite concentrations were calculated with respect to total Creatine (Cr) concentration (Creatine plus Phosphocreatine): total N-acetyl-aspartate (NAA) (equal to NAA plus NAAG), total Choline (Cho) (equal to Glycerylphosphorylcholine GPC plus Phosphocholine) and myo-Inositol (m-Ins). LCModel standard error estimates (%SD, Cramer-Rao lower bounds (CRLB)) were used to assess the confidence of the concentration estimates.

6.2.5 Statistical analysis

Statistical analysis was performed on data which passed quality control criteria. Initially, all in-vivo data was fitted using LCModel and spectra with a signal-to-noise ratio, SNR < 6 and full width at half maximum, FWHM > 0.14 were deemed to be of

poor quality and eliminated from further analysis. The values for SNR and FWHM were calculated by LCModel as part of the fitting process. LCModel estimates were retained if the %SD was equal to or lower than 21% for Cr and for the metabolite of interest.

Statistical comparisons and correlations were performed using STATA statistical software Version 10.1 (StataCorp LP College Station, TX). Data for each metabolite were tested for normal distribution and for homogeneity of variances. Differences in metabolite ratios between groups were estimated using the unpaired two sample Student's t test (t). The relationship between disability and metabolite ratios was tested in patients using multiple linear regression, using the clinical scores, in turn, as the dependent variable and the metabolite ratios as independent variables.

6.3 Results

6.3.1 Excluded patients and description of study groups

The water suppression technique or shimming procedure failed due to technical errors in 4 healthy subjects, 2 patients with re-implantation and 1 patient without re-implantation. In addition, spectra of 1 healthy subject and 1 patient without re-implantation demonstrating CRLB %SD of [Cr] > 21% (%SD = 32 and %SD = 73 respectively) were excluded. Thus, the final MRS data following exclusions came from: 14 healthy subjects; 13 men and 1 woman with and average age of 36.1 yrs (sd; 10.7).

The re-implantation group consisted of 8 men with average age of 35 years (sd; 10.8). All patients underwent ventral root re-implantation within one month from the day of their injury. The mean duration from injury to assessment for this study was 5.5 years (sd; 4.3). M-Ins/Cr ratio was excluded from the analysis in three healthy subjects because of %SD of m-Ins >21%. NAA/Cr was excluded in three different healthy subjects and one patient with re-implantation because of %SD for tNAA >21%.

Following exclusions, 3 patients were included in the control group (patients without re-implantation). These were all men and had an average age of 39.3, (sd; 10.3). However, the spectrum of one control patient showed an FWHM of 25 Hz (group mean; 18.2 Hz, sd; 6.5) deeming the data of this patient unreliable for statistical analysis and, therefore excluded (Figure 6.2 (D)). Consequently, that left only 2 control patients, rendering group comparisons of metabolite concentrations and correlations with disability scores of little value.

6.3.2 Spectroscopic voxel

Typical location and size of the VOI in the spinal cord is shown in Figure 6.1 (A and B). The average size of the spectroscopic voxel was 5.9 mm (sd; 0.3 mm) in the anteroposterior dimension, 49 mm (sd; 5 mm) in the cranio-caudal dimension and 7.4 (sd; 0.7 mm) in the transverse dimension. The mean volume of the spectroscopic voxel was 2.1 ml (sd; 0.6 ml).

(A) 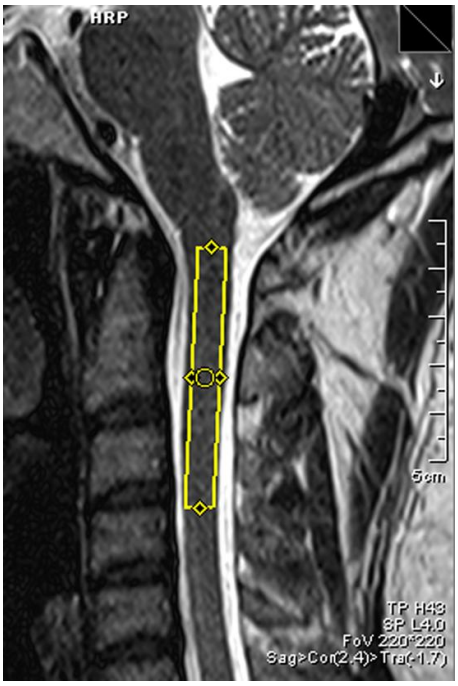

(B) 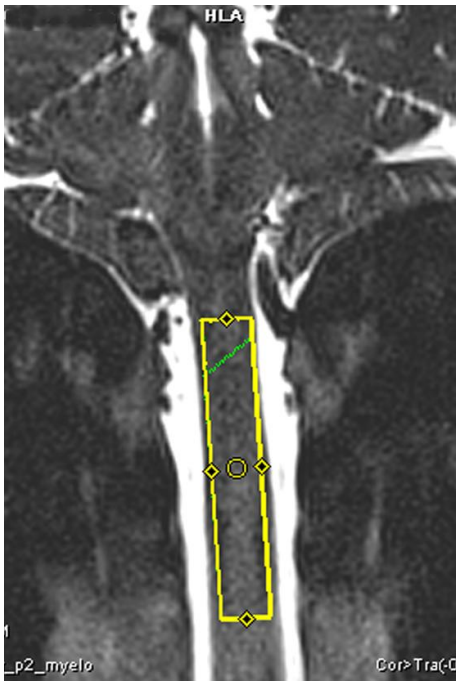

Figure 6.1: *Location of the spectroscopic voxel between C1 and C3 on the T2-weighted image of a healthy subject in the sagittal (A) and coronal (B) dimension.*

The mean FWHM and SNR values estimated by LCModel were 11 Hz (sd; 2.2 Hz) and 2.4 (sd; 0.8) respectively for the healthy subjects. The corresponding values for the re-implantation group were 10 Hz (sd; 4 Hz) and 2.9 (sd; 1.0) respectively. A Student's t test showed no significant difference in FWHM between the healthy subjects and re-implantation groups ($t(21) = 0.12$, $p = 0.91$). The overall chemical shift was fairly small in terms of volume shift and mis-positioning of the VOI. Representative spectra for each patient group are shown in Figure 6.2.

(A)

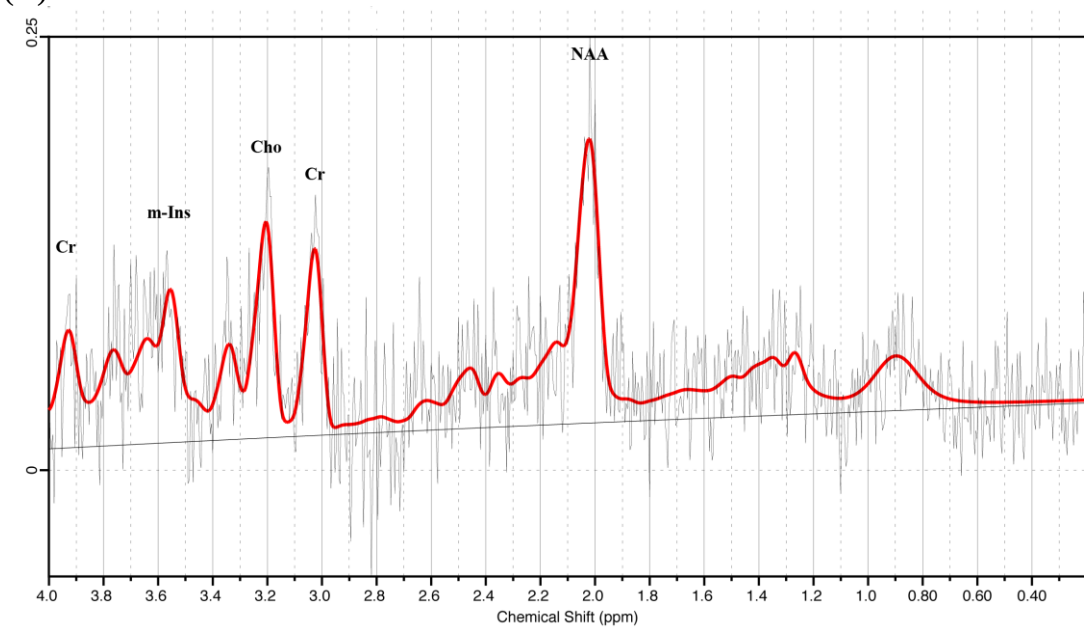

(B)

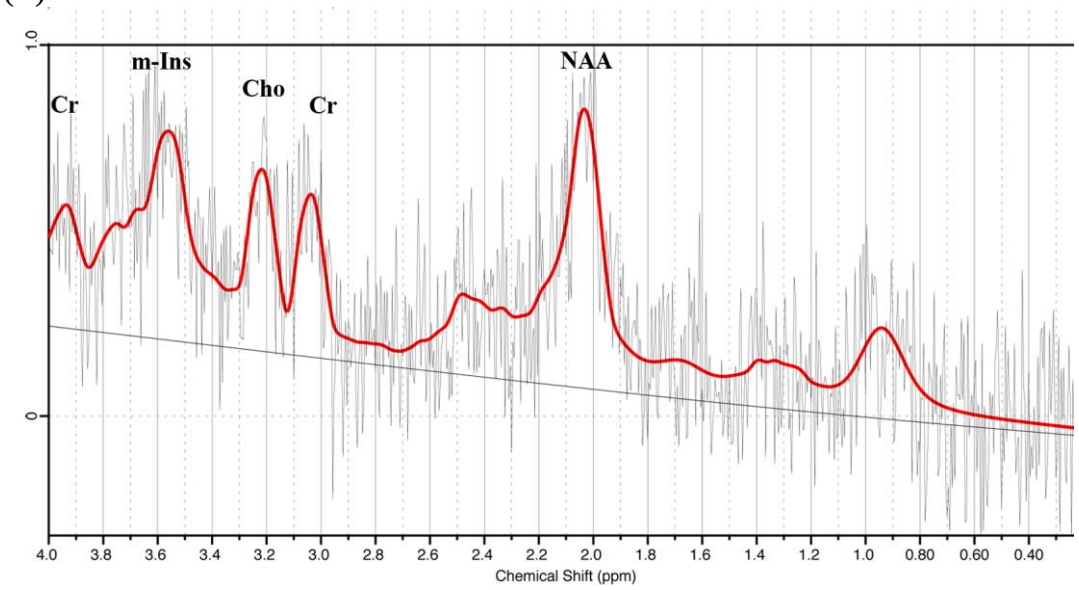

Figure 6.2 (A and B): *Representative spectra derived from each patient group; (A) healthy subject, (B) patient with re-implantation surgery.* The s*pectrum derived from the healthy subject (A) shows reduced m-Ins/Cr ratio (m-Ins/Cr =1.37; %SD 11) in comparison with a spectrum obtained from a patient with re-implantation (B) (m-Ins/Cr = 2.11 (%SD 10).*

(C)

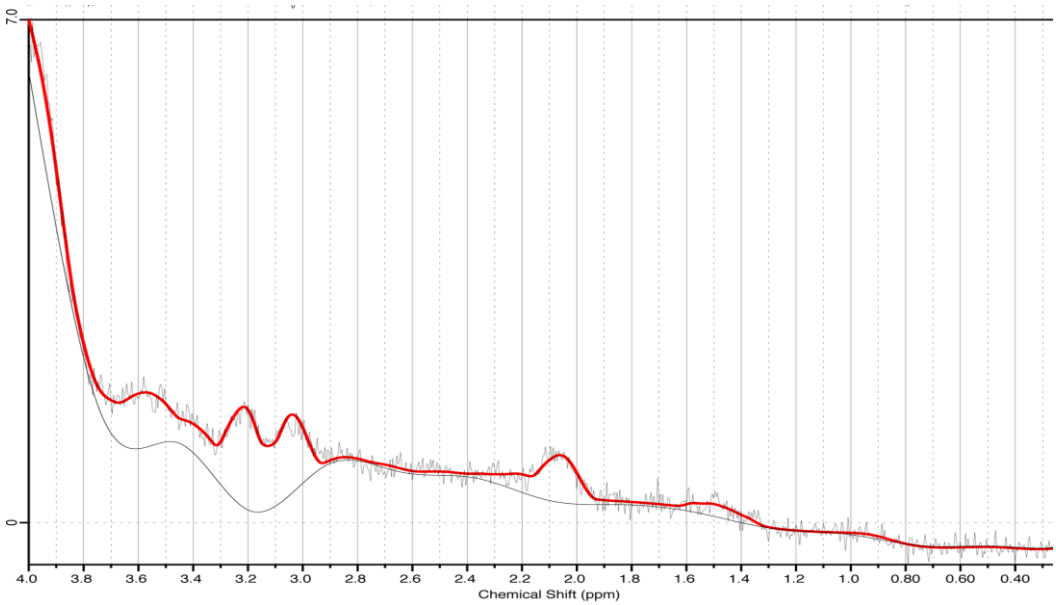

(D)

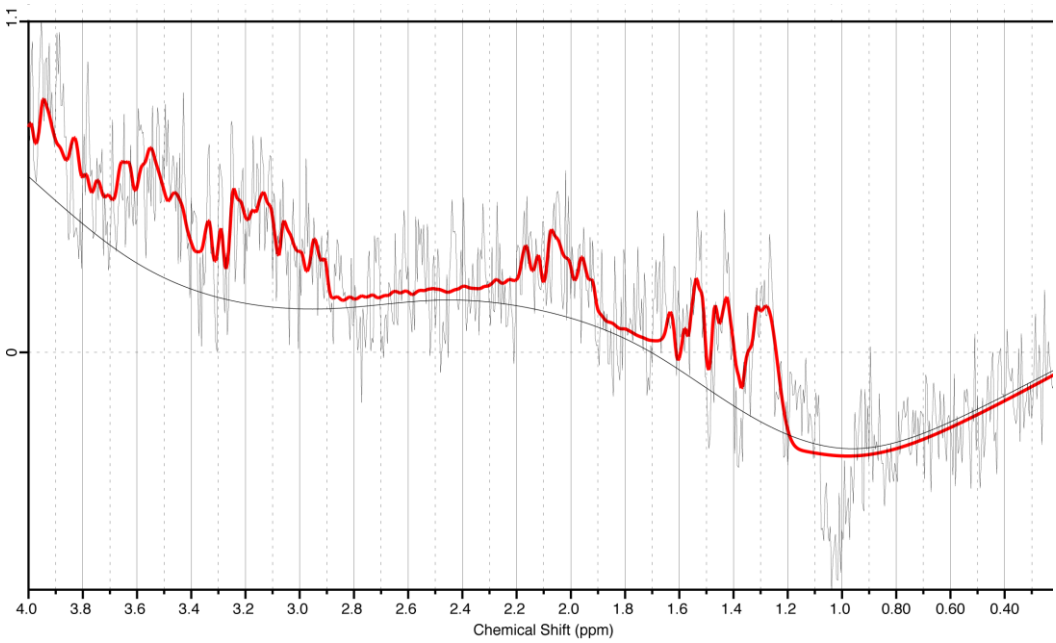

Figure 6.2 (C and D): *(C) A spectrum obtained from a patient without re-implantation surgery*. FWHM= 13, SNR = 6, %SD Cr = 7, %SD NAA = 11, %SD m-Ins = 16, %SD Cho = 8, (D) An unreliable spectrum of a control patient. FWHM = 25, SNR = 1, %SD Cr = 20, %SD NAA = 25, %SD m-Ins = 17, %SD Cho = 16.

6.3.3 Metabolite concentrations

The group mean %SD values obtained by LCModel analysis for the main metabolites in healthy volunteers were 11 for Cr, 13 for NAA, 16 for m-Ins and 14 for Cho. For the patient group with re-implantation surgery mean %SD values for each metabolite were 12, for Cr, m-Ins and Cho and 15 for NAA (Table 6.1).

Table 6.1: *Cramer-Rao lower bounds (CRLB) quantified by LCModel in the spinal cord between C1 and C3 spinal level for each metabolite (%).*

	Cr (sd)	**NAA (sd)**	**m-Ins (sd)**	**Cho (sd)**
Healthy	11 (3)	13 (5)	16 (6)	14 (4)
Re-implantation	12 (3)	15 (8)	12 (5)	12 (4)
No re-implantation	11 (8)	23 (11)	12 (7)	11 (5)

The mean concentrations of metabolites quantified by LCModels in the spinal cord between C1 and C3 relative to total Cr are presented in Table 6.2. Comparison with a Student's t test revealed a statistically significant difference in m-Ins/Cr ratio between healthy subjects and the re-implantation group (t (19) = -3.73; 95%CI = -1.05 to -0.29; p = 0.001) (Table 6.2). No significant differences in absolute Cr concentrations were observed between groups. There was no significant difference in Cho/Cr (t (20) = -0.76; 95%CI = -0.11 to 0.05; p = 0.45) or NAA/Cr concentration

ratios between healthy subjects and patients with re-implantation (t (15) = -0.19; 95%CI = -0.38 to 0.31; p = 0.85) (Table 6.2).

Table 6.2: *Mean concentrations of metabolites quantified by LCModels in the spinal cord between C1 and C3 in healthy controls and patients with re-implantation and comparisons of metabolite concentrations between the two groups. Asterix (*) denotes statistically significant difference between groups. Concentrations are quantified relative to total creatine (Cr).*

Ratio	**Controls Mean (SD)**	**Re-implantation Mean (SD)**	**p value**
NAA/Cr	1.19 (0.29)	1.21 (0.38)	0.85
m-Ins/Cr	1.18 (0.38)*	1.86 (0.41)*	0.001*
Cho/Cr	0.30 (0.08)	0.33 (0.45)	0.45

6.3.4 Correlation of metabolite ratios with disability scores and patient variables in patients with re-implantation surgery

Multiple regression analysis of m-Ins/Cr ratio of the patients with re-implantation showed that m-Ins/Cr ratio was independently associated with both DASH scale and time from injury (R^2 = 84%; F = 13.56; p = 0.0096). In particular, a higher m-Ins/Cr ratio correlated with greater disability, as measured by the DASH scale (t (7) = 2.86; 95%CI = -0.001 to -0.02; p = 0.035) (Figure 6.3), and with shorter time from injury (t (7) = -5.15; 95%CI = -0.02, -0.006; p = 0.004) (Figure 6.4). Comparison of predictor coefficients shows that a one standard deviation increase in DASH score leads to a 0.55 standard deviation increase in predicted m-Ins/Cr ratio and a one

standard deviation increase in the length of time since the injury (in months) results in 0.99 standard deviation decrease in m-Ins/Cr ratio. The addition of age, MRC grade for individual muscles, "global MRC score", or MHQ or pain scores did not improve the regression model. Changes in m-Ins/Cr ratio did not correlate with changes in NAA/Cr (p = 0.29).

Multiple regression analysis of NAA/Cr and Cho/Cr ratios in patients with re-implantation surgery did not show significant correlations with disability, scores, MRC scale or pain scores. However, Spearman's correlation coefficient revealed a positive correlation of Cho/Cr with "global MRC score" (r = 0.814, p = 0.0138, (95%CI = 0.258 to 0.965).

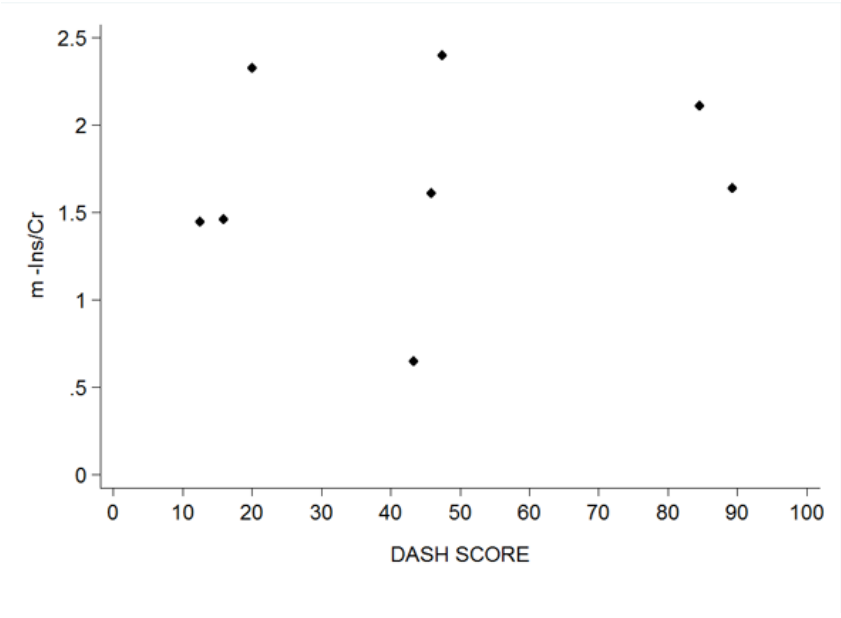

Figure 6.3: *Scatter plot showing the relationship between m-Ins and Dash score* (R^2 = 84%; F = 13.56; p = 0.0096).

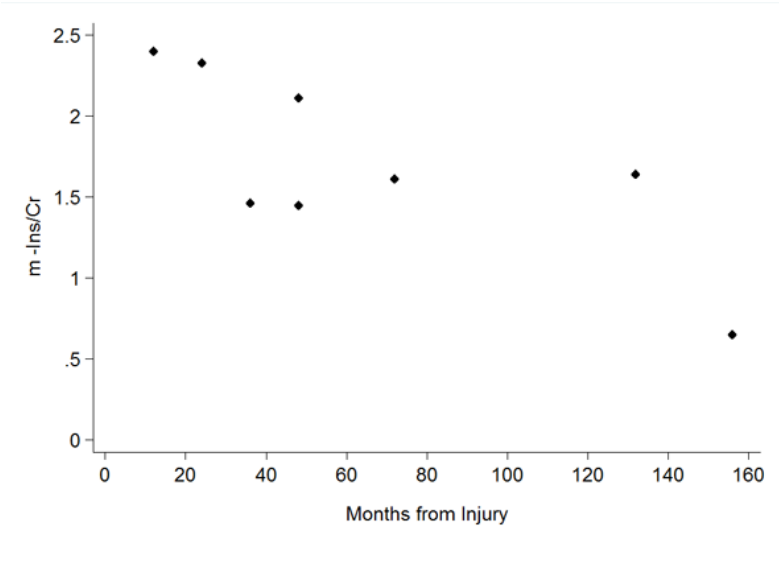

Figure 6.4: *Scatter plot showing the relationship between m-Ins and months from injury* (R^2 = 84%; F = 13.56; p = 0.0096).

6.4 Discussion

To date, only a small number of ^{1}H-MRS studies of the spinal cord have been performed due to the technical difficulties. The local field inhomogeneities and the small voxel size are the main difficulties encountered. The aim is to simultaneously obtain narrow line-width and adequate SNR in an acceptable acquisition period. The present thesis assesses the feasibility of volume selective 3T ^{1}H-MRS of the spinal cord and evaluates its potential use as a prognostic tool in central nervous injury of the spinal cord in humans. We have compared a cohort of patients with complete brachial plexus avulsion injury who have undergone re-implantation surgery with healthy volunteers aiming to demonstrate differences in major metabolite

concentrations including Cr, NAA, m-Ins and Cho. In the following section, the feasibility of volume selective 3T ^{1}H-MRS of the cervical spinal cord is discussed and its weaknesses are addressed.

6.4.1 Feasibility of volume selective 3T ^{1}H-MRS of the spinal cord and quality of spectra

When in vivo ^{1}H-MRS spectra obtained from the spinal cord above the level of injury were analysed using LCModel, concentrations of Cho, M-Ins, NAA and Cr were reliably quantified according to CRLB in 25 out of 34 patients scanned in total (73.5%).

In 7 out 9 (77.7%) failed scans were attributed to inadequate shimming or water suppression due to either patient/physiological movements or operator errors, rather than due to protocol design. Therefore, in 27 out of total 34 scans (79.4%), metabolite peaks of interest were adequately resolved. However, another 2 patients were excluded their CRLB %SD of total Cr was > 21%. CRLB is a statistical estimate of uncertainty of metabolite concentrations and < 21% has been arbitrarily chosen based on previous experience and thought to represent reliable metabolite concentrations (Ciccarelli et al. 2007).

In general, the use of larger voxels improves SNR but this has trade-offs against fat contamination and partial-volume effects. As suggested by previous reports of ^{1}H-MRS of the cervical spinal cord (Cooke et al. 2004), we aimed to use the largest

possible voxel, which was placed parallel to the spinal cord, in such a way that the voxel was entirely within the spinal cord to avoid fat and CSF contamination. We optimised our protocol in healthy volunteers and obtained an averaged voxel size of 5.9 mm (± 0.3) (anteroposterior) x 7.4 mm (± 0.7) (transverse) x 49 mm (± 5) (craniocaudal) resulting in an average volume of 2.1 ml. This is comparable to previous studies investigating the optimal voxel size in the cervical spinal cord with average voxel volumes of 2.2 ml. (Cooke et al. 2004) and 2.4 ml (Marliani et al. 2007). In contrast to the study of Cooke et al., (Cooke et al. 2004) we increased the length of the voxel to the maximum possible with the voxel always centered at C2, covering the length of the spinal cord from the tip of C2 to the level of C3, thereby increasing the voxel size while keeping the number of tissue interfaces to minimum. These maneuvers increased the resultant spectroscopy signal. We were unable to increase the transverse dimension to 9 mm average in the transverse direction, as suggested by Cooke et al., (Cooke et al. 2004), as the voxel would enter the CSF space.

The average SNR was 2.4, comparable with other ^{1}H-MRS studies of the human spinal cord, (Marliani et al. 2007; Marliani et al. 2010). To reduce scanning time and patient discomfort and based on previously acquired pilot data, we opted for collecting 160 repetitions with a TR of 3 sec and cardiac gating. This resulted in total nominal acquisition time of 8 min (in practice, close to 10min). Our long TR provided an 8% boost in SNR (Traber et al. 2004). In the study of Marliani et al., (Marliani et al. 2010) who achieved SNR of 4, 400 repetitions, a TR of 2 sec and no cardiac gating were used, resulting in a 13 min and 20 sec scanning time but increased sensitivity to cardiac pulsation. A 15 % loss in signal and 25 % increase in

FWHM has been demonstrated in non-gated compared to gated data (Cooke et al. 2004); for this reason we used cardiac gating. It is worth remembering SNR reported by the LCModel is, by definition and design, only a 'rough' indication of spectral quality, since it is simply calculated as the maximum in the spectrum minus baseline over the analysis window. The %SD reported for each metabolite in LCModel is a better indicator of the reliability of the metabolite estimates as it accounts for both spectral resolution and noise level. Therefore, the reported %SD of our metabolites in 25 out of 27 scans (92.6%) confirms that our data quality was adequate.

With regards to mis-positioning of the VOI for the metabolites, great effort was made to ensure that the target region of the cervical cord was on resonance between field map and acquisition. Despite maximal efforts, the location of the VOI was shifted between -4.9% and +14.3% of 7 mm, i.e. -0.34 mm, (sd; 1.00 mm) in the transverse plane, and between -1.5% and +4.2% of 49 mm, i.e. -0.74 mm, (sd; 2.06 mm) in the cranio-caudal direction. This was considered acceptable given the size and positioning procedure applied in this study.

6.4.2 Interpretation of metabolite concentration ratios obtained

6.4.2.1 Inositol/Cr ratio

In this study, patients with re-implantation showed a significantly greater m-Ins/Cr ratio in the cervical spinal cord above the level of injury when compared with healthy subjects. In addition, m-Ins was positively correlated with increasing

disability in patients with re-implantation. These are novel findings, which have not been observed in previous ^{1}H-MRS studies of patients with spinal cord injury lesions (Holly et al. 2009; Elliott et al. 2011). M-Ins increases have been observed in white matter lesions in patients with multiple sclerosis (Fernando et al. 2004; Marliani et al. 2010). Increased m-Ins is thought to be due to reactive gliosis, including astrocytic proliferation and hypertrophy, possibly in response to the Wallerian degeneration of avulsed neuronal fibres. This is in agreement with observations in histopathological studies including: (i) increased vimentin (VIM) and glial fibrillary acidic protein (GFAP) immunoreactivity, markers of astrocytic proliferation and gliosis, in the pericontusional zone described in animal models of acute and chronic stage after spinal cord injury (Verma et al. 2008; Erschbamer et al. 2011); and (ii) proliferation of astrocytes forming a non-permissive glial scar surrounding the transitional zone, found in models of nerve root avulsion injury (Risling et al. 1983; Risling et al. 1983; Koliatsos et al. 1994). Alternatively, given the roles of m-Ins in intracellular signalling pathways, changes in m-Ins/Cr ratios may be due to alterations of cell signalling in spinal cord segments that no longer have bilateral axonal connections with the remainder of the spinal cord and/or brain (Erschbamer et al. 2011).

Furthermore, in the current thesis it was demonstrated that m-Ins/Cr concentration ratio is negatively correlated with length of time from injury. Increases in m-Ins and corresponding GFAP immunoreactivity in experimental models of spinal cord injury at 7 days, but not 24 hours after the insult (Schuhmann et al. 2003) and remaining at 4 months (Erschbamer et al. 2011). In sum, these findings suggest that there may be in initial increase in the m-Ins/Cr ratio in the acute stage, but a progressive decrease

in the chronic stage of disease in patients with re-implantation surgery. This can is yet to be demonstrated with either prospective studies or by comparing with a control group of patients with BP avulsion injury but without surgical intervention, which was the initial but unsuccessful aim in the current thesis.

6.4.2.2 NAA/Cr ratio

No significant difference in NAA/Cr concentration between patients who have undergone re-implantation surgery and healthy volunteers or a correlation with disability scores was observed in this study. Decreases in NAA in various neuropathologies of the brain are thought to represent irreversible loss of neurons and/or metabolic dysfunction because under normal conditions NAA is synthesised in and exported from the mitochondria, predominantly of neurons (Moffett et al. 2007; Sajja et al. 2009). On the aims of re-implantation surgery is to counteract the effects of the avulsion injury, prevent apoptosis of injured motoneurons and support axonal regeneration (Linda et al. 1985; Risling et al. 1992; Koliatsos et al. 1994; Bergerot et al. 2004). The lack of difference in NAA/Cr ratio between the two groups in this study may be due to the either the small number of patients and low statistical power, or due to a true replenishment of nerve fibers in the re-implantation group. Furthermore, in successful ventral root re-implantation, one would expect an increase in NAA/Cr ratio with time. In this cohort of patients, however, there was no significant correlation between NAA/Cr ratio and time from injury. It could be hypothesized that NAA/Cr concentration has normalised over time.

A key question is whether patients who have not undergone re-implantation surgery show significantly reduced levels of NAA/Cr levels compared with healthy subjects and patients who underwent re-implantation. Unfortunately, we were able to scan only 3 such patients, and the small number of patients and spectral quality does not allow reliable statistical comparison among groups. Nonetheless, an attempt to interpret the data has shown observation 42% and 43% reductions in NAA/Cr ratio in patients without re-implantation compared with patients who underwent re-implantation and healthy subject respectively. Analysis of variance showed revealed a significant difference among the three groups studied ($F(2,7) = 5.53$; $p = 0.0141$). Planned comparisons revealed that healthy subjects have a mean of 0.03 (95% CI: -0.32 to 0.38) higher than patients who have had re-implantation surgery (mean -.067, 95% CI: -1.12 to -0.22), which is not a statistically significant difference (p 0.86). However, the control group (avulsion injury without reimplantation) has a mean of -0.67 (95% CI: -1.12 to -0.22) lower NAA/Cr ratio than healthy subjects with a significant difference ($p = 0.006$). This finding also suggests that NAA/Cr levels may normalise with time. However, taking into consideration the small number of patients in the control group (avulsion injury without reimplantation), it was felt more appropriate to use a non-parametric test to assess comparisons. A Kruskal-Wallis was, therefore, also used to explore whether there is a difference between the three groups in NAA/Cr ratio, which showed only a marginal difference among groups ($p = 0.057$). In summary, there is a suggestion from the results presented that there is a trend towards significance in the difference of NAA/Cr ratio between the three groups. However, this needs to be confirmed in subsequent studies with larger patient groups.

6.4.2.3 Cho/Cr ratio

There was no significant difference in Cho/Cr ratio, which reflects inflammation with membrane turnover, between healthy subjects and patients with re-implantation. Our results are in accord with previous human studies in patients with cervical spondylotic myelopathy (Holly et al. 2009) or chronic whiplash injury (Elliott et al. 2011). In contrast, elevations in Cho/Cr has been observed in normal-appearing gray matter after traumatic brain injury (Friedman et al. 1999; Garnett et al. 2000) in the acute setting and in pericontusional brain regions in experimental brain studies following an initial decrease in Cho/Cr ratio compared to controls (Schuhmann et al. 2003). Again, it may be that in the chronic phase Cho/Cr levels normalise, as shown in a study of experimental model of crushing spinal cord injury by Qian et al., (Qian et al. 2010) who demonstrated recovery of Cho/Cr ratio in the epicentre and caudal regions of the spinal cord at 56 days post injury.

Although Cho:Cr ratio did not differ between groups, it showed a positive correlation with increasing "global MRC score" i.e. greater neurological recovery, suggesting increased inflammation and membrane turnover in patients with better neurological status.

6.4.2.4 Absolute Cr concentration

No differences in absolute Cr concentrations were observed between groups confirming that Cr is a reliable internal standard when investigating the effects of spinal cord injury above the level of injury upon metabolite concentration.

6.5 Limitations

The main limitation of this study is the limited number of patients that were available in both the re-implantation group and control group. The main reasons for this is the rarity of the injury and institutional constrains in scanning patients with metal implants. Most of these patients had been involved in high impact motor vehicle accidents resulting in multiple fractures requiring fixation with metal implants most of which have not been cleared for 3 Tesla MRI. At the time of scanning, the "default" field strength indicated for and "MR safe" implant was 1.5 Tesla, evidence that is adequate for scanning in the clinical setting as benefit outweighs risks. However, for research purposes, specific evidence of testing at 3 Tesla was required to deem a metal implant safe in the institution we scanned our patients. Every effort was made to acquire sufficient data that proved implants safe, however, most manufacturers have not performed or would not release their data. The major concern was the risk of metal heating that could result in internal burns especially with older implant designs, rather than implant movement.

Furthermore, as already discussed, findings of this current thesis were limited by the absence of a control group. Future and collaborative work, perhaps with a multi-centre setting, may be able to address this question.

Spectroscopy analysis was limited to NAA, Choline and myo-inositol, whereas other potentially measurable metabolites such as Lactate (Lac) and Glutamine/Glutamate (Gln/Glu) were not studied. Lac resonance is at the very limit of detectability in most brain MRS studies due to the low concentration of lactate under normal conditions but is often detectable in pathological conditions where anaerobic metabolism ensues. However, our patients are well into the chronic stage of their injury and such elevations would not persist years after the injury. Secondly, lactate resonance is difficult to distinguish due overlapping lipid resonances and requires long echo time (~140 ms) or other spectral editing techniques. To our knowledge, Lac spectra from the spinal cord have been acquired in one study of cervical spondylotic myelopathy patients in the acute stage, where Lac peaks were demonstrated in 7 out of 21 patients, 6 of which had T2 signal abnormality in the same region of the spinal cord (Holly et al. 2009). Furthermore, Gln/Glu quantification is complex and challenging and to our knowledge has not been reported in the spinal cord to date. We aim to perform pre- treatment MRS and prospective longitudinal follow up MRS studies during the rehabilitation period to demonstrate temporal changes in the spinal cord and correlate to clinical recovery, which will also enable us to obtain Lac spectra during the acute stage.

6.6 Future directions

To date, there is no imaging available to indicate the success of the re-implantation including progress of regeneration and the relationship between imaging and

neurological improvement and surgical outcome in patients with spinal cord re-implantation. Standard MR imaging provides excellent macroscopic anatomical detail but limited specific information regarding the cellular function of the spinal cord microarchitecture. MRS has the potential to provide microcellular biochemical information as well as advance our current understanding of nerve regeneration following re-implantation.

Future work should focus on recruiting a larger cohort of patients including patients without surgical intervention perhaps by recruiting patients from other centers to show reproducibility of finding presented here.

In addition, a great deal of information could be obtained by retrospectively assessing patients prior to patients' surgery and at intervals after surgical intervention. Perhaps, this method may demonstrate any metabolic changes over time. For example, it is interesting to find out whether NAA is reduced in the spinal cord after brachial plexus injury in the acute phase, and then normalizes over time.

Lastly, the combination of functional MRI with metabolic and structural MRI may allow to better understand recovery after spinal cord injury and fully characterize CNS plasticity, which is the ultimate goal of multi-modal imaging.

6.7 Conclusion

In closing, the present study set out to investigate the metabolic changes that occur in the spinal cord with ^{1}H-MRS. Findings suggest that it is feasible to quantify metabolites of the upper cervical cord above the site of injury, close to focal traumatic lesion, with volume selective 3T ^{1}H-MRS using the LCModel. Patients with re-implantation surgery showed increased m-Ins/Cr ratio compared to controls, which was associated with (1) the level of function of the affected arm and (2) time from injury. These differences in metabolite concentrations may prove a useful tool in predicting outcome and provide insights into the underlying pathological processes in these patients.

Overall conclusion

This thesis set out to investigate three different perspectives of the management of complete brachial plexus avulsion injury. The first experiment of this thesis investigates the long-term functional improvement of re-implantation surgery in patients with complete brachial plexus avulsion injury using standardized assessments. The second study relates to the potential use of olfactory ensheathing cell transplantation as an adjunct therapy to root reimplantation surgery. It involves a prospective observational study of the olfactory ensheathing cell yield from biopsies of nasal mucosa from different locations. A new surgical technique for harvest is described. Specimen- and patient-related characteristics, in addition to, location are assessed in an attempt to determine what factors affect yield and could result in adequate yields for transplantation. The third experiment describes the use of ^{1}H-MR spectroscopy in predicting outcome in patients undergoing brachial plexus re-implantation surgery, which may also provide a more robust measure for comparing different strategies of brachial plexus repair.

Brachial plexus re-implantation surgery is a relatively new surgical strategy for the management of brachial plexus avulsion injury. In this thesis, we assessed the functional recovery of such patients with clinical and neurophysiological means, as well as, patient reported outcome measures and compared functional recovery to a control group of patients who have had complete brachial plexus avulsion injury but no implantation surgery. Previous preliminary reports investigating the functional

recovery of re-implantation surgery have been non-specific in determining recovery in a homogeneous group of patients, incorporating patients with incomplete brachial plexus injury in studies and therefore failing to confidently revealing the true effects of this strategy. More importantly, previous reports are not supported by objective assessment methods such as neurophysiological evidence of recovery and lack a comparison control group of patients.

In this thesis, it was shown that patients with brachial plexus re-implantation surgery following complete brachial plexus avulsion demonstrated some improved motor and sensory function in the proximal muscles of the upper limb when compared to patients with complete brachial plexus avulsion injury who have not had re-implantation surgery. In particularly, patients with re-implantation surgery showed greater return of function in the deltoid, pectoralis and infraspinatous power on clinical examination with a significantly improved recovery in the global function of the upper limb assessed by a "global MRC power "score incorporating 7 different upper limb muscles. In addition there was a significant difference in the voluntary control between the two groups with patients with re-implantation surgery demonstrating evidence of reinnervation in the infraspinatous, biceps and triceps muscles in patients with re-implantation surgery when compared to as demonstrated by needle EMG studies. There was also evidence of ongoing reinnervation in deltoid, biceps and triceps in patients who have had re-implantation surgery, demonstrated by the presence of polyphasic nascent units in electrophysiological studies. Furthermore, an exciting finding was the presence of motor unit action potentials in distal muscles of the upper limb including the FDIO and FDS in two separate patients who have undergone re-implantation patients while there was no

evidence of reinnervation of distal muscles of the upper limb in the control group. Interestingly, an improved recovery in sensory function was also revealed in the re-implantation group. Sensory testing in affected dermatomes showed generally improved recovery in the re-implantation group in C5, C6 and T1 dermatomes with a significant higher frequency in return of sensation in C5 dermatome for both soft touch and pinprick sensation in the re-implantation group compared to controls.

Despite the evidence of improved function in the aforementioned muscles in clinical and neurophysiological assessment, the functional recovery was limited and operated patients did not report a significant difference in function compared to those without re-implantation in the patient reported outcome measures. Research has focused in finding adjuvant therapies to re-implantation surgery by which the re-innervation seen with re-implantation surgery can be further enhanced.

One such strategy involves the use of cell transplantation at the time of re-implantation of avulsed roots. While OEC mediated repair of spinal cord injury has been well described in animal experiments, the translation to human studies is partly limited by the difficulty in achieving adequate culture yields of human OECs for autotransplantation. Previous reports have documented their success in localizing olfactory mucosa but studies investigating actual human OEC yields have been insufficient. In the second experiment, it is shown that biopsies from the cranial portions of the superior turbinate using a new safe and reproducible endoscopic surgical technique produce greater OEC yields. The success rate in obtaining olfactory mucosa from the nasal cavity was also significantly higher compared to previous reports. In addition, it is demonstrated that increasing age and nasal

mucosal disease adversely affect the culture yield, while other factors including smoking and antero-posterior location of the biopsy did not affect culture yields. While location and patient characteristics are not the sole limiting factors in achieving adequate culture yields, the findings presented in this thesis assist in better predicting the adequacy of the patients' own olfactory mucosa, avoiding exposing patients to the potential risks of the biopsy procedure.

Lastly, in the third experiment the use of ^{1}H-MR spectroscopy in predicting outcome in patients who have undergone brachial plexus re-implantation surgery is explored. Studies of ^{1}H-MR spectroscopy of the spinal cord are scarce due to the small size and central location in the spinal cord resulting in low signal to noise ratio and susceptibility artefacts. In this thesis, it is demonstrated that ^{1}H-MR spectroscopy can reliably quantify concentrations of major metabolites including Cho, M-Ins, NAA and Cr. In addition, it is shown that ^{1}H-MR spectroscopy above the level of injury is sensitive to pathological changes occurring in the spinal cord of patients with brachial plexus avulsion injury with and without re-implantation surgery to predict outcome. Major findings include (i) a positive correlation between m-Ins/Cr, a marker of gliosis, and disability, as measured by the DASH scale (ii) a negative association between m-Ins/Cr time from injury and (iii) a positive association between Cho/Cr, a marker of inflammation and membrane turnover, and global upper limb function. Whilst the use of ^{1}H-MR spectroscopy was intended for outcome prediction, it also provided interesting findings regarding the underlying pathophysiological changes. For example, the decrease of m-Ins/Cr with time suggests that there may be a decrease in gliosis near the site of injury with time and increased Cho/Cr levels in patients with improved function may suggest ongoing

attempt for repair. With the advent of more sensitive radiofrequency coils, higher magnetic field strength magnets and prospective studies ^{1}H-MR spectroscopy may prove an invaluable tool for understanding the underlying processing that take place in spinal cord injury and repair.

Appendix

Appendix 1 - Visual Analogue Scale (VAS)

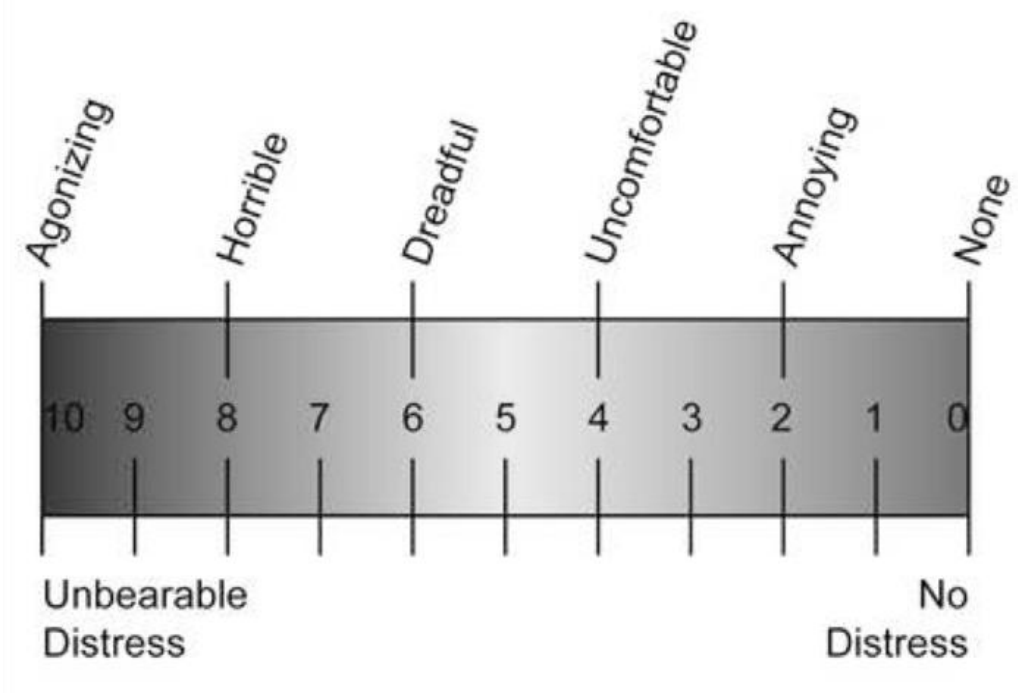

Appendix 2 - Disabilities of the Arm, Shoulder and Hand (DASH)

DISABILITIES OF THE ARM, SHOULDER AND HAND

THE **DASH**

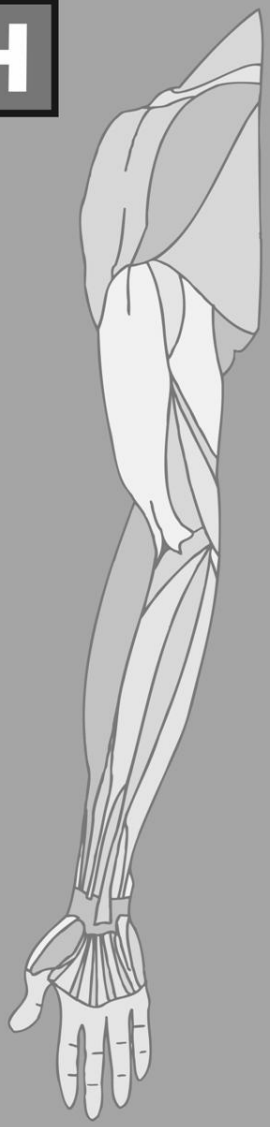

INSTRUCTIONS

This questionnaire asks about your symptoms as well as your ability to perform certain activities.

Please answer *every question*, based on your condition in the last week, by circling the appropriate number.

If you did not have the opportunity to perform an activity in the past week, please make your *best estimate* on which response would be the most accurate.

It doesn't matter which hand or arm you use to perform the activity; please answer based on your ability regardless of how you perform the task.

Disabilities of the Arm, Shoulder and Hand

Please rate your ability to do the following activities in the last week by circling the number below the appropriate response.

	NO DIFFICULTY	MILD DIFFICULTY	MODERATE DIFFICULTY	SEVERE DIFFICULTY	UNABLE
1. Open a tight or new jar.	1	2	3	4	5
2. Write.	1	2	3	4	5
3. Turn a key.	1	2	3	4	5
4. Prepare a meal.	1	2	3	4	5
5. Push open a heavy door.	1	2	3	4	5
6. Place an object on a shelf above your head.	1	2	3	4	5
7. Do heavy household chores (e.g., wash walls, wash floors).	1	2	3	4	5
8. Garden or do yard work.	1	2	3	4	5
9. Make a bed.	1	2	3	4	5
10. Carry a shopping bag or briefcase.	1	2	3	4	5
11. Carry a heavy object (over 10 lbs).	1	2	3	4	5
12. Change a lightbulb overhead.	1	2	3	4	5
13. Wash or blow dry your hair.	1	2	3	4	5
14. Wash your back.	1	2	3	4	5
15. Put on a pullover sweater.	1	2	3	4	5
16. Use a knife to cut food.	1	2	3	4	5
17. Recreational activities which require little effort (e.g., cardplaying, knitting, etc.).	1	2	3	4	5
18. Recreational activities in which you take some force or impact through your arm, shoulder or hand (e.g., golf, hammering, tennis, etc.).	1	2	3	4	5
19. Recreational activities in which you move your arm freely (e.g., playing frisbee, badminton, etc.).	1	2	3	4	5
20. Manage transportation needs (getting from one place to another).	1	2	3	4	5
21. Sexual activities.	1	2	3	4	5

DISABILITIES OF THE ARM, SHOULDER AND HAND

	NOT AT ALL	SLIGHTLY	MODERATELY	QUITE A BIT	EXTREMELY
22. During the past week, *to what extent* has your arm, shoulder or hand problem interfered with your normal social activities with family, friends, neighbours or groups? *(circle number)*	1	2	3	4	5

	NOT LIMITED AT ALL	SLIGHTLY LIMITED	MODERATELY LIMITED	VERY LIMITED	UNABLE
23. During the past week, were you limited in your work or other regular daily activities as a result of your arm, shoulder or hand problem? *(circle number)*	1	2	3	4	5

Please rate the severity of the following symptoms in the last week. *(circle number)*

	NONE	MILD	MODERATE	SEVERE	EXTREME
24. Arm, shoulder or hand pain.	1	2	3	4	5
25. Arm, shoulder or hand pain when you performed any specific activity.	1	2	3	4	5
26. Tingling (pins and needles) in your arm, shoulder or hand.	1	2	3	4	5
27. Weakness in your arm, shoulder or hand.	1	2	3	4	5
28. Stiffness in your arm, shoulder or hand.	1	2	3	4	5

	NO DIFFICULTY	MILD DIFFICULTY	MODERATE DIFFICULTY	SEVERE DIFFICULTY	SO MUCH DIFFICULTY THAT I CAN'T SLEEP
29. During the past week, how much difficulty have you had sleeping because of the pain in your arm, shoulder or hand? *(circle number)*	1	2	3	4	5

	STRONGLY DISAGREE	DISAGREE	NEITHER AGREE NOR DISAGREE	AGREE	STRONGLY AGREE
30. I feel less capable, less confident or less useful because of my arm, shoulder or hand problem. *(circle number)*	1	2	3	4	5

DASH DISABILITY/SYMPTOM SCORE = $[(\frac{\text{sum of n responses}}{n}) - 1] \times 25$, where n is equal to the number of completed responses.

A DASH score may <u>not</u> be calculated if there are greater than 3 missing items.

DISABILITIES OF THE ARM, SHOULDER AND HAND

WORK MODULE (OPTIONAL)

The following questions ask about the impact of your arm, shoulder or hand problem on your ability to work (including homemaking if that is your main work role).

Please indicate what your job/work is:_____

p I do not work. (You may skip this section.)

Please circle the number that best describes your physical ability in the past week. Did you have any difficulty:

	NO DIFFICULTY	MILD DIFFICULTY	MODERATE DIFFICULTY	SEVERE DIFFICULTY	UNABLE
1. using your usual technique for your work?	1	2	3	4	5
2. doing your usual work because of arm, shoulder or hand pain?	1	2	3	4	5
3. doing your work as well as you would like?	1	2	3	4	5
4. spending your usual amount of time doing your work?	1	2	3	4	5

SPORTS/PERFORMING ARTS MODULE (OPTIONAL)

The following questions relate to the impact of your arm, shoulder or hand problem on playing *your musical instrument or sport or both*.
If you play more than one sport or instrument (or play both), please answer with respect to that activity which is most important to you.

Please indicate the sport or instrument which is most important to you:_

o I do not play a sport or an instrument. (You may skip this section.)

Please circle the number that best describes your physical ability in the past week. Did you have any difficulty:

	NO DIFFICULTY	MILD DIFFICULTY	MODERATE DIFFICULTY	SEVERE DIFFICULTY	UNABLE
1. using your usual technique for playing your instrument or sport?	1	2	3	4	5
2. playing your musical instrument or sport because of arm, shoulder or hand pain?	1	2	3	4	5
3. playing your musical instrument or sport as well as you would like?	1	2	3	4	5
4. spending your usual amount of time practising or playing your instrument or sport?	1	2	3	4	5

SCORING THE OPTIONAL MODULES: Add up assigned values for each response; divide by 4 (number of items); subtract 1; multiply by 25.
An optional module score may <u>not</u> be calculated if there are any missing items.

INSTITUTE FOR WORK & HEALTH
INSTITUT DE RECHERCHE SUR LE TRAVAIL ET LA SANTÉ

Appendix 3 – Michigan Hand Outcomes Questionnaire

Study ID _____

MICHIGAN HAND OUTCOMES

QUESTIONNAIRE (MHQ)

Today's date: _____
Month Day Year

Instructions: This survey asks for your views about your hands and your health. This information will help keep track of how you feel and how well you are able to do your usual activities.

Answer ***EVERY*** question by marking the answer as indicated. If you are unsure about how to answer a question, please give the best answer you can.

I. The following questions refer to the function of your hand(s)/wrist(s) ***during the past week***. (Please circle one answer for each question). Please answer ***EVERY*** question, even if you do not experience any problems with the hand and/or wrist.

A. The following questions refer to your ***right*** hand/wrist.

	Very Good	Good	Fair	Poor	Very Poor
1. Overall, how well did your ***right*** hand work?	1	2	3	4	5
2. How well did your ***right*** fingers move?	1	2	3	4	5
3. How well did your ***right*** wrist move?	1	2	3	4	5
4. How was the strength in your ***right*** hand?	1	2	3	4	5
5. How was the sensation (feeling) in your ***right*** hand?	1	2	3	4	5

B. The following questions refer to your ***left*** hand/wrist.

	Very Good	Good	Fair	Poor	Very Poor
1. Overall, how well did your ***left*** hand work?	1	2	3	4	5
2. How well did your ***left*** fingers move?	1	2	3	4	5
3. How well did your ***left*** wrist move?	1	2	3	4	5
4. How was the strength in your ***left*** hand?	1	2	3	4	5
5. How was the sensation (feeling) in your ***left*** hand?	1	2	3	4	5

II. The following questions refer to the ability of your hand(s) to do certain tasks ***during the past week***. (Please circle one answer for each question). If you do not do a certain task, please estimate the difficulty with which you would have in performing it.

A. How difficult was it for you to perform the following activities using your ***right hand*** ?

	Not at All Difficult	A Little Difficult	Somewhat Difficult	Moderately Difficult	Very Difficult
1. Turn a door knob	1	2	3	4	5
2. Pick up a coin	1	2	3	4	5
3. Hold a glass of water	1	2	3	4	5
4. Turn a key in a lock	1	2	3	4	5
5. Hold a frying pan	1	2	3	4	5

B. How difficult was it for you to perform the following activities using your ***left hand*** ?

	Not at All Difficult	A Little Difficult	Somewhat Difficult	Moderately Difficult	Very Difficult
1. Turn a door knob	1	2	3	4	5
2. Pick up a coin	1	2	3	4	5
3. Hold a glass of water	1	2	3	4	5
4. Turn a key in a lock	1	2	3	4	5
5. Hold a frying pan	1	2	3	4	5

C. How difficult was it for you to perform the following activities using ***both of your hands***?

	Not at All Difficult	A Little Difficult	Somewhat Difficult	Moderately Difficult	Very Difficult
1. Open a jar	1	2	3	4	5
2. Button a shirt/blouse	1	2	3	4	5
3. Eat with a knife/fork	1	2	3	4	5
4. Carry a grocery bag	1	2	3	4	5
5. Wash dishes	1	2	3	4	5
6. Wash your hair	1	2	3	4	5
7. Tie shoelaces/knots	1	2	3	4	5

III. The following questions refer to how you did in your ***normal work*** (including both housework and school work) during the ***past four weeks***. (Please circle one answer for each question).

	Always	Often	Sometimes	Rarely	Never
1. How often were you unable to do your work because of problems with your hand(s)/wrist(s)?	1	2	3	4	5
2. How often did you have to shorten your work day because of problems with your hand(s)/ wrist(s)?	1	2	3	4	5
3. How often did you have to take it easy at your work because of problems with your hand(s)/ wrist(s)?	1	2	3	4	5
4. How often did you accomplish less in your work because of problems with your hand(s)/ wrist(s)?	1	2	3	4	5
5. How often did you take longer to do the tasks in your work because of problems with your hand(s)/ wrist(s)?	1	2	3	4	5

IV. The following questions refer to how much ***pain*** you had in your hand(s)/wrist(s) ***during the past week***. (Please circle one answer for each question).

A. The following questions refer to **pain** in your ***right*** hand/wrist.

1. How often did you have pain in your ***right*** hand/wrist?
   1. Always
   2. Often
   3. Sometimes
   4. Rarely
   5. Never

If you answered **Never** to **question IV-A1** above, please skip the following questions and go to the next page.

2. Please describe the pain you had in your ***right*** hand/wrist.
   1. Very mild
   2. Mild
   3. Moderate
   4. Severe
   5. Very severe

	Always	Often	Sometimes	Rarely	Never
3. How often did the pain in your ***right*** hand/wrist interfere with your sleep?	1	2	3	4	5
4. How often did the pain in your ***right*** hand/wrist interfere with your daily activities (such as eating or bathing)?	1	2	3	4	5
5. How often did the pain in your ***right*** hand/wrist make you unhappy?	1	2	3	4	5

B. The following questions refer to **pain** in your ***left*** hand/wrist.

1. How often did you have pain in your ***left*** hand/wrist?
   1. Always
   2. Often
   3. Sometimes
   4. Rarely
   5. Never

If you answered **Never** to **question IV-B1** above, please skip the following questions and go to the next page.

2. Please describe the pain you had in your ***left*** hand/wrist.
   1. Very mild
   2. Mild
   3. Moderate
   4. Severe
   5. Very severe

	Always	Often	Sometimes	Rarely	Never
3. How often did the pain in your ***left*** hand/wrist interfere with your sleep?	1	2	3	4	5
4. How often did the pain in your ***left*** hand/wrist interfere with your daily activities (such as eating or bathing)?	1	2	3	4	5
5. How often did the pain in your ***left*** hand/wrist make you unhappy?	1	2	3	4	5

V. A. The following questions refer to the appearance (look) of your ***right*** hand **during the past week**. (Please circle one answer for each question).

	Strongly Agree	Agree	Neither Agree **nor** Disagree	Disagree	Strongly Disagree
1. I am satisfied with the appearance (look) of my ***right*** hand.	1	2	3	4	5
2. The appearance (look) of my ***right*** hand sometimes made me uncomfortable in public.	1	2	3	4	5
3. The appearance (look) of my ***right*** hand made me depressed.	1	2	3	4	5
4. The appearance (look) of my ***right*** hand interfered with my normal social activities.	1	2	3	4	5

B. The following questions refer to the appearance (look) of your ***left*** hand **during the past week**. (Please circle one answer for each question).

	Strongly Agree	Agree	Neither Agree **nor** Disagree	Disagree	Strongly Disagree
1. I am satisfied with the appearance (look) of my ***left*** hand.	1	2	3	4	5
2. The appearance (look) of my ***left*** hand sometimes made me uncomfortable in public.	1	2	3	4	5
3. The appearance (look) of my ***left*** hand made me depressed.	1	2	3	4	5
4. The appearance (look) of my ***left*** hand interfered with my normal social activities.	1	2	3	4	5

VI. A. The following questions refer to your satisfaction with your ***right*** hand/wrist **during the past week**. (Please circle one answer for each question).

	Very Satisfied	Somewhat Satisfied	Neither Satisfied **nor** Dissatisfied	Somewhat Dissatisfied	Very Dissatisfied
1. Overall function of your ***right*** hand	1	2	3	4	5
2. Motion of the fingers in your ***right*** hand	1	2	3	4	5
3. Motion of your ***right*** wrist	1	2	3	4	5
4. Strength of your ***right*** hand	1	2	3	4	5
5. Pain level of your ***right*** hand	1	2	3	4	5
6. Sensation (feeling) of your ***right*** hand	1	2	3	4	5

B. The following questions refer to your satisfaction with your ***left*** hand/wrist **during the past week**. (Please circle one answer for each question).

	Very Satisfied	Somewhat Satisfied	Neither Satisfied **nor** Dissatisfied	Somewhat Dissatisfied	Very Dissatisfied
1. Overall function of your ***left*** hand	1	2	3	4	5
2. Motion of the fingers in your ***left*** hand	1	2	3	4	5
3. Motion of your ***left*** wrist	1	2	3	4	5
4. Strength of your ***left*** hand	1	2	3	4	5
5. Pain level of your ***left*** hand	1	2	3	4	5
6. Sensation (feeling) of your ***left*** hand	1	2	3	4	5

Please provide the following information about yourself. (Please circle one answer for each question.)

1. Are you right-handed or left-handed?
   a. Right-handed
   b. Left-handed
   c. Both

2. Which hand gives you the most problem?
   a. Right hand
   b. Left hand
   c. Both

3. Have you changed your job since you had problem with your hand(s)?
   a. Yes
   b. No

   Please describe the type of job you did **before** you had problem with your hand(s). _____

   _____

   Please describe the type of job you are doing **now**. _____

   _____

4. What is your gender?
   a. Male
   b. Female

5. What is your ethnic background?
   a. White
   b. Black
   c. Hispanic
   d. Asian or Pacific Islander
   e. American Indian or Alaskan Native
   f. Other (Please specify.) _____

6. What is the highest level of education you received?
   a. Less than high school graduate
   b. High school graduate
   c. Some college
   d. College graduate
   e. Professional or graduate school

7. What is your approximate family income including wages, disability payment, retirement income and welfare?
   a. Less than $10,000
   b. $10,000 - $19,999
   c. $20,000 - $29,999
   d. $30,000 - $39,999
   e. $40,000 - $49,999
   f. $50,000 - $59,999
   g. $60,000 - $69,999
   h. More than $70,000
8. Is your injury covered by Workers' Compensation?
   a. Yes
   b. No

Thank you very much for completing this questionnaire.

Appendix 4 – SF36 version 2

SF36 VERSION 2

OVERALL HEALTH

The following questions ask for your views about your health and how you feel about life in general. If you are unsure about how to answer any question, try and think about your overall health and give the best answer you can. Do not spend too much time answering, as your immediate response is likely to be the most accurate.

---

1. In general, would you say your health is:

(Please tick **one** box)

- Excellent ☐
- Very good ☐
- Good ☐
- Fair ☐
- Poor ☐

---

2. Compared to 3 months ago, how would you rate your health in general now?

(Please tick **one** box)

- Much better than 3 months ago ☐
- Somewhat better than 3 months ago ☐
- About the same ☐
- Somewhat worse now than 3 months ago ☐
- Much worse now than 3 months ago ☐

3. **The following questions are about activities you might do during a typical day. Does your health limit you in these activities? If so, how much?**

	(Please tick **one** box on each line)	Yes, limited a lot	Yes, limited a little	No, not limited at all
a)	**Vigorous activities,** such as running, lifting heavy objects, participating in strenuous sports	☐	☐	☐
b)	**Moderate activities,** such as moving a table, pushing a vacuum, bowling or playing golf	☐	☐	☐
c)	Lifting or carrying groceries	☐	☐	☐
d)	Climbing **several** flights of stairs	☐	☐	☐
e)	Climbing **one** flight of stairs	☐	☐	☐
f)	Bending kneeling or stooping	☐	☐	☐
g)	Walking **more than a mile**	☐	☐	☐
h)	Walking **half a mile**	☐	☐	☐
i)	Walking **100 yards**	☐	☐	☐
j)	Bathing and dressing yourself	☐	☐	☐

---

4. **During the <u>past 2 weeks</u>, how much time have you had any of the following problems with your work or other regular daily activities <u>as a result of your physical health</u>?**

	(Please tick **one** box) on each line	All of the time	Most of the time	Some of the time	A little of the time	None of the time
a)	Cut down on the **amount of time** you spent on work or other activities	☐	☐	☐	☐	☐
b)	**Accomplished less** than you would like	☐	☐	☐	☐	☐
c)	Were limited in the **kind** of work or other activities	☐	☐	☐	☐	☐
d)	Had difficulty performing the work or other activities (eg it took more effort)	☐	☐	☐	☐	☐

5. **During the past 2 weeks, how much time have you had any of the following problems with your work or other regular daily activities as a result of any emotional problems (such as feeling depressed or anxious)?**

(Please tick **one** box) on each line	All of the time	Most of the time	Some of the time	A little of the time	None of the time
a) Cut down on the **amount of time** you spent on work or other activities	☐	☐	☐	☐	☐
b) **Accomplished less** than you would like	☐	☐	☐	☐	☐
c) Didn't do work or other activities as **carefully** as usual	☐	☐	☐	☐	☐

---

6. **During the past 2 weeks, to what extent have your physical health or emotional problems interfered with your normal social activities with family, neighbours or groups?**

(Please tick **one** box)

- Not at all ☐
- Slightly ☐
- Moderately ☐
- Quite a bit ☐
- Extremely ☐

---

7. **How much bodily pain have you had during the past 2 weeks ?**

(Please tick **one** box)

- None ☐
- Very mild ☐
- Mild ☐
- Moderate ☐
- Severe ☐
- Very Severe ☐

8. **During the past 2 weeks, how much did pain interfere with your normal work (including bothoutside the home and housework)?**

(Please tick **one** box)

- Not at all ☐
- Slightly ☐
- Moderately ☐
- Quite a bit ☐
- Extremely ☐

---

9. **These questions are about how you feel and how things have been with you during the past 2 weeks. For each question please give one answer that comes closest to the way you have been feeling.**

(Please tick **one** box on each line)

	How much time during the last 2 weeks:	All of the time	Most of the time	A good bit of the time	Some of the time	A little of the time	None of the time
a)	Did you feel full of life?	☐	☐	☐	☐	☐	☐
b)	Have you been a very nervous person?	☐	☐	☐	☐	☐	☐
c)	Have you felt so down in the dumps that nothing would cheer you up?	☐	☐	☐	☐	☐	☐
d)	Have you felt calm and peaceful?	☐	☐	☐	☐	☐	☐
e)	Did you have a lot of energy?	☐	☐	☐	☐	☐	☐
f)	Have you felt downhearted and low?	☐	☐	☐	☐	☐	☐
g)	Did you feel worn out?	☐	☐	☐	☐	☐	☐
h)	Have you been a happy person?	☐	☐	☐	☐	☐	☐
i)	Did you feel tired?	☐	☐	☐	☐	☐	☐

10. During the past 2 weeks, how much of the time has your physical health or emotional problems interefered with your social activities (like visiting friends, relatives etc.).

(Please tick **one** box)

- All of the time ☐
- Most of the time ☐
- Some of the time ☐
- A little of the time ☐
- None of the time ☐

---

11. How TRUE or FALSE is each of the following statements for you?

(Please tick **one** box on each line)

		Definitely true	Mostly true	Not sure	Mostly false	Definitely false
a)	I seem to get ill more easily than other people	☐	☐	☐	☐	☐
b)	I am as healthy as anybody I know	☐	☐	☐	☐	☐
c)	I expect my health to get worse	☐	☐	☐	☐	☐
d)	My health is excellent	☐	☐	☐	☐	☐

---

12. During the last 12 months, how many hours on average per day have you spent caring for the person suffering from Parkinson's disease?

_____ **Hours per day**

If you did not have to spend this time caring, what would you otherwise have done withthese hours? *(please tick all those relevant activities and the number of hours which would have been spent on each).*

For example, Paid employment	☑	*4 hours*
Paid employment	☐	___ hours
Leisure activities such as gardening/reading/relaxing	☐	___ hours
Other (e.g. shopping, housework)	☐	___ hours

If other, please specify _____

Completed by: ..... **Date completed:** ...../...../.....

Appendix 5 – Experimental studies involving OEC mediated repair of the nervous system

Type of lesion	Study	Source of OEC	Results
T10 dorsal root rhizotomy	Ramon-Cueto et al. 1994	ONL and GL Purified	Regeneration of dorsal root axons into the dorsal spinal gray matter
Multiple rhizotomy at L3 to L6	Navarro et al. (1999)	ONL and GL, frozen OEC, purified	Recovery of electrophysiological functions.
Rhizotomy of L4 dorsal root	Li et al. (2004)	ONL and GL, not purified	Intermingling of OEC with astrocytes at the DREZ permitted axons to grow into the spinal cord.
Cervical or lumbar dorsal root crush	Ramer et al. (2004b)	LP, purified	Increased angiogenesis and altered astrogliosis. No regeneration of axons into the spinal cord
Multiple rhizotomy at C3–T3	Gomez et al. (2003)	ONL and GL, frozen OEC, purified	No regeneration or sprouting observed. No migration of OEC. Endogenous SC rather than OEC associated with axons
Rhizotomy of L4 dorsal root	Riddell et al. (2004)	Whole bulbs, purified	Electrophysiological and histological analysis show no effects
Cervical or lumbar dorsal root crush	Ramer et al. (2004)	LP, purified	No regeneration of axons into spinal cord.
Demyelinating lesion at the thoracolumbar spinal cord	(Franklin et al. 1996)	OEC cell line, purified	*In vivo* remyelination of larger-diameter axons by peripheral-like myelin sheaths.
Demyelinating lesion at T10–T11	(Imaizumi et al. 1998)	ONL, not purified	Remyelination and recovery of electrophysiological properties.
Demyelinating lesion at T10–T11	Kato et al. (2000)	Human olfactory nerve, not purified	Peripheral-like remyelination.
Demyelinating lesion in the dorsal funiculus at T13	Lakatos et al. (2003b)	Outer layer of bulb, purified and not purified	Limited capacity of OEC to remyelinate was improved by co-transplantation of meningeal cells.
Demyelinating lesion at T7 and/or T9 in monkeys	Radtke et al. (2004)	ONL and GL from pigs, purified	Remyelination of dorsal funiculus axons in non-human primate spinal cord by pig OEC.
Demyelinating lesion at T10–T11	Akiyama et al. (2004)	ONL, purified	OEC and SC remyelinated equally and both cell types improved conduction velocity.
Demyelinating lesion at T9	Sasaki et al. (2006a)	ONL, purified	Remyelination, reconstitution of nodes of Ranvier, recruitment of Na^+ and K^- channels and increased

			conduction velocity.
Unilateral electrolytic lesion of CST at C1–C2	(Li et al. 1997)	ONL and GL, not purified	OEC and axons bridged the lesion and this was accompanied by functional recovery
Electrolytic lesion of CST at C1–C2	(Li et al. 1998)	ONL and GL, not purified	Corticospinal axons traversed the lesion site, were enwrapped by peripheral myelin, and reentered the caudal spinal cord, where they became myelinated by central myelin.
Unilateral heat lesion of dorsal CST at C1	Keyvan-Fouladi et al. (2003)	ONL and GL, not purified	Delayed transplantation resulted in functional recovery. Axons entered and traversed transplant and formed collateral branches.
Dorsal CST transection at T8–T9	Chuah et al. (2004)	Mix of ONL and mucosa, purified	Increased collateral branching of uninjured ventral CST.
Ruitenberg et al. (2005)	Unilateral CST transection at C4	ONL, purified	OEC promoted axonal regeneration only when genetically modified to express NT-3.
Photochemical injury at T12–L1	Verdu et al. (2001)	Whole bulbs, frozen OEC, purified	Reduced astrogliosis and cavity formation.
Photochemical injury at T8	Verdu et al. (2003)	Whole bulbs, purified	Preservation of spinal cord. Electrophysiological and behavioral recovery.
Photochemical injury at T8	Garcia-Alias et al. (2004)	Whole bulbs, purified	Both OEC and SC transplantation resulted in behavioral recovery, OEC transplantation resulted in more electrophysiological recovery and less astrocytic reactivity.
Photochemical injury at T8	Lopez-Vales et al. (2004)	Whole bulbs, purified	Upregulation of COX-2 and VEGF, neoangiogenesis and improved locomotor function.
Dorsal column transection at T11	Imaizumi et al. (2000a)	Anterior tips of bulb, not purified	Xenotransplantation of OEC and SC equally resulted in remyelination and long-distance recovery of electrophysiological properties
Dorsal column transection at T11	Imaizumi et al. (2000b)	Anterior tips of bulb, not purified	Both OEC and SC transplantation resulted in remyelination and recovery of conduction velocity
Dorsal column transection at C4	Lu et al. (2006)	LP from 5-day-old pups, purified	OEC did not migrate, but rather diffused within one hour after injection from the injection site into the lesion. This paper challenges the migratory properties of OEC. Similar results with OEC, bone marrow stromal cells and fibroblasts.
Non-lesioned dorsal funiculus at T13	Lakatos et al. (2003a)	Outer layer of bulb, purified	Less GFAP and CSPG expression after OEC transplantation compared with SC transplantation.
Dorsolateral funiculus crush at C4	Ramer et al. (2004a)	LP from mice, purified	OEC showed limited survival and migration, but reduced cavity formation, enhanced SC invasion, reduced astrocytic response and induced axonal sprouting and angiogenesis.
Dorsal funiculus transection	Sasaki et al. (2004)	ONL, purified	OEC associated with axons and formed myelin.

at T9			
Dorsal funiculus crush at T8–T9	Andrews and Stelzner (2004)	ONL and GL, purified and not purified	Both heterogeneous and enriched populations of OEC stimulated axon growth. A conditioning lesion had an additive effect.
Dorsolateral funiculus crush at C3–C4	Richter et al. (2005)	ONL or LP, purified	Comparison between LP–OEC and ONL–OEC. LP–OEC were superior in migration ability, in reducing lesion size and in stimulating outgrowth of axonal subpopulations.
Dorsal funiculus transection at T9	Sasaki et al. (2006a)	ONL, purified	Neuroprotective effect on the survival of cortical projection neurons
Unilateral rubrospinal tract transection at C4	Ruitenberg et al. (2003)	ONL and GL, purified	Neuroprotective effects of OEC. Effects on lesion size reduction, sprouting and functional recovery were augmented when OEC were transduced with neurotrophin encoding AdV vectors.
Hemisection at upper cervical level	Li et al. (2003)	ONL and GL, not purified	Functional repair of breathing and climbing.
Hemisection at C2–C3	Polentes et al. (2004)	ONL and GL, purified	Recovery of respiratory function
Injection alone compared with injection after hemisection at T9	Deng et al. (2006)	LP, purified	Rat and human OEC survived and migrated equally, but both cell types migrated for longer distances when injected in the uninjured cord than after hemisection. They stopped dividing after 24 h.
Complete transection and removal of segment including dorsal roots at T9	(Ramon-Cueto et al. 1998)	ONL and GL, purified	OEC induced axonal growth into SC-containing channels and further into host spinal cord resulting in long-distance regeneration (2.5 cm). Extensive migration of OEC.
Unilateral electrolytic lesion of CST at C1–C2	(Li et al. 1997)	ONL and GL, not purified	OEC and axons bridged the lesion and this was accompanied by functional recovery
Electrolytic lesion of CST at C1–C2	(Li et al. 1998)	ONL and GL, not purified	Corticospinal axons traversed the lesion site, were enwrapped by peripheral myelin, and reentered the caudal spinal cord, where they became myelinated by central myelin.
Complete transection + removal of segment including dorsal roots at T9	(Ramon-Cueto et al. 1998)	ONL and GL, purified	OEC induced axonal growth into SC-containing channels and further into host spinal cord resulting in long-distance regeneration (2.5 cm). Extensive migration of OEC.
Complete transection at T10	Lu et al. (2001)	LP OEC and pieces of lamina propria, not purified	Both OEC and pieces of lamina propria transplantation resulted in functional recovery and regrowth of axons traversing the transection site.
Complete transection at T10	Lu et al. (2002)	Pieces of lamina propria, not purified	Locomotor recovery and axonal regrowth after delayed transplantation.
Complete transection at T8	Cao et al. (2004)	ONL, purified	Increased axonal outgrowth and functional recovery. Effects were enhanced when OEC were transduced by

			GDNF-encoding retroviruses.
Complete transection at T8	Lopez-Vales et al. (2006)	Whole bulbs, frozen OEC, purified	Electrophysiological, histological and behavioral recovery. Better results with acute transplantation than with delayed.
Complete transection at T8	Lopez-Vales et al. (2007)	Whole bulbs, frozen OEC, purified	Electrophysiological, histological and behavioral recovery after 45 days delayed transplantation.
Complete transection at T8	Lee et al. (2004)	ONL and GL, not purified	Migration of OEC may be dependent on lesion type. OEC, labeled by magnetodendrimers, did not migrate in transected cords.
Complete transection at T10.	Steward et al. (2006)	Delayed implantation of pieces of lamina propria, not purified	Replication of experiment by Lu et al. (2002). In contrast to this study, no recovery in motor function or enhanced axonal outgrowth was observed.
Moderate contusion at T9	Takami et al. (2002)	ONL, purified	First study on OEC implantation after contusion. Delayed transplantation of OEC, SC or OEC/SC resulted in equal tissue sparing. SC transplants resulted in more GFAP and CSPG expression, but were most effective in promoting axonal sparing/ regeneration, myelination and in improving functional recovery.
Moderate contusion at T9–T10	Plant et al. (2003)	ONL, purified	Immediate and delayed transplantation promoted tissue sparing. Delayed transplantation resulted in more axonal regeneration/sparing and improvement in functional outcome. First and only study that reports positive effects of OEC transplantation after contusion.
Moderate to severe contusion at T8 or T9	Resnick et al. (2003)	Whole bulbs, purified	Survival of OEC, but no improvement in functional outcome.
Boyd et al. (2004)	Clip compression at T10	Fetal ONL, not purified	After delayed transplantation, OEC remained in cystic cavities and did not associate with axons. Numerous SC–axon units were observed, surrounded by OEC cytoplasmic processes.
Barakat et al. (2005)	Moderate contusion at T8	ONL, purified	In contrast to OEC, SC survived, supported axon growth and improved functional outcome after delayed transplantation
Moderate contusion at T8	Pearse et al. (2007)	ONL, purified	Poor survival and no migration of OEC. No axon regeneration into injury site and no major behavioral improvements. More myelination in SC graft than in OEC graft.
Reimplantation of avulsed ventral root S1	Li et al. (2007a,b)	ONL and GL, not purified	OEC migration into the root and increased axon growth into the ventral root.

Reference List

Aguayo, A. J., M. Vidal-Sanz, et al. (1987). "Growth and connectivity of axotomized retinal neurons in adult rats with optic nerves substituted by PNS grafts linking the eye and the midbrain." Ann N Y Acad Sci **495**: 1-9.

Andrews, M. R. and D. J. Stelzner (2007). "Evaluation of olfactory ensheathing and schwann cells after implantation into a dorsal injury of adult rat spinal cord." J Neurotrauma **24**(11): 1773-1792.

Annamalai, S., N. A. Kumar, et al. (2003). "An association between acquired epiphora and the signs and symptoms of chronic rhinosinusitis: a prospective case-control study." Am J Rhinol **17**(2): 111-114.

Arnold, D. L. and S. N. De (1997). "Magnetic resonance spectroscopy in vivo: applications in neurological disorders." Ital.J.Neurol.Sci. **18**(6): 321-329.

Au, E. and A. J. Roskams (2003). "Olfactory ensheathing cells of the lamina propria in vivo and in vitro." Glia **41**(3): 224-236.

Audoin, B., G. R. Davies, et al. (2006). "Localization of grey matter atrophy in early RRMS : A longitudinal study." J Neurol **253**(11): 1495-1501.

Bar, K. J., G. J. Saldanha, et al. (1998). "GDNF and its receptor component Ret in injured human nerves and dorsal root ganglia." Neuroreport **9**(1): 43-47.

Barakat, D. J., S. M. Gaglani, et al. (2005). "Survival, integration, and axon growth support of glia transplanted into the chronically contused spinal cord." Cell Transplant. **14**(4): 225-240.

Barber, P. C. and R. M. Lindsay (1982). "Schwann cells of the olfactory nerves contain glial fibrillary acidic protein and resemble astrocytes." Neuroscience **7**(12): 3077-3090.

Barker, P. B. (2001). "N-acetyl aspartate--a neuronal marker?" Ann Neurol **49**(4): 423-424.

Barker, P. B., S. N. Breiter, et al. (1994). "Quantitative proton spectroscopy of canine brain: in vivo and in vitro correlations." Magn Reson Med **32**(2): 157-163.

Barnett, S. C., C. L. Alexander, et al. (2000). "Identification of a human olfactory ensheathing cell that can effect transplant-mediated remyelination of demyelinated CNS axons." Brain **123 (Pt 8)**: 1581-1588.

Barnett, S. C., A. M. Hutchins, et al. (1993). "Purification of olfactory nerve ensheathing cells from the olfactory bulb." Dev.Biol. **155**(2): 337-350.

Bates, T. E., M. Strangward, et al. (1996). "Inhibition of N-acetylaspartate production: implications for 1H MRS studies in vivo." Neuroreport **7**(8): 1397-1400.

Beaton, D. E., J. N. Katz, et al. (2001). "Measuring the whole or the parts? Validity, reliability, and responsiveness of the Disabilities of the Arm, Shoulder and Hand outcome measure in different regions of the upper extremity." J.Hand Ther. **14**(2): 128-146.

Behar, K. L., J. A. den Hollander, et al. (1983). "High-resolution 1H nuclear magnetic resonance study of cerebral hypoxia in vivo." Proc.Natl.Acad.Sci.U.S.A **80**(16): 4945-4948.

Bergerot, A., P. J. Shortland, et al. (2004). "Co-treatment with riluzole and GDNF is necessary for functional recovery after ventral root avulsion injury." Exp.Neurol. **187**(2): 359-366.

Berman, J. S., R. Birch, et al. (1998). "Pain following human brachial plexus injury with spinal cord root avulsion and the effect of surgery." Pain **75**(2-3): 199-207.

Bianco, J. I., C. Perry, et al. (2004). "Neurotrophin 3 promotes purification and proliferation of olfactory ensheathing cells from human nose." Glia **45**(2): 111-123.

Bigbee, A. J., T. X. Hoang, et al. (2007). "At-level neuropathic pain is induced by lumbosacral ventral root avulsion injury and ameliorated by root reimplantation into the spinal cord." Exp.Neurol. **204**(1): 273-282.

Blamire, A. M., S. Cader, et al. (2007). "Axonal damage in the spinal cord of multiple sclerosis patients detected by magnetic resonance spectroscopy." Magn Reson.Med. **58**(5): 880-885.

Blits, B., T. P. Carlstedt, et al. (2004). "Rescue and sprouting of motoneurons following ventral root avulsion and reimplantation combined with intraspinal adeno-associated viral vector-mediated expression of glial cell line-derived neurotrophic factor or brain-derived neurotrophic factor." Exp.Neurol. **189**(2): 303-316.

Boruch, A. V., J. J. Conners, et al. (2001). "Neurotrophic and migratory properties of an olfactory ensheathing cell line." Glia **33**(3): 225-229.

Bottomley, P. A. (1987). "Spatial localization in NMR spectroscopy in vivo." Ann N Y Acad Sci **508**: 333-348.

Brand, A., C. Richter-Landsberg, et al. (1993). "Multinuclear NMR studies on the energy metabolism of glial and neuronal cells." Dev.Neurosci. **15**(3-5): 289-298.

Bray, G. M., M. P. Villegas-Perez, et al. (1987). "The use of peripheral nerve grafts to enhance neuronal survival, promote growth and permit terminal reconnections in the central nervous system of adult rats." J.Exp.Biol. **132**: 5-19.

Brooks, W. M., C. A. Stidley, et al. (2000). "Metabolic and cognitive response to human traumatic brain injury: a quantitative proton magnetic resonance study." J.Neurotrauma **17**(8): 629-640.

Brulatout, S., P. Meric, et al. (1996). "A one-dimensional (proton and phosphorus) and two-dimensional (proton) in vivo NMR spectroscopic study of reversible global cerebral ischemia." J Neurochem **66**(6): 2491-2499.

Bundesen, L. Q., T. A. Scheel, et al. (2003). "Ephrin-B2 and EphB2 regulation of astrocyte-meningeal fibroblast interactions in response to spinal cord lesions in adult rats." J.Neurosci. **23**(21): 7789-7800.

Cader, S., H. Johansen-Berg, et al. (2007). "Discordant white matter N-acetylasparate and diffusion MRI measures suggest that chronic metabolic dysfunction contributes to axonal pathology in multiple sclerosis." Neuroimage **36**(1): 19-27.

Cao, Q., X. M. Xu, et al. (2005). "Functional recovery in traumatic spinal cord injury after transplantation of multineurotrophin-expressing glial-restricted precursor cells." J.Neurosci. **25**(30): 6947-6957.

Carew, J. D., G. Nair, et al. (2011). "Magnetic resonance spectroscopy of the cervical cord in amyotrophic lateral sclerosis." Amyotroph.Lateral.Scler. **12**(3): 185-191.

Carlstedt, T. (1977). "Observations on the morphology at the transition between the peripheral and the central nervous system in the cat. I. A preparative

procedure useful for electron microscopy of the lumbosacral dorsal." Acta Physiol Scand.Suppl **446**: 5-22.

Carlstedt, T. (2008). "Root repair review: basic science background and clinical outcome." Restor.Neurol.Neurosci. **26**(2-3): 225-241.

Carlstedt, T., P. Anand, et al. (2000). "Spinal nerve root repair and reimplantation of avulsed ventral roots into the spinal cord after brachial plexus injury." J.Neurosurg. **93**(2 Suppl): 237-247.

Carlstedt, T., P. Anand, et al. (2004). "Restoration of hand function and so called "breathing arm" after intraspinal repair of C5-T1 brachial plexus avulsion injury. Case report." Neurosurg.Focus. **16**(5): E7.

Carlstedt, T., H. Linda, et al. (1986). "Reinnervation of hind limb muscles after ventral root avulsion and implantation in the lumbar spinal cord of the adult rat." Acta Physiol Scand. **128**(4): 645-646.

Carlstedt, T. and G. Noren (1995). "Repair of ruptured spinal nerve roots in a brachial plexus lesion. Case report." J.Neurosurg. **82**(4): 661-663.

Carlstedt, T. P., R. G. Hallin, et al. (1993). "Functional recovery in primates with brachial plexus injury after spinal cord implantation of avulsed ventral roots." J Neurol Neurosurg Psychiatry **56**(6): 649-654.

Carpentier, A., D. Galanaud, et al. (2006). "Early morphologic and spectroscopic magnetic resonance in severe traumatic brain injuries can detect "invisible brain stem damage" and predict "vegetative states"." J.Neurotrauma **23**(5): 674-685.

Cecil, K. M. and R. E. Lenkinski (1998). "Proton MR spectroscopy in inflammatory and infectious brain disorders." Neuroimaging Clin N Am **8**(4): 863-880.

Chard, D. T., C. M. Griffin, et al. (2002). "Brain atrophy in clinically early relapsing-remitting multiple sclerosis." Brain **125**(Pt 2): 327-337.

Chen, M. S., A. B. Huber, et al. (2000). "Nogo-A is a myelin-associated neurite outgrowth inhibitor and an antigen for monoclonal antibody IN-1." Nature **403**(6768): 434-439.

Chew, D. J., V. H. Leinster, et al. (2008). "Cell death after dorsal root injury." Neurosci Lett **433**(3): 231-234.

Choi, D., D. Li, et al. (2008). "A prospective observational study of the yield of olfactory ensheathing cells cultured from biopsies of septal nasal mucosa." Neurosurgery **62**(5): 1140-1144.

Chuah, M. I. and C. Au (1991). "Olfactory Schwann cells are derived from precursor cells in the olfactory epithelium." J.Neurosci.Res. **29**(2): 172-180.

Chuah, M. I., J. Cossins, et al. (2000). "Glial growth factor 2 induces proliferation and structural changes in ensheathing cells." Brain Res. **857**(1-2): 265-274.

Chung, K. C., J. B. Hamill, et al. (1999). "The Michigan Hand Outcomes Questionnaire (MHQ): assessment of responsiveness to clinical change." Ann Plast Surg **42**(6): 619-622.

Chung, K. C., M. S. Pillsbury, et al. (1998). "Reliability and validity testing of the Michigan Hand Outcomes Questionnaire." J.Hand Surg.Am. **23**(4): 575-587.

Ciccarelli, O., C. A. Wheeler-Kingshott, et al. (2007). "Spinal cord spectroscopy and diffusion-based tractography to assess acute disability in multiple sclerosis." Brain **130**(Pt 8): 2220-2231.

Cooke, F. J., A. M. Blamire, et al. (2004). "Quantitative proton magnetic resonance spectroscopy of the cervical spinal cord." Magn Reson.Med. **51**(6): 1122-1128.

Creasey, G. H., C. H. Ho, et al. (2004). "Clinical applications of electrical stimulation after spinal cord injury." J Spinal Cord Med **27**(4): 365-375.

Cullheim, S., T. Carlstedt, et al. (1989). "Motoneurons reinnervate skeletal muscle after ventral root implantation into the spinal cord of the cat." Neuroscience **29**(3): 725-733.

Cullheim, S., T. Carlstedt, et al. (1999). "Axon regeneration of spinal motoneurons following a lesion at the cord-ventral root interface." Spinal Cord. **37**(12): 811-819.

Cuschieri, A. and L. H. Bannister (1975). "The development of the olfactory mucosa in the mouse: electron microscopy." J.Anat. **119**(Pt 3): 471-498.

Daly, P. F., R. C. Lyon, et al. (1987). "Phospholipid metabolism in cancer cells monitored by 31P NMR spectroscopy." J Biol Chem **262**(31): 14875-14878.

De, S. N., P. M. Matthews, et al. (1998). "Axonal damage correlates with disability in patients with relapsing-remitting multiple sclerosis. Results of a longitudinal magnetic resonance spectroscopy study." Brain **121 (Pt 8)**: 1469-1477.

De Stefano, N., S. Narayanan, et al. (2001). "Evidence of axonal damage in the early stages of multiple sclerosis and its relevance to disability." Arch Neurol **58**(1): 65-70.

Dobkin, B. H., A. Curt, et al. (2006). "Cellular transplants in China: observational study from the largest human experiment in chronic spinal cord injury." Neurorehabil.Neural Repair **20**(1): 5-13.

Doucette, J. R. (1984). "The glial cells in the nerve fiber layer of the rat olfactory bulb." Anat.Rec. **210**(2): 385-391.

Doucette, R. (1990). "Glial influences on axonal growth in the primary olfactory system." Glia **3**(6): 433-449.

Doucette, R. (1991). "PNS-CNS transitional zone of the first cranial nerve." J.Comp Neurol. **312**(3): 451-466.

Doucette, R. (1993). "Glial cells in the nerve fiber layer of the main olfactory bulb of embryonic and adult mammals." Microsc.Res.Tech. **24**(2): 113-130.

Douek, E., L. H. Bannister, et al. (1975). "Recent advances in the pathology of olfaction." Proc.R.Soc.Med. **68**(8): 467-470.

Duarte, J. M., H. Lei, et al. (2012). "The neurochemical profile quantified by in vivo 1H NMR spectroscopy." Neuroimage **61**(2): 342-362.

Eggers, R., M. R. Tannemaat, et al. (2010). "A spatio-temporal analysis of motoneuron survival, axonal regeneration and neurotrophic factor expression after lumbar ventral root avulsion and implantation." Exp Neurol **223**(1): 207-220.

Elliott, J. M., A. R. Pedler, et al. (2011). "Spinal cord metabolism and muscle water diffusion in whiplash." Spinal Cord.

Erschbamer, M., J. Oberg, et al. (2011). "1H-MRS in spinal cord injury: acute and chronic metabolite alterations in rat brain and lumbar spinal cord." Eur.J.Neurosci. **33**(4): 678-688.

Fawcett, J. W. (1997). "Astrocytic and neuronal factors affecting axon regeneration in the damaged central nervous system." Cell Tissue Res **290**(2): 371-377.

Feinberg, J. (2006). "EMG: myths and facts." HSS.J. **2**(1): 19-21.

Fernando, K. T., M. A. McLean, et al. (2004). "Elevated white matter myo-inositol in clinically isolated syndromes suggestive of multiple sclerosis." Brain **127**(Pt 6): 1361-1369.

Feron, F., C. Perry, et al. (2005). "Autologous olfactory ensheathing cell transplantation in human spinal cord injury." Brain **128**(Pt 12): 2951-2960.

Feron, F., C. Perry, et al. (1998). "New techniques for biopsy and culture of human olfactory epithelial neurons." Arch.Otolaryngol.Head Neck Surg. **124**(8): 861-866.

Flaherty, S. A. (1996). "Pain measurement tools for clinical practice and research." AANA.J. **64**(2): 133-140.

Flogel, U., W. Willker, et al. (1994). "Regulation of intracellular pH in neuronal and glial tumour cells, studied by multinuclear NMR spectroscopy." NMR Biomed. **7**(4): 157-166.

Forman, D. S. and R. A. Berenberg (1978). "Regeneration of motor axons in the rat sciatic nerve studied by labeling with axonally transported radioactive proteins." Brain Res. **156**(2): 213-225.

Fraher, J. P. (1992). "The CNS-PNS transitional zone of the rat. Morphometric studies at cranial and spinal levels." Prog Neurobiol **38**(3): 261-316.

Fraher, J. P. and G. F. Kaar (1985). "The development of alpha and gamma motoneuron fibres in the rat. II. A comparative ultrastructural study of their central and peripheral myelination." J.Anat. **141**: 89-103.

Frahm, J., H. Bruhn, et al. (1989). "Localized high-resolution proton NMR spectroscopy using stimulated echoes: initial applications to human brain in vivo." Magn Reson.Med. **9**(1): 79-93.

Frahm, J., T. Michaelis, et al. (1991). "On the N-acetyl methyl resonance in localized 1H NMR spectra of human brain in vivo." NMR Biomed. **4**(4): 201-204.

Franklin, R. J., J. M. Gilson, et al. (1996). "Schwann cell-like myelination following transplantation of an olfactory bulb-ensheathing cell line into areas of demyelination in the adult CNS." Glia **17**(3): 217-224.

Friedman, S. D., W. M. Brooks, et al. (1999). "Quantitative proton MRS predicts outcome after traumatic brain injury." Neurology **52**(7): 1384-1391.

Garnett, M. R., A. M. Blamire, et al. (2000). "Early proton magnetic resonance spectroscopy in normal-appearing brain correlates with outcome in patients following traumatic brain injury." Brain **123 (Pt 10)**: 2046-2054.

Gomez-Anson, B., D. G. MacManus, et al. (2000). "In vivo 1H-magnetic resonance spectroscopy of the spinal cord in humans." Neuroradiology **42**(7): 515-517.

Gong, Q., M. S. Bailey, et al. (1994). "Localization and regulation of low affinity nerve growth factor receptor expression in the rat olfactory system during development and regeneration." J Comp Neurol **344**(3): 336-348.

Graziadei, P. P. and G. A. Graziadei (1979). "Neurogenesis and neuron regeneration in the olfactory system of mammals. I. Morphological aspects of differentiation and structural organization of the olfactory sensory neurons." J.Neurocytol. **8**(1): 1-18.

Graziadei, P. P. and G. A. Monti Graziadei (1980). "Neurogenesis and neuron regeneration in the olfactory system of mammals. III. Deafferentation and reinnervation of the olfactory bulb following section of the fila olfactoria in rat." J.Neurocytol. **9**(2): 145-162.

Gu, H. Y., H. Chai, et al. (2004). "Survival, regeneration and functional recovery of motoneurons in adult rats by reimplantation of ventral root following spinal root avulsion." Eur.J.Neurosci. **19**(8): 2123-2131.

Haase, A., J. Frahm, et al. (1985). "1H NMR chemical shift selective (CHESS) imaging." Phys.Med.Biol **30**(4): 341-344.

Hallin, R. G., T. Carlstedt, et al. (1999). "Spinal cord implantation of avulsed ventral roots in primates; correlation between restored motor function and morphology." Exp.Brain Res. **124**(3): 304-310.

Havton, L. A. and T. Carlstedt (2009). "Repair and rehabilitation of plexus and root avulsions in animal models and patients." Curr Opin Neurol **22**(6): 570-574.

Herminghaus, S., U. Pilatus, et al. (2002). "Increased choline levels coincide with enhanced proliferative activity of human neuroepithelial brain tumors." NMR Biomed **15**(6): 385-392.

Hoang, T. X. and L. A. Havton (2006). "A single re-implanted ventral root exerts neurotropic effects over multiple spinal cord segments in the adult rat." Exp.Brain Res. **169**(2): 208-217.

Holly, L. T., B. Freitas, et al. (2009). "Proton magnetic resonance spectroscopy to evaluate spinal cord axonal injury in cervical spondylotic myelopathy." J.Neurosurg.Spine **10**(3): 194-200.

Horska, A., L. Farage, et al. (2009). "Brain metabolism in Rett syndrome: age, clinical, and genotype correlations." Ann Neurol **65**(1): 90-97.

Htut, M., P. Misra, et al. (2006). "Pain phenomena and sensory recovery following brachial plexus avulsion injury and surgical repairs." J Hand Surg Br **31**(6): 596-605.

Htut, M., V. P. Misra, et al. (2007). "Motor recovery and the breathing arm after brachial plexus surgical repairs, including re-implantation of avulsed spinal roots into the spinal cord." J.Hand Surg.Eur.Vol. **32**(2): 170-178.

Hu, P. and E. M. McLachlan (2003). "Selective reactions of cutaneous and muscle afferent neurons to peripheral nerve transection in rats." J Neurosci **23**(33): 10559-10567.

Huang, H., L. Chen, et al. (2003). "Influence of patients' age on functional recovery after transplantation of olfactory ensheathing cells into injured spinal cord injury." Chin Med.J.(Engl.) **116**(10): 1488-1491.

Imaizumi, T., K. L. Lankford, et al. (1998). "Transplanted olfactory ensheathing cells remyelinate and enhance axonal conduction in the demyelinated dorsal columns of the rat spinal cord." J.Neurosci. **18**(16): 6176-6185.

Ito, D., C. Ibanez, et al. (2006). "Comparison of cell populations derived from canine olfactory bulb and olfactory mucosal cultures." Am.J.Vet.Res. **67**(6): 1050-1056.

Iwanami, A., S. Kaneko, et al. (2005). "Transplantation of human neural stem cells for spinal cord injury in primates." J.Neurosci.Res. **80**(2): 182-190.

Jacobs, M. A., A. Horska, et al. (2001). "Quantitative proton MR spectroscopic imaging of normal human cerebellum and brain stem." Magn Reson.Med. **46**(4): 699-705.

Jafek, B. W., B. Murrow, et al. (2002). "Biopsies of human olfactory epithelium." Chem.Senses **27**(7): 623-628.

Jani, H. R. and G. Raisman (2004). "Ensheathing cell cultures from the olfactory bulb and mucosa." Glia **47**(2): 130-137.

Kachramanoglou, C., S. Law, et al. (2012). "Culture of Olfactory Ensheathing Cells for Central Nerve Repair: The Limitations and Potential of Endoscopic Olfactory Mucosal Biopsy." Neurosurgery.

Kachramanoglou, C., D. Li, et al. (2011). "Novel strategies in brachial plexus repair after traumatic avulsion." Br.J.Neurosurg. **25**(1): 16-27.

Kandenwein, J. A., T. Kretschmer, et al. (2005). "Surgical interventions for traumatic lesions of the brachial plexus: a retrospective study of 134 cases." J.Neurosurg. **103**(4): 614-621.

Kantarci, K. (2007). "1H magnetic resonance spectroscopy in dementia." Br J Radiol **80 Spec No 2**: S146-152.

Karimi-Abdolrezaee, S., E. Eftekharpour, et al. (2006). "Delayed transplantation of adult neural precursor cells promotes remyelination and functional neurological recovery after spinal cord injury." J.Neurosci. **26**(13): 3377-3389.

Kato, N., M. Htut, et al. (2006). "The effects of operative delay on the relief of neuropathic pain after injury to the brachial plexus: a review of 148 cases." J.Bone Joint Surg.Br. **88**(6): 756-759.

Kawaja, M. D., J. G. Boyd, et al. (2009). "Technical strategies to isolate olfactory ensheathing cells for intraspinal implantation." J.Neurotrauma **26**(2): 155-177.

Kelley, D. A., L. L. Wald, et al. (1999). "Lactate detection at 3T: compensating J coupling effects with BASING." J Magn Reson Imaging **9**(5): 732-737.

Kendi, A. T., F. U. Tan, et al. (2004). "MR spectroscopy of cervical spinal cord in patients with multiple sclerosis." Neuroradiology **46**(9): 764-769.

Keyvan-Fouladi, N., Y. Li, et al. (2002). "How do transplanted olfactory ensheathing cells restore function?" Brain Res.Brain Res.Rev. **40**(1-3): 325-327.

Keyvan-Fouladi, N., G. Raisman, et al. (2003). "Functional repair of the corticospinal tract by delayed transplantation of olfactory ensheathing cells in adult rats." J.Neurosci. **23**(28): 9428-9434.

Kim, D. H., E. Adalsteinsson, et al. (2002). "Regularized higher-order in vivo shimming." Magn Reson.Med. **48**(4): 715-722.

Kirshner, B. and G. Guyatt (1985). "A methodological framework for assessing health indices." J Chronic Dis **38**(1): 27-36.

Kishino, A., Y. Ishige, et al. (1997). "BDNF prevents and reverses adult rat motor neuron degeneration and induces axonal outgrowth." Exp Neurol **144**(2): 273-286.

Koliatsos, V. E., R. E. Clatterbuck, et al. (1993). "Evidence that brain-derived neurotrophic factor is a trophic factor for motor neurons in vivo." Neuron **10**(3): 359-367.

Koliatsos, V. E., W. L. Price, et al. (1994). "Ventral root avulsion: an experimental model of death of adult motor neurons." J.Comp Neurol. **342**(1): 35-44.

Kozerke, S., M. Schar, et al. (2002). "Volume tracking cardiac 31P spectroscopy." Magn Reson Med **48**(2): 380-384.

Krudewig, C., U. Deschl, et al. (2006). "Purification and in vitro characterization of adult canine olfactory ensheathing cells." Cell Tissue Res. **326**(3): 687-696.

Lakatos, A., S. C. Barnett, et al. (2003). "Olfactory ensheathing cells induce less host astrocyte response and chondroitin sulphate proteoglycan expression than Schwann cells following transplantation into adult CNS white matter." Exp.Neurol. **184**(1): 237-246.

Lakatos, A., R. J. Franklin, et al. (2000). "Olfactory ensheathing cells and Schwann cells differ in their in vitro interactions with astrocytes." Glia **32**(3): 214-225.

Lane, A. P., G. Gomez, et al. (2002). "The superior turbinate as a source of functional human olfactory receptor neurons." Laryngoscope **112**(7 Pt 1): 1183-1189.

Lanza, D. C., D. T. Moran, et al. (1993). "Endoscopic human olfactory biopsy technique: a preliminary report." Laryngoscope **103**(7): 815-819.

Laubenberger, J., D. Haussinger, et al. (1996). "HIV-related metabolic abnormalities in the brain: depiction with proton MR spectroscopy with short echo times." Radiology **199**(3): 805-810.

Lee, D. H., G. C. Claussen, et al. (2004). "Clinical nerve conduction and needle electromyography studies." J Am Acad Orthop Surg **12**(4): 276-287.

Leopold, D. A., T. Hummel, et al. (2000). "Anterior distribution of human olfactory epithelium." Laryngoscope **110**(3 Pt 1): 417-421.

Li, B. S., H. Wang, et al. (2003). "Metabolite ratios to assumed stable creatine level may confound the quantification of proton brain MR spectroscopy." Magn Reson Imaging **21**(8): 923-928.

Li, L., W. Wu, et al. (1995). "Rescue of adult mouse motoneurons from injury-induced cell death by glial cell line-derived neurotrophic factor." Proc Natl Acad Sci U S A **92**(21): 9771-9775.

Li, L., C. J. Xian, et al. (2002). "Effect of lumbar 5 ventral root transection on pain behaviors: a novel rat model for neuropathic pain without axotomy of primary sensory neurons." Exp Neurol **175**(1): 23-34.

Li, Y., T. Carlstedt, et al. (2004). "Interaction of transplanted olfactory-ensheathing cells and host astrocytic processes provides a bridge for axons to regenerate across the dorsal root entry zone." Exp.Neurol. **188**(2): 300-308.

Li, Y., P. Decherchi, et al. (2003). "Transplantation of olfactory ensheathing cells into spinal cord lesions restores breathing and climbing." J.Neurosci. **23**(3): 727-731.

Li, Y., P. M. Field, et al. (1997). "Repair of adult rat corticospinal tract by transplants of olfactory ensheathing cells." Science **277**(5334): 2000-2002.

Li, Y., P. M. Field, et al. (1998). "Regeneration of adult rat corticospinal axons induced by transplanted olfactory ensheathing cells." J.Neurosci. **18**(24): 10514-10524.

Li, Y., D. Li, et al. (2005). "Interaction of olfactory ensheathing cells with astrocytes may be the key to repair of tract injuries in the spinal cord: the 'pathway hypothesis'." J Neurocytol **34**(3-5): 343-351.

Li, Y. and G. Raisman (1994). "Schwann cells induce sprouting in motor and sensory axons in the adult rat spinal cord." J.Neurosci. **14**(7): 4050-4063.

Li, Y., Y. Sauve, et al. (2003). "Transplanted olfactory ensheathing cells promote regeneration of cut adult rat optic nerve axons." J.Neurosci. **23**(21): 7783-7788.

Lima, C., P. Escada, et al. (2010). "Olfactory mucosal autografts and rehabilitation for chronic traumatic spinal cord injury." Neurorehabil Neural Repair **24**(1): 10-22.

Lima, C., J. Pratas-Vital, et al. (2006). "Olfactory mucosa autografts in human spinal cord injury: a pilot clinical study." J Spinal Cord Med **29**(3): 191-203; discussion 204-196.

Linda, H., F. Piehl, et al. (1992). "Expression of GAP-43 mRNA in the adult mammalian spinal cord under normal conditions and after different types of lesions, with special reference to motoneurons." Exp Brain Res **91**(2): 284-295.

Linda, H., M. Risling, et al. (1985). "'Dendraxons' in regenerating motoneurons in the cat: do dendrites generate new axons after central axotomy?" Brain Res **358**(1-2): 329-333.

Lovell, M. A., B. W. Jafek, et al. (1982). "Biopsy of human olfactory mucosa. An instrument and a technique." Arch Otolaryngol **108**(4): 247-249.

Mannion, R. J. and C. J. Woolf (2000). "Pain mechanisms and management: a central perspective." Clin J Pain **16**(3 Suppl): S144-156.

Marliani, A. F., V. Clementi, et al. (2010). "Quantitative cervical spinal cord 3T proton MR spectroscopy in multiple sclerosis." AJNR Am.J.Neuroradiol. **31**(1): 180-184.

Marliani, A. F., V. Clementi, et al. (2007). "Quantitative proton magnetic resonance spectroscopy of the human cervical spinal cord at 3 Tesla." Magn Reson.Med. **57**(1): 160-163.

McKeon, R. J., R. C. Schreiber, et al. (1991). "Reduction of neurite outgrowth in a model of glial scarring following CNS injury is correlated with the expression of inhibitory molecules on reactive astrocytes." J.Neurosci. **11**(11): 3398-3411.

McMahon, S. B. and R. Kett-White (1991). "Sprouting of peripherally regenerating primary sensory neurones in the adult central nervous system." J.Comp.Neurol. **304**(2): 307-315.

MedicalResearchCouncil (1976). Aids to the examination of the peripheral system. M. R. Council, Her Majesty's Stationery Office.

Miedzybrodzki, R., P. Tabakow, et al. (2006). "The olfactory bulb and olfactory mucosa obtained from human cadaver donors as a source of olfactory ensheathing cells." Glia **54**(6): 557-565.

Mikulis, D. J., M. L. Wood, et al. (1994). "Oscillatory motion of the normal cervical spinal cord." Radiology **192**(1): 117-121.

Miller, B. L., R. A. Moats, et al. (1993). "Alzheimer disease: depiction of increased cerebral myo-inositol with proton MR spectroscopy." Radiology **187**(2): 433-437.

Miragall, F., G. Kadmon, et al. (1988). "Expression of cell adhesion molecules in the olfactory system of the adult mouse: presence of the embryonic form of N-CAM." Dev Biol **129**(2): 516-531.

Moffett, J. R., B. Ross, et al. (2007). "N-Acetylaspartate in the CNS: from neurodiagnostics to neurobiology." Prog.Neurobiol. **81**(2): 89-131.

Montani, G., S. Tonelli, et al. (2006). "Neuropeptide Y in the olfactory microvillar cells." Eur J Neurosci **24**(1): 20-24.

Moran, D. T., J. C. Rowley, III, et al. (1982). "The fine structure of the olfactory mucosa in man." J.Neurocytol. **11**(5): 721-746.

Morrison, E. E. and R. M. Costanzo (1990). "Morphology of the human olfactory epithelium." J.Comp Neurol. **297**(1): 1-13.

Morrison, E. E. and R. M. Costanzo (1992). "Morphology of olfactory epithelium in humans and other vertebrates." Microsc.Res.Tech. **23**(1): 49-61.

Narakas, A. O. (1993). "Lesions found when operating traction injuries of the brachial plexus." Clin.Neurol.Neurosurg. **95 Suppl**: S56-S64.

Nash, H. H., R. C. Borke, et al. (2001). "New method of purification for establishing primary cultures of ensheathing cells from the adult olfactory bulb." Glia **34**(2): 81-87.

Navarro, X., A. Valero, et al. (1999). "Ensheathing glia transplants promote dorsal root regeneration and spinal reflex restitution after multiple lumbar rhizotomy." Ann.Neurol. **45**(2): 207-215.

Nibu, K., G. Li, et al. (1999). "Olfactory neuron-specific expression of NeuroD in mouse and human nasal mucosa." Cell Tissue Res **298**(3): 405-414.

Nomura, H., A. Furuta, et al. (2002). "Dorsal root rupture injury induces extension of astrocytic processes into the peripheral nervous system and expression of GDNF in astrocytes." Brain Res **950**(1-2): 21-30.

Novikov, L., L. Novikova, et al. (1995). "Brain-derived neurotrophic factor promotes survival and blocks nitric oxide synthase expression in adult rat spinal motoneurons after ventral root avulsion." Neurosci.Lett. **200**(1): 45-48.

Novikov, L., L. Novikova, et al. (1997). "Brain-derived neurotrophic factor promotes axonal regeneration and long-term survival of adult rat spinal motoneurons in vivo." Neuroscience **79**(3): 765-774.

Olsson, T., C. Lundberg, et al. (2000). "Genetic regulation of nerve avulsion-induced spinal cord inflammation." Ann.N.Y.Acad.Sci. **917**: 186-196.

Parr, A. M., I. Kulbatski, et al. (2007). "Transplantation of adult rat spinal cord stem/progenitor cells for spinal cord injury." J.Neurotrauma **24**(5): 835-845.

Pascual, J. I., G. Gudino-Cabrera, et al. (2002). "Spinal implants of olfactory ensheathing cells promote axon regeneration and bladder activity after bilateral lumbosacral dorsal rhizotomy in the adult rat." J.Urol. **167**(3): 1522-1526.

Pasterkamp, R. J. and J. Verhaagen (2001). "Emerging roles for semaphorins in neural regeneration." Brain Res.Brain Res.Rev. **35**(1): 36-54.

Pastrana, E., M. T. Moreno-Flores, et al. (2007). "BDNF production by olfactory ensheathing cells contributes to axonal regeneration of cultured adult CNS neurons." Neurochem.Int. **50**(3): 491-498.

Petroff, O. A., G. D. Graham, et al. (1992). "Spectroscopic imaging of stroke in humans: histopathology correlates of spectral changes." Neurology **42**(7): 1349-1354.

Piehl, F., H. Hammarberg, et al. (1998). "Changes in the mRNA expression pattern, with special reference to calcitonin gene-related peptide, after axonal injuries in rat motoneurons depends on age and type of injury." Exp.Brain Res. **119**(2): 191-204.

Piehl, F., G. Tabar, et al. (1995). "Expression of NMDA receptor mRNAs in rat motoneurons is down-regulated after axotomy." Eur.J.Neurosci. **7**(10): 2101-2110.

Pouwels, P. J. and J. Frahm (1997). "Differential distribution of NAA and NAAG in human brain as determined by quantitative localized proton MRS." NMR Biomed. **10**(2): 73-78.

Provencher, S. W. (1993). "Estimation of metabolite concentrations from localized in vivo proton NMR spectra." Magn Reson.Med. **30**(6): 672-679.

Qian, J., J. J. Herrera, et al. (2010). "Neuronal and axonal degeneration in experimental spinal cord injury: in vivo proton magnetic resonance spectroscopy and histology." J.Neurotrauma **27**(3): 599-610.

Ragnarsson, K. T. (2008). "Functional electrical stimulation after spinal cord injury: current use, therapeutic effects and future directions." Spinal Cord **46**(4): 255-274.

Raisman, G. (1985). "Specialized neuroglial arrangement may explain the capacity of vomeronasal axons to reinnervate central neurons." Neuroscience **14**(1): 237-254.

Ramon Y Cajal, S. (1928). Degeneration and regeneration of the nervous system. London, Oxford University Press.

Ramon-Cueto, A. (2000). "Olfactory ensheathing glia transplantation into the injured spinal cord." Prog.Brain Res. **128**: 265-272.

Ramon-Cueto, A. and J. Avila (1998). "Olfactory ensheathing glia: properties and function." Brain Res.Bull. **46**(3): 175-187.

Ramon-Cueto, A. and M. Nieto-Sampedro (1992). "Glial cells from adult rat olfactory bulb: immunocytochemical properties of pure cultures of ensheathing cells." Neuroscience **47**(1): 213-220.

Ramon-Cueto, A. and M. Nieto-Sampedro (1994). "Regeneration into the spinal cord of transected dorsal root axons is promoted by ensheathing glia transplants." Exp.Neurol. **127**(2): 232-244.

Ramon-Cueto, A., G. W. Plant, et al. (1998). "Long-distance axonal regeneration in the transected adult rat spinal cord is promoted by olfactory ensheathing glia transplants." J.Neurosci. **18**(10): 3803-3815.

Rawson, N. E., J. G. Brand, et al. (1995). "Functionally mature olfactory neurons from two anosmic patients with Kallmann syndrome." Brain Res **681**(1-2): 58-64.

Rawson, N. E., G. Gomez, et al. (1997). "Selectivity and response characteristics of human olfactory neurons." J Neurophysiol **77**(3): 1606-1613.

Richardson, P. M., U. M. McGuinness, et al. (1980). "Axons from CNS neurons regenerate into PNS grafts." Nature **284**(5753): 264-265.

Risling, M., H. Aldskogius, et al. (1983). "Effects of sciatic nerve resection on L7 spinal roots and dorsal root ganglia in adult cats." Exp.Neurol. **82**(3): 568-580.

Risling, M., S. Cullheim, et al. (1983). "Reinnervation of the ventral root L7 from ventral horn neurons following intramedullary axotomy in adult cats." Brain Res. **280**(1): 15-23.

Risling, M., K. Fried, et al. (1993). "Regrowth of motor axons following spinal cord lesions: distribution of laminin and collagen in the CNS scar tissue." Brain Res Bull **30**(3-4): 405-414.

Risling, M., K. Fried, et al. (1992). "Changes in nerve growth factor receptor-like immunoreactivity in the spinal cord after ventral funiculus lesion in adult cats." J.Neurocytol. **21**(2): 79-93.

Robinson, L. R. (2000). "Role of neurophysiologic evaluation in diagnosis." J Am Acad Orthop Surg **8**(3): 190-199.

Roisen, F. J., K. M. Klueber, et al. (2001). "Adult human olfactory stem cells." Brain Res **890**(1): 11-22.

Rubio, M. P., C. Munoz-Quiles, et al. (2008). "Adult olfactory bulbs from primates provide reliable ensheathing glia for cell therapy." Glia **56**(5): 539-551.

Sajja, B. R., J. S. Wolinsky, et al. (2009). "Proton magnetic resonance spectroscopy in multiple sclerosis." Neuroimaging Clin.N.Am. **19**(1): 45-58.

Schuhmann, M. U., D. Stiller, et al. (2003). "Metabolic changes in the vicinity of brain contusions: a proton magnetic resonance spectroscopy and histology study." J.Neurotrauma **20**(8): 725-743.

Schwob, J. E. (2005). "Restoring olfaction: a view from the olfactory epithelium." Chem Senses **30 Suppl 1**: i131-132.

Sheth, R. N., M. J. Dorsi, et al. (2002). "Mechanical hyperalgesia after an L5 ventral rhizotomy or an L5 ganglionectomy in the rat." Pain **96**(1-2): 63-72.

Sibtain, N. A., F. A. Howe, et al. (2007). "The clinical value of proton magnetic resonance spectroscopy in adult brain tumours." Clin Radiol **62**(2): 109-119.

Silver, J. and J. H. Miller (2004). "Regeneration beyond the glial scar." Nat Rev Neurosci **5**(2): 146-156.

Simmons, M. L., C. G. Frondoza, et al. (1991). "Immunocytochemical localization of N-acetyl-aspartate with monoclonal antibodies." Neuroscience **45**(1): 37-45.

Simone, I. L., C. Tortorella, et al. (2001). "Axonal damage in multiple sclerosis plaques: a combined magnetic resonance imaging and 1H-magnetic resonance spectroscopy study." J.Neurol.Sci. **182**(2): 143-150.

Singhal, A., R. Nagarajan, et al. (2010). "Two-dimensional MR spectroscopy of minimal hepatic encephalopathy and neuropsychological correlates in vivo." J Magn Reson Imaging **32**(1): 35-43.

Smith, C. G. (1941). The incidence of atrophy of olfactory nerves in man. **34:** 533-539.

SooHoo, N. F., A. P. McDonald, et al. (2002). "Evaluation of the construct validity of the DASH questionnaire by correlation to the SF-36." J Hand Surg Am **27**(3): 537-541.

Spinner, R. J., A. Y. Shin, et al. (2008). "Update on Brachial Plexus Surgery in Adults." Techniques in Hand and Upper Extremity Surgery **9**(4): 220-232.

Strange, K., F. Emma, et al. (1994). "Osmoregulatory changes in myo-inositol content and Na+/myo-inositol cotransport in rat cortical astrocytes." Glia **12**(1): 35-43.

Swash, M. (1986). "Diagnosis of brachial root and plexus lesions." J Neurol **233**(3): 131-135.

Takahashi, S., T. Iwanaga, et al. (1984). "Neuron-specific enolase, neurofilament protein and S-100 protein in the olfactory mucosa of human fetuses. An immunohistochemical study." Cell Tissue Res **238**(2): 231-234.

Takami, T., M. Oudega, et al. (2002). "Schwann cell but not olfactory ensheathing glia transplants improve hindlimb locomotor performance in the moderately contused adult rat thoracic spinal cord." J.Neurosci. **22**(15): 6670-6681.

Tavakkolizadeh, A., A. Saifuddin, et al. (2001). "Imaging of adult brachial plexus traction injuries." J Hand Surg Br **26**(3): 183-191.

Techangamsuwan, S., I. Imbschweiler, et al. (2008). "Similar behaviour and primate-like properties of adult canine Schwann cells and olfactory ensheathing cells in long-term culture." Brain Res. **1240**: 31-38.

Terzis, J. K. and K. C. Papakonstantinou (2000). "The surgical treatment of brachial plexus injuries in adults." Plast.Reconstr.Surg. **106**(5): 1097-1122.

Tiberio, M., D. T. Chard, et al. (2006). "Metabolite changes in early relapsing-remitting multiple sclerosis. A two year follow-up study." J Neurol **253**(2): 224-230.

Tkac, I., J. M. Dubinsky, et al. (2007). "Neurochemical changes in Huntington R6/2 mouse striatum detected by in vivo 1H NMR spectroscopy." J Neurochem **100**(5): 1397-1406.

Tourbah, A., J. L. Stievenart, et al. (1996). "In vivo localized NMR proton spectroscopy of normal appearing white matter in patients with multiple sclerosis." J.Neuroradiol. **23**(2): 49-55.

Traber, F., W. Block, et al. (2004). "1H metabolite relaxation times at 3.0 tesla: Measurements of T1 and T2 values in normal brain and determination of regional differences in transverse relaxation." J Magn Reson Imaging **19**(5): 537-545.

Trojanowski, J. Q., P. D. Newman, et al. (1991). "Human olfactory epithelium in normal aging, Alzheimer's disease, and other neurodegenerative disorders." J Comp Neurol **310**(3): 365-376.

Valverde, F. and L. Lopez-Mascaraque (1991). "Neuroglial arrangements in the olfactory glomeruli of the hedgehog." J.Comp Neurol. **307**(4): 658-674.

van der Graaf, M. (2010). "In vivo magnetic resonance spectroscopy: basic methodology and clinical applications." Eur Biophys J **39**(4): 527-540.

Vaynman, S. and F. Gomez-Pinilla (2005). "License to run: exercise impacts functional plasticity in the intact and injured central nervous system by using neurotrophins." Neurorehabil Neural Repair **19**(4): 283-295.

Veech, R. L. (1991). "The metabolism of lactate." NMR Biomed **4**(2): 53-58.

Vejsada, R., Y. Sagot, et al. (1995). "Quantitative comparison of the transient rescue effects of neurotrophic factors on axotomized motoneurons in vivo." Eur J Neurosci **7**(1): 108-115.

Vent, J., A. M. Robinson, et al. (2004). "Pathology of the olfactory epithelium: smoking and ethanol exposure." Laryngoscope **114**(8): 1383-1388.

Verma, P., G. Garcia-Alias, et al. (2008). "Spinal cord repair: bridging the divide." Neurorehabil.Neural Repair **22**(5): 429-437.

Vetrugno, R., R. Liguori, et al. (2003). "Sympathetic skin response: basic mechanisms and clinical applications." Clin Auton Res **13**(4): 256-270.

Ware, J. E., Jr. and C. D. Sherbourne (1992). "The MOS 36-item short-form health survey (SF-36). I. Conceptual framework and item selection." Med Care **30**(6): 473-483.

Webb, P. and A. Macovski (1991). "Rapid, fully automatic, arbitrary-volume in vivo shimming." Magn Reson.Med. **20**(1): 113-122.

Whitesides, J. G., III and A. S. LaMantia (1996). "Differential adhesion and the initial assembly of the mammalian olfactory nerve." J.Comp Neurol. **373**(2): 240-254.

Woodhall, E., A. K. West, et al. (2001). "Cultured olfactory ensheathing cells express nerve growth factor, brain-derived neurotrophic factor, glia cell line-derived neurotrophic factor and their receptors." Brain Res.Mol.Brain Res. **88**(1-2): 203-213.

Wu, G., M. Ringkamp, et al. (2002). "Degeneration of myelinated efferent fibers induces spontaneous activity in uninjured C-fiber afferents." J Neurosci **22**(17): 7746-7753.

Wu, W. (1993). "Expression of nitric-oxide synthase (NOS) in injured CNS neurons as shown by NADPH diaphorase histochemistry." Exp.Neurol. **120**(2): 153-159.

Yamagishi, M., S. Hasegawa, et al. (1988). "Examination and classification of human olfactory mucosa in patients with clinical olfactory disturbances." Arch Otorhinolaryngol **245**(5): 316-320.

Zimmerman, R. A. and Z. J. Wang (1997). "The value of proton MR spectroscopy in pediatric metabolic brain disease." AJNR Am J Neuroradiol **18**(10): 1872-1879.